DOTTORATO DI RICERCA IN SCIENZE DELLA TERRA

Università degli Studi di Firenze

Guglielmo Rossi

"A physically based distributed slope stability simulator to analyze shallow landslides triggering in real time and on a large scale"

settori scientifico disciplinari: GEO-04 / GEO-05

Tutore: Prof. Filippo Catani

Coordinatore: Prof. Federico Sani

XXIII CICLO

Firenze, 31 Dicembre 2010

Contents

Introduction and problem statement

Soil slips and debris flows are among the most dangerous shallow landslides: the threat they pose to human activities and life is mainly due to the high velocity that they can reach during the runout and to the nearly total absence of premonitory signals. These movements are usually triggered by heavy rainfall and they have the same extemporaneous character. Moreover, small and apparently harmless debris flows, triggered by small zones of unstable slopes, can group from different sources in channels greatly increasing mass displacement and destructive powers reaching up to 20 m/s velocities. There are several examples that testify the destructive power and the extemporaneous character of shallow landslides. Some Italian regions are under continuous threat and every year are hit by this phenomena that usually causes infrastructural damage but occasionally even human casualties.

Despite the large number of studies, publications and applications available nowadays, the prediction of shallow landslides over large areas in real or near real-time remains a very complex task. This is mainly due to: the necessary simplification introduced in hydrological and geotechnical models, the errors introduced by the rainfall predictions, the consequences of the uncertainties in the knowledge of morphometric, mechanical and hydrological parameters of soils and the extremely high computational effort required to operate on the basin scale.

The main objective of this PhD thesis is to address the aforementioned problems while developing a physically based distributed slope stability simulator to analyze shallow landslide triggering in real time and on a large scale. The expression “real

time" indicates that the simulator has to be fast enough to be compatible with a warning system for civil protection purposes.

To achieve this objective a physical model was developed with these main characteristics:

- The capability of computing the factor of safety at each time step and not only at the end of the rainfall event;
- The variable-depth computation of slope stability;
- The introduction of the contribution of soil suction in unsaturated conditions
- The probabilistic treatment of the uncertainties in the main hydrological and mechanical parameters and, thus, of the factor of safety.

A model with the aforementioned capabilities cannot be applied continuously over a large area without resorting to supercomputers and parallel processing. For this reason, the entire model programming code was developed to run over multiprocessor systems and was tested for performances with an increasing number of processing units to design an optimal cost/benefit approach covering the entire prediction chain, from rainfall data acquisition to the factor of safety computation.

This thesis follows a logical path through the physical and technological problems that affected the development of the stability simulator and the respective solutions proposed.

The first two chapters present a summary of the knowledge of landslides and the state of the art of slope stability models. They are introductory writings that permit one to understand different landslide types, the threat of shallow landslides, and the problems related to these phenomenas. More specifically, the second chapter is focused on landslide forecasting problems and the issues connected to the state of the art of the stability models. The respective software is also analyzed.

The third chapter concentrates on the physical model implemented in the stability simulator and on the innovative solutions proposed to achieve the thesis objectives.

In the forth chapter, the technological philosophy that drove the software code development is explained and the innovative stability simulator and its structure are presented.

In the following chapter, the fifth, the test areas involved in the development and in the validations are described. The chapter presents the fieldwork performed in the largest test area and the measurements methodology adopted and proposed to collect data to be used in the stability simulator on a large scale.

The sixth chapter presents the results and the validations of the developed stability simulator evaluating the performance in three fields: spatial reliability, temporal reliability and runtime performances.

Lastly, the potential of this stability simulator is briefly analyzed considering the reliability and computing performance obtained through the validation test.

1. Knowledge on landslides

1.1. Landslides classification

The movement of rock, soil, or debris caused by gravity is defined as a landslide. This includes a very large family of movements because the fall of a block from a rocky cliff and a mudslide are both defined as "landslides", but they are different phenomena. They involve different materials, geometry and dynamics of collapsed material. It is hard to define a unique and unambiguous classification and the question is an open debate among researchers.

Some classifications have been proposed by Varnes (1958), Hutchinson (1988) Hungr et al. (2001) but the most widely used classification of slope movement is that which was again modified by Varnes in 1978 and then revised in 1996 . Landslides are classified into five types of movement and differentiated by two classes of material involved: falls, topples, slides (rotational and translational) lateral spreads and flows. A sixth type, the complex movement, is defined as a combination of two

or more basic types of movement. According to the classification of Varnes, if a slide, flow or a complex landslide involves only a few meters, a soil depth is defined as a shallow landslide. The two classes of materials are: rocks and soils. Soils can be subdivided in two classes: predominantly fine soils and predominantly coarse soils (Varnes, 1996).

1.1.1. Falls

A fall starts with the detachment of soil or rock from a steep slope along a surface on which little or no shear displacement takes place. The material then descends mainly through the air by falling, bouncing, or rolling. These landslides involve steep slopes and the main causes of triggering are: vibration, undercutting, differential weathering, excavation, or stream erosion.

Figure 1.1: Topple example.

1.1.2. Topples

Topples are the forward rotation out of the slope of mass of soil or rock regarding a point or axis below the centre of gravity of the displaced mass. The main triggering causes are similar to falls, toppling is sometimes driven by gravity exerted by material upslope of the displaced mass and sometimes by water or ice in cracks in the mass.

Figure 1.2: At the left, the rotational slide of Conchita landslide (California, USA). At the right a fall example.

1.1.3. Slides

A slide (figures 1.2 and 1.3) is characterized by a sliding movement along one or more planes. There are two types of slides: rotational slides and translational slides. Rotational slides develop along a curved surface of sliding and are typical in homogeneous materials. Instead, translational slides occur along planar or slightly wavy plans. Usually this plane is controlled by structural or stratigraphic discontinuities like the boundary between bedrock and soil. Translational slides in shallow soils are usually called soil-slips (Campbell, 1975; Moser & Hohensinn, 1983; Ellen, 1988; Crosta & Frattini, 2002).

Figure 1.3: Slide example (Tessina, Italy).

1.1.4. Lateral Spreads

Spread is defined as an extension of a cohesive soil or rock mass combined with a general subsidence of the fractured mass of cohesive material into softer underlying material (Cruden & Varnes, 1996). In spreads, the dominant mode of movement is lateral extension accommodated by shear or tensile fractures (Varnes, 1978).

Figure 1.4: Rock avalanche.

1.1.5. Flows

A flow can be described as a spatially continuous movement in which surfaces of shear are short-lived, closely spaced, and usually not preserved (Cruden & Varnes, 1996). The distribution of velocity of the moving mass is similar to that which we can find in a viscous liquid. This dynamical property leads to a huge deformation amount within the entire sliding mass and mainly differentiates flows from the other types of landslides like slides where usually the landslide body moves rigidly along a slip surface.

We can observe very different types of flows depending on the material involved and they can be characterized by different velocity and triggering causes. We adopted the Varnes flows classification with some integration of Hungr's work (Hungr et al. 2001). Flows are grouped in two main categories: flows in rock and flows in soil. There are two types of rock flows:

- Rock flow: Flow movements in bedrock include deformations that are distributed among many large or small fractures, or even microfractures, without concentration of displacement along a through-going fracture. This flow movement speed is slow, and the main causes of triggering are the same as falls or topples: vibration, undercutting, differential weathering, excavation, or stream erosion.

- Rock avalanche: these are characterized by an extremely rapid, massive, flow-like motion of fragmented rock from a large rock slide or rock fall (figures 1.4 and 1.5).

Figure 1.5: Rock avalanche example.

The flows in soil share one main triggering cause: water saturation. They can affect slope that is not too steep (5-45 slope degree) and we can classify five types of flows in soil:

- Earth flows: they are from slow to rapid or intermittent plastic clayey earth movements. They usually present a characteristic tongue-shaped mass with a hummocky surface and lobed ends. Earth flows develop where water-rich unconsolidated material moves by slumping and plastic flow.

- Debris flows: d defined as very rapid to extremely rapid flows of saturated non-plastic debris in a steep channel. The flow is characterized by a low plasticity index [1] (lower than 5) and from sandy to gravely sliding mass granulometry. Debris flows' key feature is that they form and converge on a channel; either a first or second order drainage channel or even an established gully, or on a regular confined path. The running path follows the direction of the channels which greatly affects the type of movement and morphology of the flows. The runoff water in the channels can increase sliding mass speed and change

[1] The plasticity index is a measure of the plasticity of a soil. The plasticity index is the size of the range of water contents where the soil exhibits plastic properties. Soils with a high plasticity index tend to be clay, those with a lower PI tend to be silt, and those with a 0 value tend to have little or no silt or clay.

the typology of the flow. The lateral confinement can affect the sliding body depth, the vertical velocity gradient and thus the vertical and longitudinal sorting of the material. Usually the term “debris flow” is used as a general term to describe a rapid gravity controlled mass movement of a mixture of granular solids, water and air (Costa, 1984) and can be broadly interpreted as a general term to describe many other types of flow like mudflows, wet grain flows, lahars[2], tillflows[3], wet rock avalanches, debris avalanches and debris torrents.

- Mud flows: very rapid to extremely rapid flows of saturated plastic debris in a channel, involving significantly greater water content related to the source material (figure 1.6). The plasticity index is higher than 5 and the rich plastic content of clay differentiates the mud flow from a debris flow. Clay generates longer runout due to the dilution delay by water and drainage (Scott et al., 1992).

- Debris floods: very rapid, surging flows of water, heavily charged with debris in a steep channel. These flows, also called “hyperconcentrated flows”, differ from a debris flow by the amount of solid concentration: if a flow does not exceed the threshold of 80 percent of solid concentration it can be classified as a debris flood otherwise it is categorized a debris flow (Costa, 1984).

- Debris avalanches: very rapid to extremely rapid shallow flows of partially or fully saturated debris on a steep slope, without confinement in an established channel (figure 1.7).

[2] One of the greatest volcanic hazards. Lahars are similar to pyroclastic flows, fluidized masses of rock fragments and gases that move rapidly in response to gravity, but with a high content of water.

[3] Glacial melted water and debris flows.

Figure 1.6: A mud flow example.

Figure 1.7: Debris avalanches.

1.2. Shallow landslides hazard

As mentioned in landslide classification, a shallow landslide can be described as a slope movement of a few meters soil depth. Flows of soils are one of the most dangerous shallow landslides: their threat is attributed to the high velocity that they can reach during the runout and to the nearly total absence of premonitory signals. These movements are usually triggered by heavy rainfall and they have the same extemporaneous character. Moreover, small and apparently harmless debris flows, triggered by a small zone of instability slope, can group together from different sources in channels greatly increasing mass displacement and destructive power reaching speeds up to 20 m/s. High kinetic energy, due to high runout velocities, is extremely dangerous also for buildings and infrastructures. Even a soil slip is considered a shallow landslide, but, most of the time this type of landslide is the beginning of a soil flow: the soil collapses and can evolve into a flow after the involved material liquefaction due to the increasing pore pressure along the slip surface.

Figure 1.8: Sarno 1998 landslide event.

There are several examples that demonstrate the destructive power and the extemporaneous character of shallow landslides. Some Italian regions are under continuous threat and every year are hit by this phenomena that usually causes

infrastructural damage and occasionally even human casualties. From May 4th - 5th, 1998 about 150 landslide movements occurred over the span of 10 hours and hit an area of 75 km^2 near Naples (Italy), in the cities around Sarno. These landslides resulted in 137 fatalities. The landslides were favored by a strong and very spatially limited atmospheric perturbation that reached its highest strength in the Sarno (figure 1.8).

Between October and November 2000 in the entire Liguria region, heavy rainfalls occurred resulting in a total cumulative rainfall higher than 1000 mm for the 45-day period. In some places, the cumulative rainfall exceeded 70% of the average annual precipitation (Guzzetti et al., 2004). A total of 1024 landslides were triggered throughout the Imperia Province and during the night of November 23rd, two people were killed in their home (figure 1.9).

Figure 1.9: The Bestagno landslide which damaged the provincial road n°55 and killed two people.

On December 8, 2006 a storm occurred in the Armea basin and, although it was significantly smaller than the 2000 event, it triggered several superficial landslides and caused large infrastructural damages. A landslide damaged a main road, destroying a car and injuring the occupant (figure 1.10).

Figure 1.10: one of the Valle Armea landslides occurred in 2000. The landslides has damaged a main road, destroyed a car and injured the occupant.

In April 2006, four debris flows triggered by heavy rainfall occurred along the northern flank of a local mountain, Monte Vezzi (figure 1.11). These landslides affected two buildings, a quarry, a garbage compactor and four people were killed in their home. These flows were triggered in the highest part of Monte Vezzi, involving only 1 m of soil above a layer of cohesive pyroclastic deposits. These landslides were triggered by heavy localized rainfall as soil slipped and then evolved into a debris flow along the preexisting drainage channels during the downstream runoff.

Figure 1.11: Monte Vezzi landslide triggered by a heavy rainstorm in the morning of April 30, 2006.

1.2.1. Triggering of soil flows

Flows in soil usually develop on steep terrain and in areas characterized by no woodland or with brush and small trees. This triggering usually occurs in the upper part of the slope, often in relation to an abrupt slope angle change or along the edge of a natural or artificial escarpment. There are many causes that can lead to the triggering of a flow in soil. The most common is a change in the interstitial water pressure system due to rainfall: as the soil gradually saturates, pore-water pressures increase and shear strengths decrease (Sidle et al, 1982). Another cause for triggering can be the loss of the apparent cohesion component during intense rainfall (Fredlund, 1987). Other causes can be a variation to the external force system due to an earthquake or to natural erosion or to anthropic activity. However, the key cause remains strongly connected to heavy rainfall.

Figure1.12 : debris flow.

The shallow landslide triggering factor can be divided in three main groups:

- Hydrology: the initial moisture condition of a soil affects the slope stability and the movement triggering timing. The rise of the water table, variations in groundwater seepage or change in flow direction from recharge to discharge areas are hydrological factors that can

trigger a shallow landslide (Zêzere et al., 1999; Tsai & Yang, 2006; Tsai, 2008)

• Lithology and geology: soil properties like cohesion, internal friction angle and soil unit weight affect the slope stability because they directly influence the mechanical failure strength. Permeability is one of the most important factors that controls the surface and underground hydraulic circulation. The time needed to completely saturate a soil is strictly related to the permeability thus affecting the probability of reaching critical pore pressure. In addition, the stratigraphy of a terrain is important because the presence of one or more impermeable layers can cause a rapid saturation of the upper layers reaching the critical pore pressure which triggers the landslide (Iverson & LaHusen, 1989; Iverson et al., 1997; Iverson, 1997; Iverson et al., 2000; Takahashi, 1981).

• Morphology and topography: morphological features like the slope gradient greatly affect the stability of soil and the triggering threshold. Superficial and bedrock topography can control the superficial and groundwater flow and affect the moisture condition of soil (Pierson, 1980; Renau & Dietrich, 1997; Montgomery & Dietrich, 1994). A steep slope can reach instability sooner than a gradual one, but rainfall infiltration is more difficult due to major runoff probability and even water discharge can be faster leading to a more favorable initial moisture condition.

1.2.2. Runoff Dynamic

The flow behavior after the triggering phase and during the propagation along a slope has been highly analyzed with in situ analysis, laboratory models and simulations (Costa, 1984) (Hungr, 1996) (Iverson et al., 1997) (Johnson et al., 1984) (Takahashi, 1978, 1981).

The first propagation phase is characterized by high energy and erosion power. During this phase, the frontal part of flow thickness starts to rise due to the eroded material that is included in the sliding mass. Subsequently, the volume will be approximately constant along the erosion channel created by the landslide passage.

The debris flow front part is generally characterized by high, big clasts and gravel concentration while, starting from the middle, the materials become finer and the landslide tail is characterized by the finest granulometries (Takahashi, 1981). The coarsest clasts presence in the frontal part of the flow together with the high velocity reached is the main explanation for the highly destructive power of this landslide type.

The flow stopping phase generally occurs when the slope angle becomes lower than 3°. Usually this decrease in slope angle is reached with an abrupt transversal section increase (Takahashi, 1981). During this phase the flow frontal coarse section slows down until stopping and is overlaid by the main body materials and the thickness of the flow increases. The diluted material from the flow tail usually goes through the main body opening an erosion channel within the deposition area.

2. Forecasting Models

Shallow landslides, as we saw in the first chapter, are extremely dangerous because of their enormous destructive potential and because they don't have easily detectable premonitory warning signs. A warning system that can run in real time providing a reliable threat forecasting system for these landslides is one of the most desirable yet difficult to produce facilities that a civil protection office can have. The main cause for forecasting difficulty is the soil slip and the flows in soil which are usually triggered by an intense rainfall or by a complex sequence of them. Moreover, even if these types of landslides are more frequent in areas with specific combinations of morphologic and lithologic terrain characteristics, they can potentially trigger in every slope with soil. We can easily imagine the triggering parameters combination myriad that can lead to a flow in soil and as well as understand that we cannot simplify the problem as a meteorologic forecasting issue.

The main requirements for a useful civil protection warning system are reliability and updated real time information. The rapidity of these landslides force us to have a very fast triggering forecasting and warning system if there is a dangerous situation. The rapidity and the reliability largely depends on how we model the triggering phase, this is the core of a warning system. There are two different approaches to facing this problem: statistical empirical models and deterministic models.

2.1. Statistical empirical models

The Statistical empirical models are also called black box models: these models try to find a rainfall's intensity threshold through statistical analysis of meteorological events that have mobilized landslides in a given area. A forecast system based on this methodology is the easiest to implement: the amount of rain fallen and the amount expected to fall in a given area is compared with the threshold. If the threshold is exceeded, a warning status is given to the area. The name black box derives from the fact that the entire connection between rainfall and landslide warning status is "hidden" by the statistical analysis: you don't analyze the mechanism of instability but only the cause and effect statistics.

2.1.1. Black box models: the state of the art

Literature offers many examples of black box models that require only a collection of basic data such as dated landslides and rainfall records and an analysis of weather conditions that trigger the landslide. Then rainfall real time or forecasted data is plotted on a chart with thresholds and is continuously compared. Usually the thresholds are traced graphically without mathematical, physical or statistical criterion (Guzzetti et al., 2008). Where rainfall path records are available that have shown not to trigger landslides, the thresholds are defined as the best separator between the conditions that have triggered landslides and those that don't (Jibson et al., 1989; Giannecchini et al., 2005).

The scientific community refers to the idea of "threshold rainfall" as the intensity flux of rainstorm which has mobilized one or more landslides in a studied area. The

extreme complexity of the natural environment means that different initial conditions, different types of triggering landslides and multiple weather scenarios can generate mass movements in the same area. Therefore, we can't identify a single threshold value valid for large portions of territory that is also sufficiently accurate to be used in warning systems for civil protection (Van Asch et al, 1999).

It is possible find in literature different types of thresholds that can be classified by the building methodology adopted:

- Scale geographical thresholds. These can be categorized in three geographical scales of thresholds: global, regional and local. Global thresholds are usually extended to a global or continental area and establish, regardless of morphological parameters, lithology, land use or rainfall, a minimum below which there is no landslide, (Caine 1980) (Crosta and Frattini 2001, Cannon and Gartner 2005). Regional thresholds are defined as large areas (thousands of square kilometers) grouped by similar climatic and meteorological characteristics (eg Jibson, 1989; Gain, 1991, Larsen and Simon, 1993; Paronuzzi et al. 1998; Calcaterra et al. 2000; Aleotti, 2004). Local thresholds are based on focused analysis on small extension areas, typically basins or slope scales, where the meteorological and geomorphological context is homogeneous (eg Bolley and Oliaro, 1999; Annunziati et al. 2000; Montgomery et al. 2000; Floris et al. 2004; Giannecchini, 2005; Zezere et al., 2005).

- Time range thresholds. These are valid only for a time interval between one or two limits (lower and upper). These limits generally correspond to minimum and maximum rain events duration that it is analyzed to define the thresholds. The validity of time intervals can vary from a few hours (Cannon and Gartner, 2005) to months (Floris et al, 2004; Zezere et al., 2005).

- Types of triggered landslides. Each threshold usually refers to the triggering conditions of a limited number of types of landslides: debris flows (Jibson, 1989), soil slips (Baum et al., 2005), lahars (Ardoleba and Martinez, 1996), collapses in rock (Paronuzzi and Gnech). There are even

thresholds built considering whole types of landslides (Calcaterra et al. 2000; Zezere et al., 2005), except those where the role of precipitation is marginal.

- Rainfall parameters of the triggering event. Some thresholds analyze only the meteorological events that occurs immediately before or contemporary to a landslide. This rainfall is called "critical event" (Aleotti, 2004). In this case the key parameters are the duration and the intensity of rainfall. Usually the intensity (I) with the duration (D) are related by a power law and even the thresholds are traced following the same criteria. Antecedent precipitation can be used to add another key rainfall parameter to trace threshold because, even if they have low intensity, they can bring the soil to an easier triggering condition for the critical precipitation (Aleotti, 2004). The periods of antecedent rain that is considered influential varies from a few days (Aleotti, 2004; Chleborad, 2003) to months (Cardinal et al., 2006) and depends mainly on the type of landslides: deep landslides are more affected by long antecedent rains, while the shallows are more correlated with short and heavy rains.

- Special boundary conditions: suitable for landslides that occur in areas previously affected by fire (Cannon and Gartner, 2005) or earthquakes (Jan and Chen, 2005).

2.2. Deterministic models

The deterministic slope stability models can improve the level of spatial and temporal detail of the statistical empirical methods. This is possible because they are physically based: the processes involving the stability of a slope are described by mathematical relationships which link geotechnical, hydrological and morphometric characteristics of the slope portion that is analyzed. These typology models are also called "white box" models because the cause, rainfall or other destabilizing factors, and the effect, landslide triggering, are connected with an assumed physical modeled

mechanism. The physics based method allows us to apply the calculation and obtain a specific result at any point in the studied area which means the model can be used in a spatially distributed manner. Therefore, a deterministic model can get an estimate of the stability of a slope even over large areas at spatial resolution proportional to the input physical parameters resolution. These models are common for scientific research purposes where timing is not the main target, but, they also have great potential as a civil protection warning system. However, it is necessary to face problems not only related to the physics of shallow landslides but also technological problems. A shallow landslide forecasting system is usable as a warning system for civil protection purposes only if it provides reliable results in a short time. In this case there are two main challenges:

- Physical: modeling the triggering phenomena

- Technological: use advanced computing techniques and hardware resources.

A physical model that is too complex, or, the choice of a very high spatial and temporal resolution, can lead to long computation times and therefore cannot be integrated into a real-time landslide threat forecasting.

The scientific and technological challenge of the distributed deterministic model reaches the best compromise between physics complexity and high resolution analysis and use advanced computing technique and facilities to reach the levels of reliability and timing suitable for a civil protection purpose.

2.2.1. White box models: the state of the art

We can find many models in literature that attempt to describe the triggering of shallow landslides and debris flows at various approximation levels. The most widely used approximation is the infinite slope of isotropic and homogeneous soil: it is assumed that the depth to bedrock is smaller than the length of the slope analyzed.

Johnson and Rodine (1984) proposed one of the most well known hypothesis for mobilization of debris flows and shallow landslides which is known as the Bingham

model. This model assumes that triggering can occur only if the shear stress exceeds the Coulomb strength:

$$\tau > \sigma \tan(\varphi) + c'$$

This equation shows the shear failure along a surface in a granular material, τ is the shear stress acting on a surface, σ is the effective normal stress, φ is the internal friction angle of material and c′ is the effective cohesion.

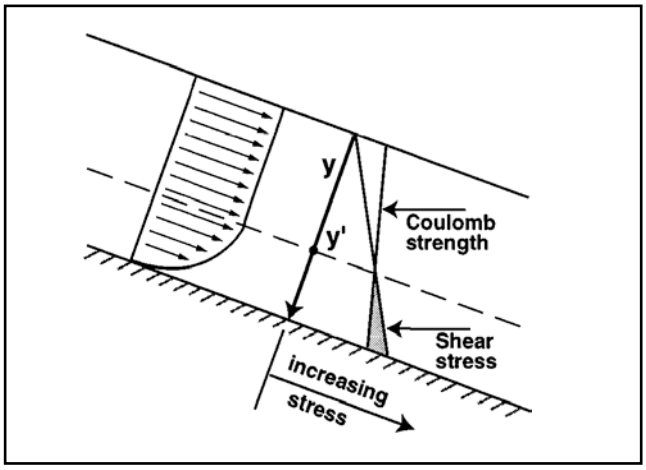

Figure 2.1:Bingham infinite slope model (from Iverson,1997)

In this case the strength, or yield strength, is assumed to be an intrinsic material property, and does not vary dynamically with the other soil properties. The failure can occur only when a soil with a particular water content exceeds a critical thickness. In such a case the shear stress at the base of the slope is higher than the yield strength (figure 2.1). Below the failure plane, the Bingham model assumes that the yield strength is not fixed but changes as a function of variables such as pore pressure and friction angle (Iverson, 1997).

Takahashi (1978) proposed an alternative hypothesis for shallow landslide triggering. The model is based on the Bagnold's concept (1954) of dispersive stress but is essentially a Coulomb failure model for a fully saturated and cohesion-less soil with slope parallel seepage. As a main assumption the soil is fully saturated and that the water flows across the slope and the slope surface (figure 2.1). The presence of surface water allows the failure at an arbitrary soil depth and in slopes of varying steepness but, because the angle of failing slopes is reduced to less than φ, this model

works better for debris flows triggered by flash floods in relatively gently slopes due to the surface-water surcharge (Iverson, 1997).

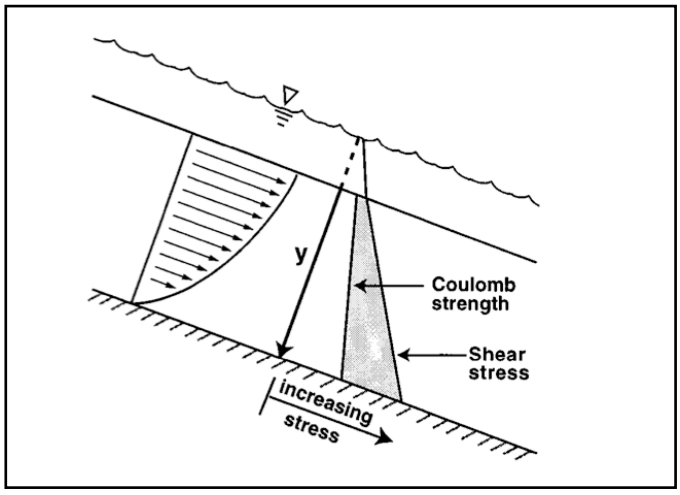

Figure 2.2:Takahashi infinite slope model (from Iverson,1997)

The debris flows are also described as a two-phase solid and fluid mixture model and it is assumed that they are triggered by the pore pressure growth beyond hydrostatic values. Some authors assume when the Coulomb failure occurs and the cohesion bonds are broken, the pore pressure can rise enough to liquefy the soil due "to the groundwater flow" (Denlinger et al., 1990); others postulate that the mobilization of debris flows may occur only when the contraction of loose soils during a quasi-static failure increase pore pressure until they reach a critical state (Casagrande, 1979) (Sassa, 1984), a behavior similar to undrained laboratory observed test cells. It is very important to consider how fast the porosity can change during soil contraction compared to the variation of the pore pressure: if this variation is slow, the pore pressure can change balancing the new porosity, but, if the porosity variation is too fast, the pore pressure increase can lead to the liquefaction of the soil.

As stated earlier in section 1.2.1, the main triggering factor for shallow landslides and debris flows is the increase in groundwater pore pressure in response to heavy rainfall. At the same time, the infiltrating water adds weight which plays a mechanical role especially where the cohesion contributes significantly to the Coulomb soil strength (Iverson, 1997). The pore pressure increase in a slope can occur in two ways: by direct infiltration of water at the slope surface and by groundwater flow from adjacent portions of the slope. The direct infiltration usually

involves a vertical flow from the surface to the deepest part of the soil while the groundwater flow usually comes from the closest saturated area. The pore pressure increase can occur also when the infiltrating or flowing water elevates the regional water table up to a shallow soil depth. The groundwater flow models used in distributed slope stability analysis use a common simplification: soils and rocks are considered as continuous porous media that obey Darcy's law, even though field evidence clearly indicates that the natural slopes flow distribution and speed can be deeply influenced by rock fractures, root channels and animal burrows (Pierson, 1983). That is a common hypothesis for two main reasons: computational and cognitive. Clearly it is very difficult, if not nearly impossible, to know all the flows preferential ways because they are casual and chaotic. It is also difficult to directly investigate these flows without making alterations to what we want to measure. Even if it is possible to have this type of knowledge it is not computationally affordable in a deterministic way due to the extreme complexity of flows net connection, and this is even more true if we want to analyze a large area and in near real time.

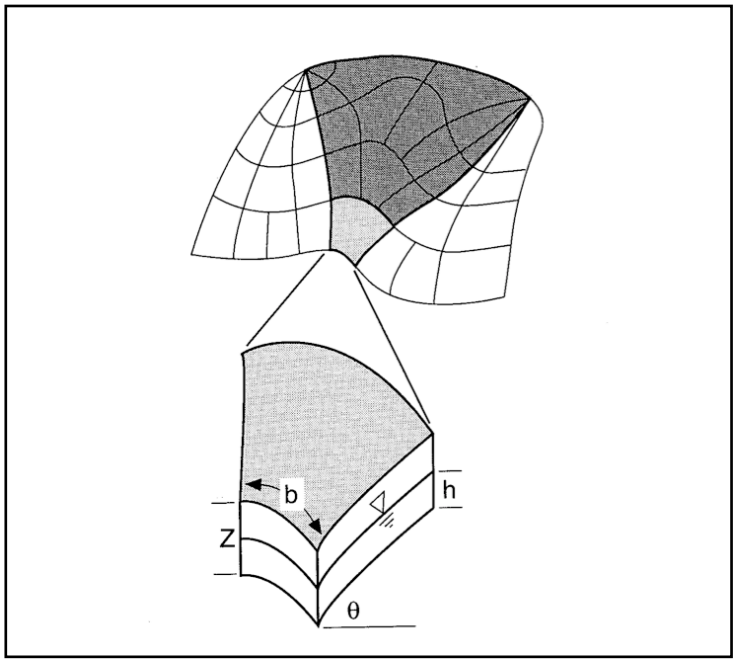

Figure 2.3:TOPOG hydrologic model topographic elements. Each element is defined by the intersections of contours lines and flow tube boundaries (from Mongomery et al.,1994)

Topography plays an important role in driving surface and groundwater flows and Montgomery & Dietrich (1994) proposed a model that explicitly considers the topographic influence on soil saturation and slope stability. They use the hydrologic model TOPOG (O'Loughlin, 1986) to predict the degree of soil saturation in

response to a steady state rainfall for topographic elements defined by the intersection of contours and flow tube boundaries (figure 2.3). The flow tube approach used by TOPOG basically permits us to include the topographic control on the pore pressure that is used to estimate the slope stability with the infinite slope model while treating the subsurface flow in the steady state. This topographic approach proves to be very efficient in capturing the spatial variability of shallow landslide hazards even though there is an over-predicted instability, depending on the topographic data quality (Dietrich et al., 2001). The flow tube approach is used in Rosso's model (Rosso et al., 2006): the hillslope hydrology is modeled by coupling Darcy's law for the seepage flow with the conservation of mass of soil water. Montgomery and Dietrich's approach models do not take into account transient movement of soil water. This simplification can negatively affect the results because the steady flow condition is unrealistic for the major part of natural slopes during and immediately after a rainfall event.

Other models use unsteady flows like those proposed by Okimura and Ichikawa (Okimura et al., 1985) or Wu and Sidle (WU et al, 1995): Okimura's model uses a finite difference approach to describe the groundwater flow, the second one couples the infinite slope stability approach with a groundwater kinematic wave model and a continuous change vegetation root strength model. This model works for varying soil depth and hydraulic conductivity but totally neglects the unsaturated zone. Casadei links a dynamic and spatially distributed shallow subsurface runoff model to an infinite slope model to predict the spatial distribution of shallow landslides also accounting for evapotranspiration and unsaturated zone storage (Casadei et al., 2003).

The major part of the above authors consider the pore pressure as deriving uniquely from the rising of a saturated layer above a fixed slip surface. Others have proposed models that instead consider the pore pressure as generated by the advance of a wetting front coming from the top. The most common approach is based on two main models that combine simplicity with high reliability: the Green-Ampt [4] infiltration model (Green et al, 1911), which infers the movements of the wetting front and finds the critical depth of triggering within the soil (Pradel et al., 1993), and Richards equation based models. Many authors use different solutions to the

4 The basic assumption behind the Green and Ampt equation is that water infiltrates into (relatively) dry soil as a sharp wetting front.

Richards equation[5] (Richards, 1931) to represent the movement of water in unsaturated soils and to assess the effect of transient rainfall on the timing and location of landslides (Iverson, 2000) (Crosta et al., 2003) (Simoni et al., 2008).

2.2.2. Existent software and code

Distributed slope stability models apply algorithms and equations to every cell of an extended area: usually the analyzed area is divided into a regular square grid that can have a side from a few to thousands of meters. Sometimes it is necessary to apply the model equations at different depths for each pixel which means the computation can be extremely time consuming depending on the thickness of the soil, the extension of the studied area, the spatial and temporal resolution and the complexity of the equation. Many softwares have been developed to handle this large amount of computations to apply stability models on a large scale and to visualize the results in many ways; all these softwares manage simpler versions of general forms of physical model equations introducing some approximations. It is usually possible to find two different software approaches: plugin oriented and stand-alone. The Plugin oriented codes are routine or add-ons that work on an existent software that provides a platform; this approach usually discharges all the file management and logical operations on the platform software and in some cases even part or all calculations are entrusted to the host software computational engine. These codes are simpler to use because they are supported by known software that is familiar to use and easier to program due to the use of host platform computational framework. Stand-alone software has a file management system and a dedicated and optimized computing routine which is developed in universal programming language (C++, Fortran, Basic...etc).

SHALSTAB, SHAllow Landslide STABility model, is a popular distributed slope stability analysis software (Dietrich et al., 1998). It has a physical core based on a distributed steady state description of the hydrological fluxes coupled with an infinite slope analysis. The basic tool is a grid-based model, a combination of C++ programs and ARC/INFO AML scripts intended to be used within an ESRI-ArcGIS software

5 Richards equation describes the fluid flow in an unsaturated porous media. Details in the next chapter (Chapter 3).

environment. This model has been classified as spatially predictive because it is not suited to forecast the timing of landslide triggering (Simoni et al., 2008).

SINMAP, Stability Index MAPping, and SINMAP 2 are other add-on tools for the ESRI-ArcGIS software. These have their theoretical basis in the infinite slope stability model with groundwater pore pressures obtained from a topographically based steady state model of hydrology (Pack et al., 1998, 2001). The input information (slope and specific catchment area) is obtained from the analysis of Digital elevation models (DEM). These parameters can be adjusted and calibrated with an interactive visual procedure that adjusts them based upon observed landslides. SINMAP allows an uncertainty of the variables through the specification of lower and upper bounds that define uniform probability distributions. Between these boundaries the parameters are assumed to vary at random in respect to the probability distribution.

Other softwares have a more complex approach to the hydrological modeling of the groundwater flow and require longer computational time. For example, SEEP/W is a stand-alone finite element software that resolves the Richards equations to account for transient groundwater flow within a slope. This software analyzes groundwater seepage and excess pore-water pressure dissipation within porous materials and can model both saturated and unsaturated flow (Krahn, 2004). SEEP/W is very efficient in resolving saturated-unsaturated and time-dependent problems and combining with the software SLOPE/W it performs the slope stability analysis adopting the limit equilibrium method. This software works very well for single slope stability analysis (Tofani et al., 2006) but is not suited to be applied to a distributed analysis.

TRIGRS, Transient Rainfall Infiltration and Grid based Regional Slope stability model, is a software developed in Fortran language, for computing the transient pore pressure distribution due to rainfall infiltration using the method proposed by Iverson (Baum et al., 2002). The results are stored in a distributed map of the factor of safety. TRIGRS, freely distributed both as source code[6] and executable files, is widely used by many authors for regional landslide hazard assessment (Baum et al., 2005; Salciarini et al., 2006; Chien-Yuan et al., 2005) and analysis under the approximation

6 The source code is a collection of files needed to convert from human-readable form to a computer-executable form. The source code may be converted into an executable file by a compiler.

of nearly saturated soil, presence of flow field and isotropic, and homogeneous hydrologic properties (Baum et al., 2002). TRIGRS is very sensitive to initial conditions, therefore, if the initial water table depth is poorly constrained, it may produce questionable results.

GEOtop-FS is one of the most advanced models for distributed slope stability and was recently proposed by Simoni (2008). This model uses the hydrological distributed model GEOtop (Rigon et al., 2006) to compute pore pressure distribution by an approximate solution of the Richards equation and an infinite slope stability analysis to compute the distributed factor of safety. The approximate solution of Richards equation used by the software works in saturated soil conditions. The factor of safety of GEOtop-FS is computed in a probabilistic approach assigning statistical distributions to soil parameters instead of a single deterministic value and analyzing the error propagation.

All these softwares use different models, approximations and programming languages but they have one common characteristic: all are suitable only for research purposes. In all these cases, speed is not the main objective. Even using modern computational hardware, workstation or personal computer, the computational time can take days for a relatively small area at high spatial and temporal resolution. It is impossible to use these softwares, even if they are state of art, in real time and for warning system purposes.

2.3. Discussion of the approach model chosen

The approach adopted in this work belongs to a white box model class because the main objectives are the development of a stability simulator with these characteristics :

- High spatial resolution.
- High temporal resolution.
- Large scale operative area.

- Fast computational time compatible with real-time analysis.

High spatial and temporal resolution are possible only with a physically based distributed model but, as we said in chapter 2.2, not usually compatible with short computational time if the analyzed area is extended more than a single slope scale. Moreover, there is still the problem of the variability of geotechnical parameters which increase when the analyzed area is increased.

The Stability simulator developed in this work proposes some solutions and computational techniques to overcome these problems and to obtain good reliability and fast runtime. The proposed solution regards as much the physical model as the programming code of the simulator, therefore, dealing with the problems related to both the physical model and technology.

3. The Physical Model

The objective of this work is to create a stability simulator that can be used on a large scale at high spatial and temporal resolutions. Above all, the main objective is to limit the running time required for an analysis because the simulator must be suitable for real-time civil protection monitoring. As we see in chapter 2, the deterministic approach is the only compatible with high spatial and temporal resolutions but that can be very time consuming. Therefore, it is important to chose a time affordable model without neglecting the reliability of the results. In this chapter, the focus is on the physical model adopted as the core of slope stability simulator and the innovation introduced to archive the objectives of this research project.

The physical model proposed is composed of two parts (figure 3.1): hydrological and geotechnical. The hydrological model receives the rainfall data as dynamical input and provides the pressure head as perturbation to the geotechnical stability

model, that provides results in factor of safety (FS) terms. The factor of safety is defined as:

$$FS = \frac{resisting \quad forces}{driving \quad forces}$$

The safety factor is a dimensionless parameter that implies the beginning of instability when it assumes the value 1, because the destabilizing forces are equal to those stabilizing.

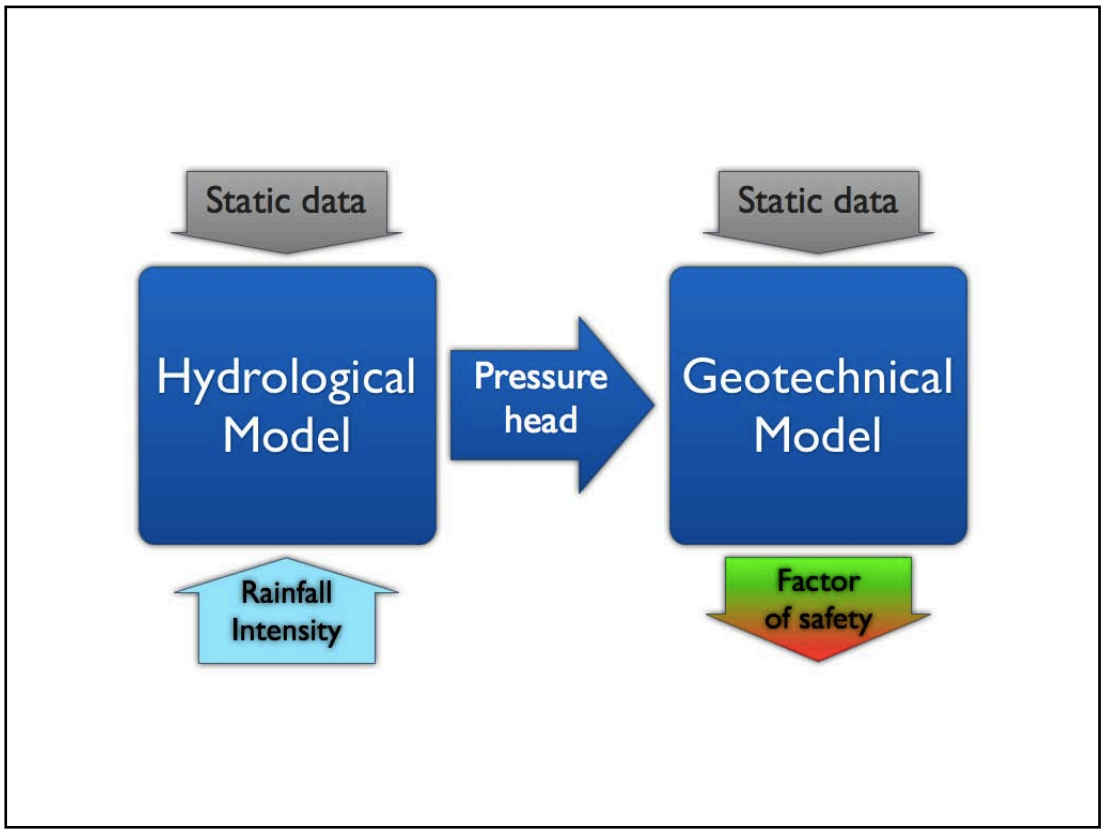

Figure 3.1: The physical model organization diagram.

This model structure is quite common and easier to implement in a real time software. The structure is inspired by the work of Iverson (Iverson, 2000) that is used in the TRIGRS software (see chapter 2.2.2).

The hydrological model is based on an analytical solution of an approximated form of Richards equation under the wet condition hypothesis and it is introduced as a modeled form of hydraulic diffusivity to improve the hydrological response. The geothecnical stability model is based on an infinite slope model that takes into account the unsaturated soil property. During the slope stability analysis the proposed

model takes into account the increase in strength and cohesion due to matric suction in unsaturated soil, that is where the pressure head is negative. Moreover, the soil mass variation on partial saturated soil caused by the water infiltration is modeled.

The model is then inserted into a Montecarlo simulation, to overcome the exact computation problems. This technique is introduced to manage the typical geothecnical parameters incertitude, which is the common weak point of the deterministic models. The Montecarlo simulation manages a probability distribution of input parameter and the results are not an exact value but a slope failure probability.

3.1. Hydrological model

The hydrological model is based on an approximate solution of the Richards equations that represents the unsteady Darcian[7] fluid flow in a porous media, in any saturation condition. Using the coordinate system (Figure 3.2) where z is normal to the slope (soil depth), x is tangent to the local surface slope and y is tangent to the local topographic contour, the general form of the equation is:

$$\frac{\partial h}{\partial t}\frac{d\theta}{dh} = \frac{\partial}{\partial x}\left[K_L(h)\left(\frac{\partial h}{\partial x} - \sin\alpha\right)\right] + \frac{\partial}{\partial y}\left[K_L(h)\left(\frac{\partial h}{\partial y}\right)\right] + \frac{\partial}{\partial z}\left[K_Z(h)\left(\frac{\partial h}{\partial z} - \cos\alpha\right)\right] \quad (3.1)$$

Where h is the groundwater pressure head, θ is the soil water volumetric content, t is time, α is the slope angle, K_L and K_Z are respectively the hydraulic conductivity in the lateral directions (x and y) and the hydraulic conductivity in slope-normal direction (z).

7 Darcian hypothesis is a slow, viscous fluid.

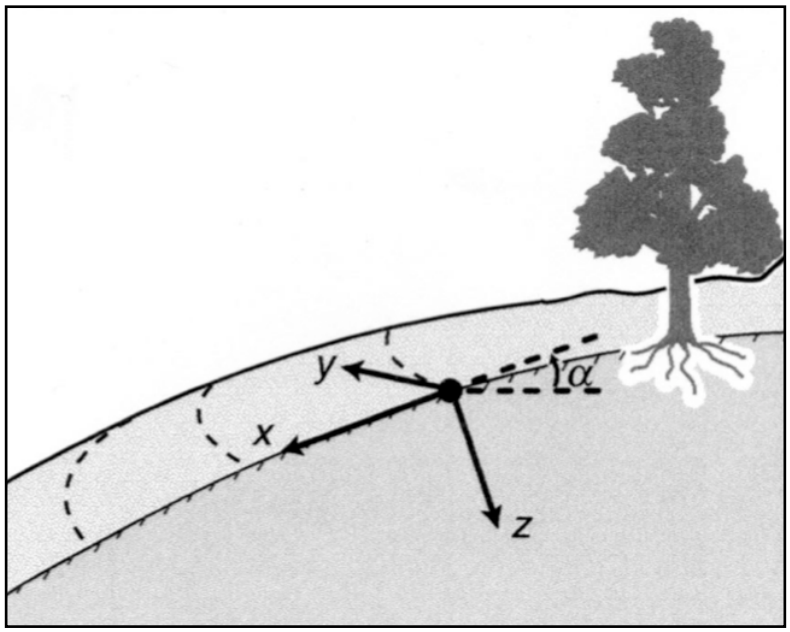

Figure3.2 : The coordinate system used in the physical model.

The general form of the Richards equation is a non-linear partial differential equation that does not have an analytical solution. There are two techniques that allow to get a solution for this general form without approximation hypothesis are a finite difference (FDM) or finite elements (FEM): these methods approximate the differential equations solutions by replacing derivative expressions with approximately equivalent difference quotients. The final solution is obtained evaluating the equation by consecutive small differences, or steps. The step must be quite smaller to have a convergent solution, that means small spatial and temporal steps and many computations compared to an analytical solution. The advantage of this approach is undoubtedly that it is not approximation dependent. However, keeping in mind the final objective, it was decided to use an analytical solution because the hypothesis to make to have an approximate solution of the general equation is not too limiting.

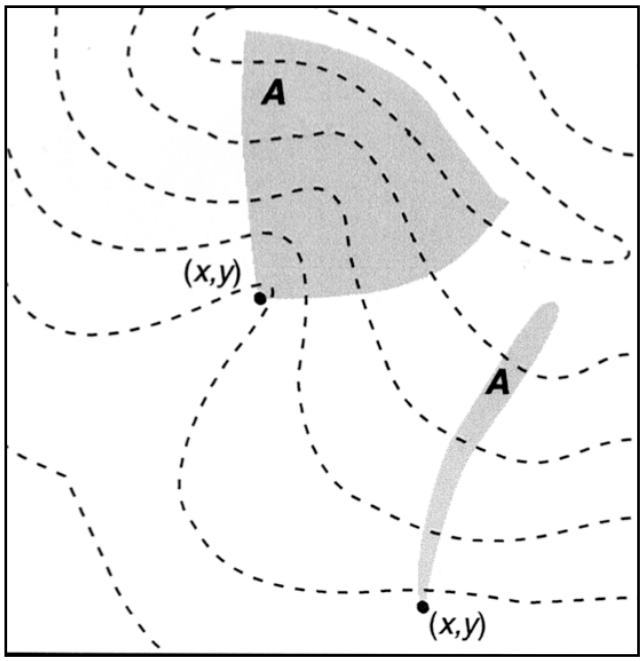

Figure 3.3: The planimetric contributing area A is defined as the area enclosed by the upslope topographic divide and hypothetical flow lines normal to topographic contours (from Iverson, 2000).

First approximation regards the timescale connected to shallows landslide phenomena. The physical process that leads to landslide triggering can operate on different timescales (Iverson, 2000): for times greater than A/D_0 the groundwater pressure head gets to a steady background distribution in response to a rainfall, where $D_0[L^2T^{-1}]$ is the maximum hydraulic diffusivity and $A[L^2]$ is the catchment area (figure 3.3) that might influence the pressure head distribution in x, y, z. Therefore, A/D_0 represents the minimum time needed for lateral pore pressure transmission from the area A. The triggering of landslides is instead the result of a rainfall over a shorter timescale of Z^2/D_0 (Z is the depth from the slope surface) which is associated with transient pore pressure transmission during and immediately after a rainstorm. Here the distinction between pore pressure transmission and water flux is relevant: rainwater can infiltrate the soil as a gravity-driven slug with uniform water content and zero pore water pressure behind the wetting front (Bear, 1972), but pore pressure change in a porous medium is largely a diffusive process that can occur with or without much water flux (Biot, 1941, 1956) (Chandler and Johnson, 1981).

So it is possible to establish a length scale ratio ε between the two timescales:

$$\varepsilon = \sqrt{\frac{Z^2 D_0}{A / D_0}} = \frac{Z^2}{\sqrt{A}} \qquad (3.2)$$

If $\varepsilon<<1$ it is possible to use the simplified solution of Richards equation using the long term and short term pressure head responses. We are mainly interested in the second response because it is linked to the shallow landslide triggering. In this case, the general form of Richards equation can be limited to the z spatial component and simplified as follow :

$$\frac{C(h)}{C_0}\frac{\partial h}{\partial t'} = \cos^2\alpha\left[K_Z\frac{\partial^2 h}{\partial Z^2} - \frac{I_Z}{K_Z}\frac{\partial K_Z}{\partial Z}\right] \qquad (3.3)$$

where *C(h)* is the change in volumetric water content per unit change in pressure head, $t' = t\,(D_0/Z^2)$, C_0 is the minimum value of *C(h)* and I_Z is the rainfall intensity rate considering Darcy's law for vertical flow in response to infiltration:

$$I_Z = -K_Z\left(\frac{\partial h}{\partial Z}\right) \qquad (3.4)$$

If the soil is prevalently dry, the diffusion term in the equation 3.3 can be neglected and the Richards equation becomes similar to that representing the "piston-flow" model described by Green-Ampt.

If we consider wet initial conditions, *C(h)* goes to C_0, K_Z goes to K_{sat} the saturated conductivity, the gravity flux can be neglected and the pressure head equation becomes:

$$\frac{\partial h}{\partial t} = \left(D_0\cos^2\alpha\right)\frac{\partial^2 h}{\partial Z^2} \qquad (3.5)$$

where D_0 is the maximum diffusivity, $D_0 = K_{sat}/C_0$. The equation 3.5 is a linear partial differential equation and allows the superposition principle: the net response at a given place and time caused by two or more stimuli is the sum of the responses which would have been caused by each stimulus individually. Mathematically that means:

$$F\left(x_1 + x_2 + ... + x_n\right) = F\left(x_1\right) + F\left(x_2\right) + ... + F\left(x_n\right) \qquad (3.6)$$

Therefore, it is possible to analyze a complex rainfall path, which means different intensity and duration, managing them as a sum of different stimuli response.

The solution of the partial differential equation 3.5 is well known in thermodynamics(Carslaw 1959); it is an analytical solution and with these boundary conditions:

$$
\begin{aligned}
&h(Z,0) = (Z - d_Z)\beta \\
&\frac{\partial h}{\partial Z}(\infty,t) = \beta \\
&\frac{\partial h}{\partial Z}(0,t) = -\frac{I_Z}{K_{sat}} + \beta \qquad (t \le T) \\
&\frac{\partial h}{\partial Z}(0,t) = \beta \qquad (t > T)
\end{aligned}
\tag{3.7}
$$

where d_Z is the steady water table depth, T is the rainfall duration and β is defined:

$$\beta = \cos^2\alpha - \left(\frac{I_Z}{K_Z}\right)\cos\alpha \tag{3.8}$$

The first boundary condition from 3.7 assumes a steady state pressure head distribution, the second assumes that at great depths below the water table the vertical groundwater becomes negligible but the steady state pressure head distribution persists. The last two conditions state that Darcy's low governs the water entry at the ground surface and that the pressure head distribution is defined by β when it is not raining (t > T) and by β plus a short time infiltration rate during rainfall (t ≤ T).

With these boundary conditions the solution of the equation (3.5) is:

$$h(Z) = Z\beta\left(1 - \frac{d_Z}{Z}\right) + Z\frac{I}{K_{sat}}\left[R\left(\frac{t}{Z^2/4D_0\cos^2\alpha}\right)\right] \qquad (t \le T) \tag{3.9}$$

$$h(Z) = Z\beta\left(1 - \frac{d_Z}{Z}\right) + Z\frac{I}{K_{sat}}\left[R\left(\frac{t}{Z^2/4D_0\cos^2\alpha}\right) - R\left(\frac{t-T}{Z^2/4D_0\cos^2\alpha}\right)\right] \qquad (t > T) \tag{3.10}$$

Where the response function R is defined:

$$R(t) = \sqrt{\frac{t}{\pi}} e^{\left(-\frac{1}{\frac{t}{Z^2/4D_0\cos^2\alpha}} \right)} - erfc\left(\frac{1}{\sqrt{\frac{t}{Z^2/4D_0\cos^2\alpha}}} \right) \qquad (3.11)$$

and *erfc* is the complementary error function.

There are another two conditions to this solution: the maximum infiltration rate and the maximum pressure head sustainable at the surface. The maximum infiltration rate is defined as the rate I_Z/K_{sat} =1, which means if the I_Z overreaches the saturated conductivity the exceeding rainfall runs off as Horton over-land flow which is not considered in this model. The maximum pressure head sustainable is ($Z\beta$), over this value we have the unrealistic physical condition of the water that leaves the soil. This restriction is rather ad hoc but necessary when using a linear model and constant flux boundary to approximate the nonlinear effects of rainfall infiltration (Iverson, 2000).

There is one parameter that is very important in the timing intensity response of this hydrological model: the hydraulic diffusivity. Unfortunately, this parameter is difficult to measure, especially on a large scale measurement campaign needed for a model applied to a large scale area. Therefore, the large scale operating philosophy suggests modeling the larger number of physical properties and to relate the parameters that are difficult to measure with others that are easier to collect.

The hydraulic diffusivity D(h) is defined as:

$$D(h) = K(h)\left(\frac{d\theta}{dh} \right)^{-1} \qquad (3.12)$$

Where the derivative part is the change in volumetric water content per unit change in pressure head and *K(h)* is the conductivity. In the proposed model the Brooks and Corey soil water retention mathematical relationship was used (Brooks et al., 1962; Brooks et al., 1964):

$$\frac{\theta - \theta_r}{\theta_s - \theta_r} = \left(\frac{h_b}{h} \right)^{\lambda} \qquad (3.13)$$

where, θ_r is the residual water content, n the porosity, h_b the bubbling pressure and λ the pore size index distribution. The diffusivity can be expressed, deriving equation 3.13 and using the Brooks and Corey expression of *K(h)*:

$$K(h) = K_{sat}\left(\frac{\theta-\theta_r}{\theta_s-\theta_r}\right)^{\left(3+\frac{2}{\lambda}\right)} \qquad (3.14)$$

Combining the equation 3.12, 3.13 and 3.14 the hydraulic diffusivity form becomes:

$$D(h) = \frac{h_b K_{sat}}{\lambda(\theta_s-\theta_r)}\left(\frac{\theta-\theta_r}{\theta_s-\theta_r}\right)^{\left(2+\frac{1}{\lambda}\right)} \qquad (3.15)$$

As stated, the proposed hydraulic model is under the wet condition hypothesis that is compatible with Brooks and Corey theory, which describes the soil water retention curve parts for matric potentials less than the bubbling pressure and not suitable for dry conditions. In wet conditions, tending at saturation, as used to obtain the solution at equation 3.5, the relation 3.15 can be simplified as:

$$D_0 = \frac{h_b K_{sat}}{\lambda\left(100\cdot n-\theta_r\right)} \qquad (3.16)$$

where θ_s is rewritten in function of the saturation degree and the porosity (θ=Sn).

3.2. Geotechnical model

The stability analysis is based on the limit equilibrium method for an infinite slope. It is observed that shallow landslides are usually characterized by an elongated shape and the influence of the toe and head portion is usually negligible, therefore it can be represented as a single slice with the slide surface approximately parallel to the ground surface. If the landslide has a low depth compared to length and width, as is common for shallow landslides, it is possible to assume a simplified geometry of the slide characterized by a planar slip surface on an infinitely extended planar slope,

both laterally and distally. This approach is known as infinite slope. It assumes that the failure is the result of translational sliding, that the failure plane and the water table are parallel to the ground surface and that the failure occurs along a single layer of infinite length. The forces acting at a point along the potential failure plane are those illustrated in figure 3.4

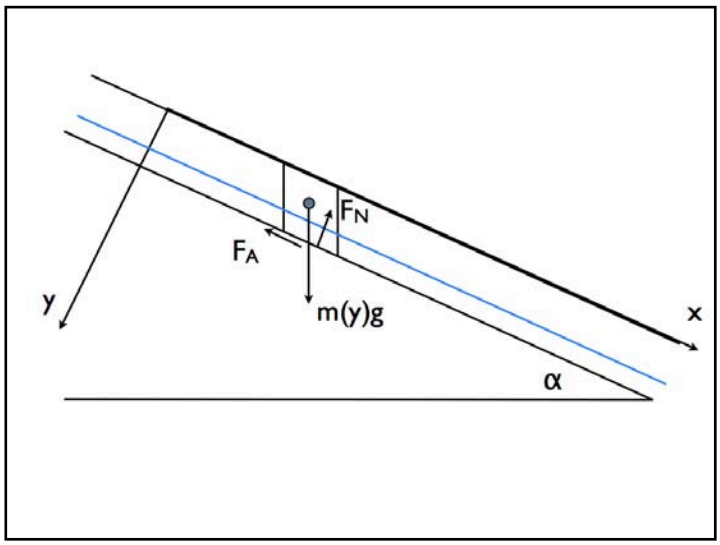

Figure 3.4: Diagram of reference system and explicit forces of geotechnical model

The hydrological model computes the pressure head in relation to the depth, therefore, it is possible to evaluate the stability at different y values. In relation to the pressure head, an evaluated point in the soil can be saturated or not.

If the soil is unsaturated, it is possible to write the equilibrium equations for each axes, x and y, of the reference system in figure 3.4 as

$$\begin{cases} m(y)g\cos(\alpha) - F_N = 0 \\ m(y)g\sin(\alpha) - F_A - F_C = 0 \end{cases} \qquad (3.17)$$

where *m(y)* is the mass of the columns of *y* depth soils, F_N the normal force, F_A the friction force and F_C the effective cohesion forces. The soil suction in an unsaturated soil can be considered as a pressure that raises the friction force. Therefore, the F_A is the static friction force plus a contribution, F_S , deriving from the soil suction

$$F_A = \mu|F_N| + F_S \qquad (3.18)$$

where μ is the dimensionless static friction coefficient that in geotechnical science is better known as the tangent of friction angle. The suction force according to Fredlund (Fredlund et al., 1993) can be expressed as the product of the suction pressure for a surface A

$$F_S = A\left(u_a - u_w\right)\tan\left(\varphi^b\right) \qquad (3.19)$$

where φ^b is an additional friction angle needed to account for the contribution of the matric suction to shear strength, u_a and u_w are respectively the air pressure in the soil and the water pressure. Solving the two equation system 3.17 and expressing all the forces, it is possible to write the equilibrium equation as

$$m(y)g\sin(\alpha) = m(y)g\cos(\alpha)\tan(\varphi) + A\left(u_a - u_w\right)\tan\left(\varphi^b\right) + c'A \qquad (3.20)$$

where c' is the effective cohesion. In this model, we consider the soil homogeneous and isotropic and we consider a two state model of soil density: wet or dry. If the soil is unsaturated, the soil density is assumed completely dry, otherwise it is considered saturated. This is a radical modeling but is quite good as a first approximation in our model. The model response, in this way, is a little bit sharp but thankful to the Montecarlo simulation, as we will see in the next paragraph, the behavior is smoothed. Considering this hypothesis, the mass at an unsaturated depth y can be written as m(y)=ρAy where ρ is the density of dry soil.

Dividing the 3.20 by the left term, considering the soil mass hypothesis and the relationship of soil unit weight ($\gamma_{NS} = \rho g$) it is possible to write the condition of stability as

$$1 \le \frac{\tan\varphi}{\tan\alpha} + \frac{c'}{\gamma_{NS} y \sin\alpha} + \frac{\left(u_a - u_w\right)\tan\left(\varphi^b\right)}{\gamma_{NS} y \sin\alpha} \qquad (3.21)$$

The right term of 3.21 is the known as the “factor of safety” (FS) because, if we analyze the equation 3.20, it is the rate between resisting forces and driving forces.

In equation 3.21 $u_a << u_w$ then the air pressure usually can be neglected, and the water pressure written in function of the pressure head h and the water unit weight γ_W:

$$u_W = \gamma_W h \qquad (3.22)$$

the additional friction angle φ^b can be related to the soil water retention curve and at the friction angle φ (Vanapalli et al., 1996)

$$\tan\left(\varphi^b\right) = \tan\varphi\left(\frac{\theta-\theta_r}{\theta_S-\theta_r}\right) \qquad (3.23)$$

Using the Van Genuchten soil water mathematical expression (Van Genuchten, 1980)

$$\frac{\theta-\theta_r}{\theta_s-\theta_r} = \frac{1}{\left[1+\left(h_b^{-1}|h|\right)^{(\lambda+1)}\right]^{\left(\frac{\lambda}{\lambda+1}\right)}} \qquad (3.24)$$

and putting together the 3.21, 3.22, 3.23 and 3.24 we obtain the following relationship for the factor of safety of unsaturated soil

$$FS = \frac{\tan\varphi}{\tan\alpha} + \frac{c'}{\gamma_{NS} y \sin\alpha} + \frac{\gamma_W h \tan(\varphi)\left(\frac{1}{\left[1+\left(h_b^{-1}|h|\right)^{(\lambda+1)}\right]^{\left(\frac{\lambda}{\lambda+1}\right)}}\right)}{\gamma_{NS} y \sin\alpha} \qquad (3.25)$$

If the pressure head is positive, at soil depth y, the soil is saturated: in this case the soil suction phenomena disappears because all pores are saturated and the capillary force is null. Therefore, the contribution due to suction in friction force equation 3.18 disappears. When the soil becomes saturated, another force must be considered: the force that comes from hydrostatic pressure, the pressure exerted by a fluid at equilibrium due to the force of gravity. The static equilibrium equations 3.17 become:

$$\begin{cases} m(y)g\cos(\alpha) - F_N - F_{hyd} = 0 \\ m(y)g\sin(\alpha) - F_A - F_C = 0 \end{cases} \qquad (3.24)$$

where the F_{hyd} is the hydrostatic force obtained from the product of a surface A with the well known hydrostatic pressure relationship:

$$F_{hyd} = \rho_w g h \quad (3.25)$$

where ρ_w is the water density and h is the height of the saturated soil in the point y that is equivalent at the pressure head value in that point. Operating like with the unsaturated soil condition, the factor of safety for a saturated depth point is

$$FS = \frac{\tan\varphi}{\tan\alpha} + \frac{c'}{\left[\gamma_{NS}(y-h)+\gamma_S h\right]\sin\alpha} - \frac{\gamma_S h \tan(\varphi)}{\left[\gamma_{NS}(y-h)+\gamma_S h\right]\sin\alpha} \quad (3.26)$$

In the model proposed when the hydrological model give a negative pressure head, unsaturated soil, the relationship 3.25 is used to compute the factor of safety, when instead the pressure head is positive the FS value is evaluate by the 3.26.

3.3. Montecarlo simulation

The drawback of the deterministic point is the incertitude of the input data: the reliability of the results are strongly connected to the quality of the parameters needed by the physical model. The parameters connected to the soil propriety are extremely variable at all spatial scales, from few meters to kilometers; this is an intrinsic characteristic of an extremely mixed and chaotic natural material composition. Moreover, if the parameters are evaluated starting from a chart, geographical, geotechnical, lithological, scale and cartographic errors are also introduced. The limits of a lithological area represented in a chart can't be sharp and clear as if they were traced, above all if we are dealing with a shallow soil part that lays on the bedrock. Evaluating the pressure head and the factor of safety from exact input parameters even in a controlled laboratory test can lead to disappointing results. Some models and slope stability simulators try to solve the problems by characterizing the parameters incertitudes, a range or a probability curve, and evaluating the error propagation function or the model itself. Even this approach is risky because there is no guarantee that in an evaluated point the result is produced

from the central value of each parameters' error distribution. The result of crossed evaluations of the most probable value with a probability distribution tail value of two parameters can lead to very different results and this it is not considered in a simple error propagation approach. Usually the approach used to limit this problem is to improve the knowledge of the input model data with huge measurements, even continuous ones produced using real time monitoring instruments. The aim of these constant measurements is to decrease the range of incertitude. This approach is possible on a slope scale, in some cases on a small basin scale, but, it is not applicable on a large scale level of hundreds or thousands of square kilometers. Even restricting the analyzed area and helping the physical model with a large amount of measurements and real time control point, the knowledge will be incomplete because some measurements can only be taken with destructive analysis. On a large scale, only a limited amount of measurements are possible and it is necessary to manage very approximative data inputs.

We propose in this work the use of a technique that helps with this type of problem: the Montecarlo simulation. This is a statistical non parametric method that is useful in solving problems linked to a deterministic exact computation. The term "Monte Carlo method" was coined in the 1940s by physicists working on nuclear weapons projects in the Los Alamos National Laboratory.

Monte Carlo methods are a class of computational algorithms that use repeated random sampling to compute their results. They are often used in simulating physical and mathematical systems and they are common studying systems with a large number of coupled degrees of freedom such as fluids, strongly coupled solids, disordered materials, and cellular structures. More broadly, Monte Carlo methods are useful for modeling phenomena with significant incertitudes in inputs and allows for determining how random variation, lack of knowledge, or error affects the sensitivity, performance, or reliability of the system that is being modeled.

These methods are widely used in mathematics: a classic use is for the evaluation of definite integrals, particularly multidimensional integrals with complicated boundary conditions. It is a successful and reliable method in risk analysis when compared to alternative methods or human intuition. When Monte Carlo simulations have been applied in space exploration and oil exploration, actual observations of

failures, cost overruns and schedule overruns are routinely better predicted by the simulations than by human intuition or alternative methods.

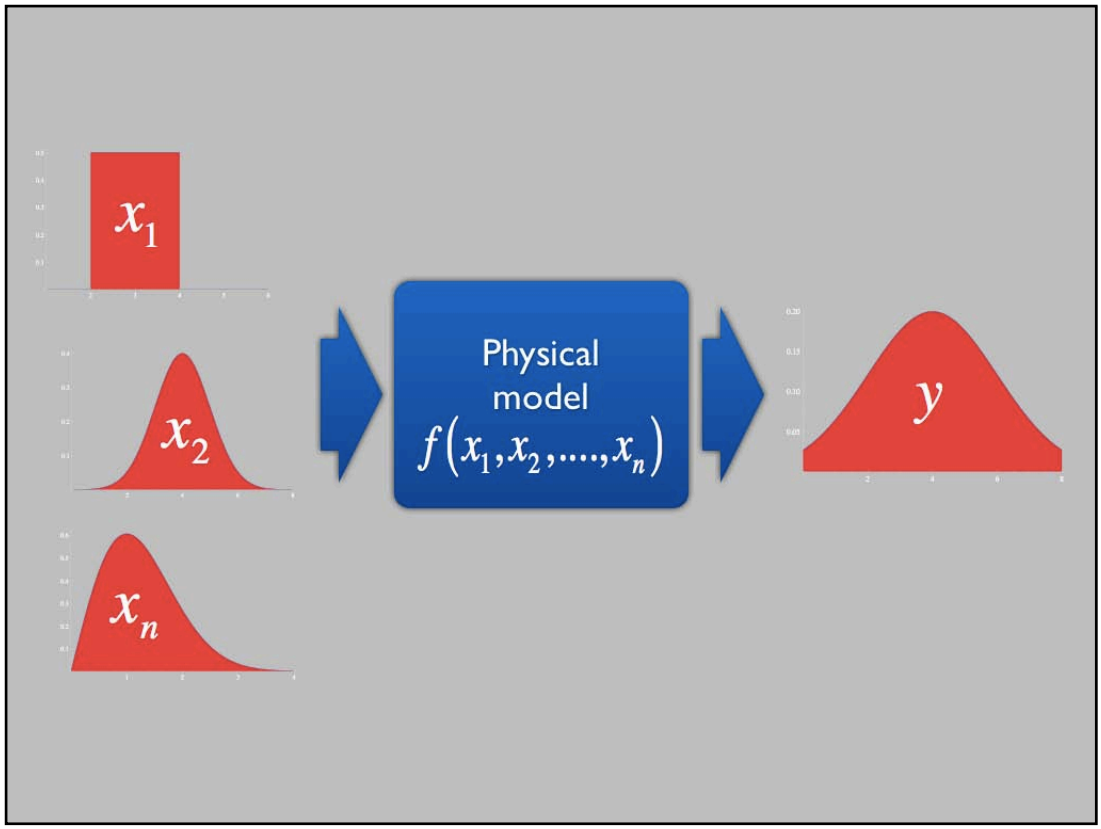

Figure 3.5: The Montecarlo simulation general diagram.

Because of their reliance on repeated computation of random or pseudo-random numbers, these methods are most suited to calculation by a computer and tend to be used when it is unfeasible or impossible to compute an exact result with a deterministic algorithm. The input parameters are randomly generated from probability distributions that most closely match data we already have or best represents our current state of knowledge in order to simulate the process of sampling from an actual population (figure 3.5). Therefore, we try to choose a distribution for the inputs. The data generated from the simulation can be represented as probability distributions or converted into error bars, reliability predictions, tolerance zones, and confidence intervals.

The Montecarlo methods approach has a defined procedural schema:

- Define a domain of possible data inputs and a probability distribution curve or a equiprobable uniform range of parameters.

- Generate data inputs randomly from the domain using a the specified probability distribution chosen.

- Perform a deterministic computation using the random inputs.

- Repeat the first three points n times

- Aggregate the results of the individual computations into the final result.

The accuracy of the final results is proportional to the square root of sampling n: in order to improve the accuracy of the aggregate result by a factor 10, the sampling values must be 100.

This method allows for the evaluation of the behavior of the physical model at the crossing of the input parameters that have different probability values. As stated previously, this is more reliable than other error propagation analysis that are strongly bounded to the knowledge and the accuracy of input data. This huge advantage is paid in computational time: the computational time can increase proportionally to the n sampling needed for a good quality simulation. The computation technique is very time consuming and, consequently, hardware demanding: it is necessary to use the most advanced programming techniques that allow the use of the computational power of modern electronic calculators. In chapter 4 this aspect is analyzed, and a solution is proposed which is adopted by our slope stability simulator software.

4. The slope stability simulator: HIRESSS

The physical representation of the landslide triggering is only half of a stability simulator software development. In this chapter, the software code HIRESSS, HIgh REsolution Slope Stability Model, is presented. This software evaluates the physical model seen in chapter 3. The techniques and solutions adopted to contain the code running time are also presented in this chapter. As discussed in chapter 2.2.2 and chapter 3 it is crucial to find a compromise between physical complexity and time computation because the final objective is a software which is suitable for a real time shallow landslide forecasting system: in order to be useful in case of danger, the slope stability evaluation has to be compatible with civil protection activation timing.

The main time demanding sources are:

- The physical model: particularly the Montecarlo simulation management.

- The high spatial resolution: the target resolution of this project is from 20 to 5 square meter pixels. These values are usually the best resolution available for the digital elevation model (DEM) on a large scale (more than 1K square meter area).

- The high temporal resolution: the target time step of the landslide's forecasting is from 30 minutes to 1 hour. This is a common temporal range for the weather forecasting data or the automated pluviometer measurement. Satellite or radar rainfall measurement data can have a data rate of 15 minutes, and the software is capable of managing this time step, but in this project it is not the main temporal resolution because it is not easily available or does not have a large scale continuous coverage.

- The large scale of analyzed area: the objective of this project extends the analyzed area over thousands of square meters. At the spatial resolution of 5 meters the physical model must be evaluated in 800 pixels every km^2 (see chapter 5).

The solution to contain or reduce the code running time of an optimized code is distributing the computation. The idea is to divide the problem into a smaller parts that can be evaluated at the same time by different processing units, the CPUs (Central Processing Units)(Figure 4.1, Figure 4.2). This approach allows the use of high performance computing (HPC) hardware that has thousands of CPUs that can operate simultaneously. These HPC hardwares are called supercomputers and they can speed up huge computational problems depending on the parallelizing grade of the problem to solve.

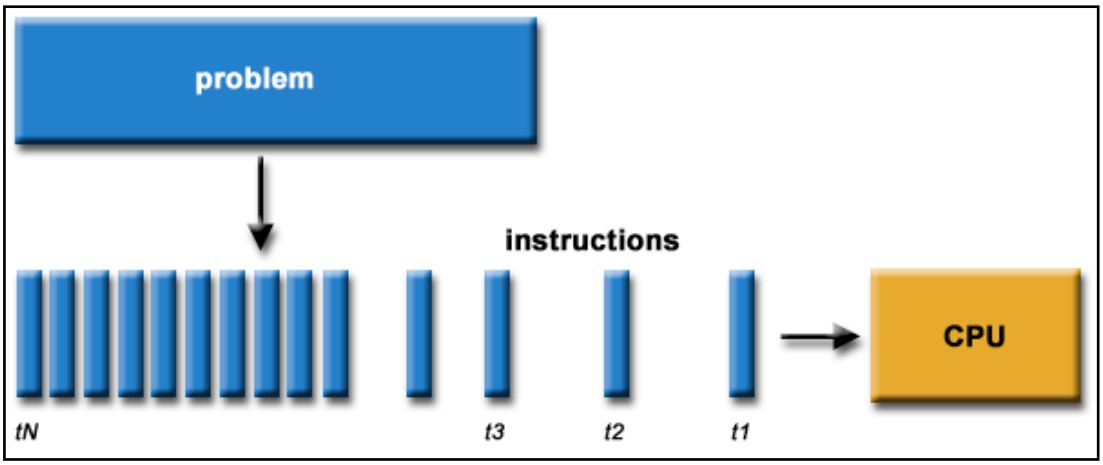

figure 4.1: the diagram of a serial processing of a problems. The problems is divided and queued to be be processed by a single CPU.

HIRESSS is conceived having in mind the use of a supercomputer, because the analysis domain and resolution proposed is not affordable by any workstation or computational hardware. It is necessary to have the computational power of thousands modern CPUs to handle in a useful amount of time for civil protection purposes the huge computation amount of a high resolution slope stability simulator. However, the parallelization of calculation improves the computational timing for small areas or for non time constrained scientific purposes also in the modern computer. The actual desktop, workstation and often also laptop computer, have more than one processing unit that can work parallels. The parallels programming presents some difficulties with the synchronization of the computation and it is a new challenge for the code writer: the first CPU dual core aimed at a large market was introduced in 2005. However, for special purposes, like scientific supercomputing, it was introduced two years earlier. Even now, after 5 years, the most common application that can be found in our computers do not have a parallelized code and they do not take advantage of multicore CPU.

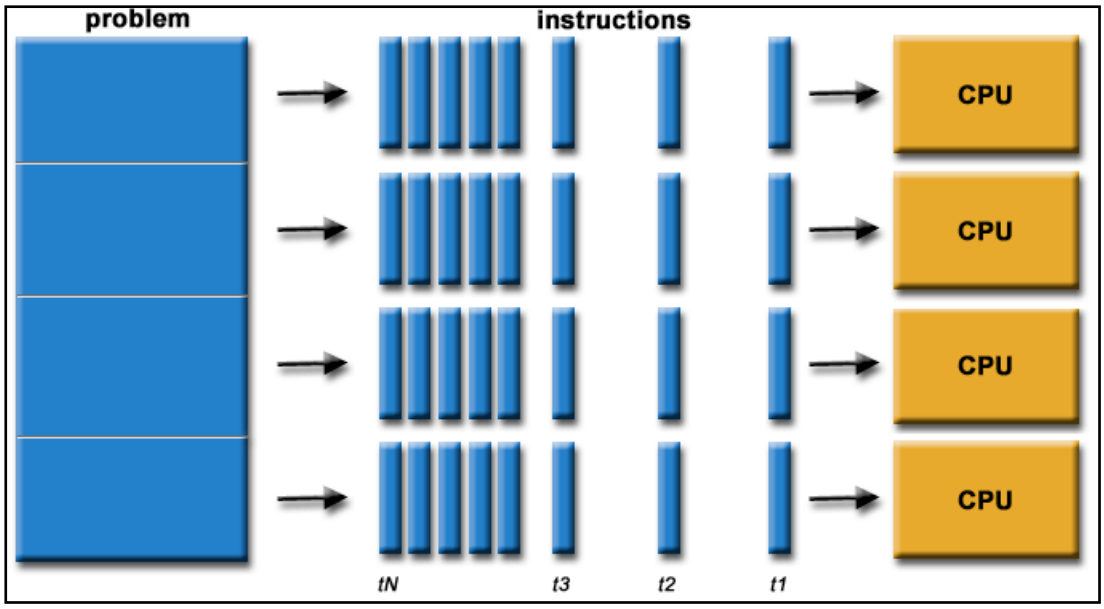

Figure 4.2: the diagram of a parallel processing of a problems.The problem is divided in smaller part. Then each smaller part is serially processed by respective CPU.

4.1. Parallel computing architectures

Architecture translates the potential of the technology into performance and capability. There are fundamentally two ways in which a larger volume of resources, which means more transistors, improves performance: parallelism and locality. These two fundamental characteristics are interconnected: the number of cycles required to execute the program is reduced whenever multiple operations are performed in parallel. However, each of the simultaneous activities require supporting resources. Whenever data references are performed close to the processor, the latency of accessing deeper levels of the storage hierarchy is avoided and the number of cycles to execute the program is reduced. However, resources are also required to provide this local storage. Therefore, the best performance is obtained with a compromising strategy which devotes resources to exploit a degree of parallelism and a degree of locality.

We can divide the parallel computing architecture into two main families: shared memory and distributed memory. A third architecture family is a hybrid of these two and it is now the most commonly used in the supercomputer because, as stated previously, the best performance is produced by a combination of parallelism and locality

4.1.1. Shared memory architecture

One of the most important classes of parallel machines is shared memory architecture. Basically, there is a unified data container, the memory, where every CPUs reads the inputs or stores the computed information or variable (figure 4.3). The data stored in memory is visible by all CPUs, therefore, the communication between the processing units is simplified because it is only necessary "to post" an exchange of information on this shared "board", the memory.

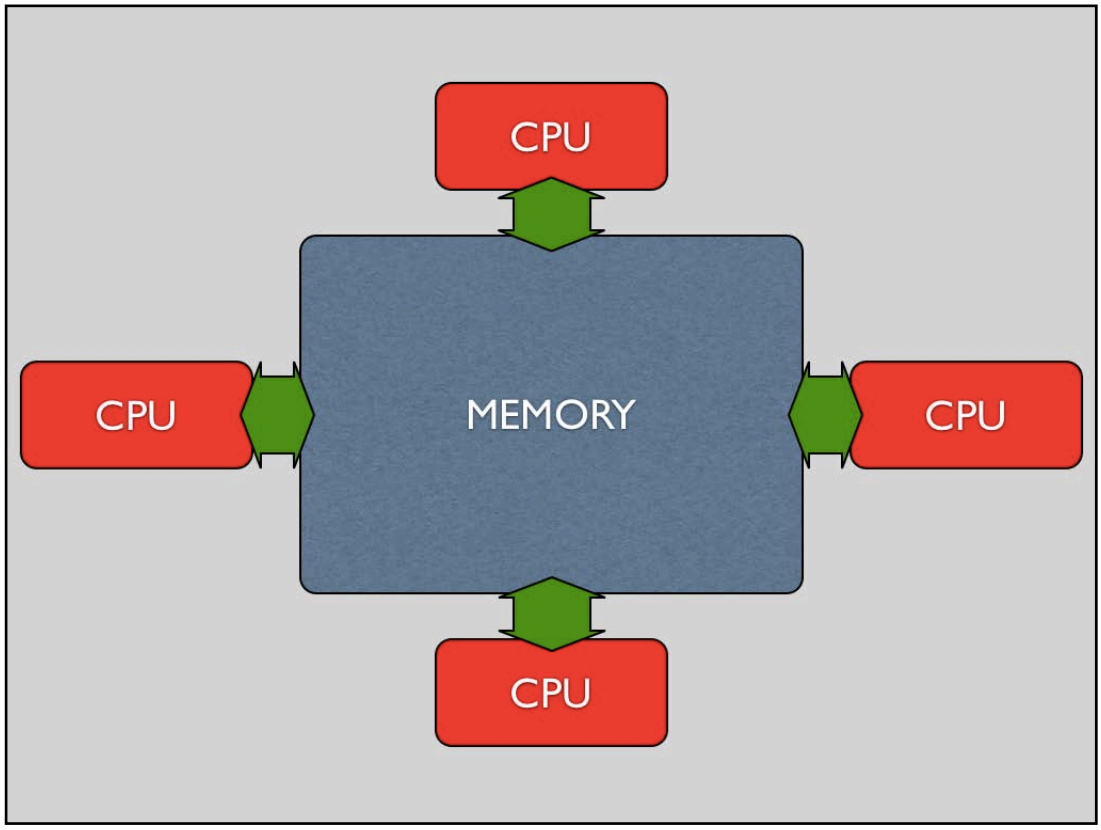

figure 4.3: shared memory architecture diagram.

Therefore, the key property of this class is that communication occurs implicitly as a result of conventional memory access instructions, loads and stores. Shared memory multiprocessors serve to provide better throughput on multiprogramming workloads, as well as to support parallel programs.

The primary programming model for these machines is essentially that of timesharing on a single processor, except that real parallelism replaces interleaving in time. Formally, a process is a virtual address space and one or more threads[8] of control. Processes can be configured so that portions of their address space are

8 A thread is the smallest unit of processing that can be scheduled by an operating system.

shared or are mapped to a common physical location. Multiple threads within a process, by definition, share portions of the address space. Cooperation and coordination among threads is accomplished by reading and writing shared variables and pointers[9] referring to shared addresses. Writing to a logically shared address by one thread are visible to read by the other threads. The communication architecture employs conventional memory operations to provide communication through shared addresses, as well as special atomic operations for synchronization. Completely independent processes typically share the kernel portion of the address space, although this is only accessed by operating system code. Nonetheless, the shared address space model is used within the operating system to coordinate the execution of the processes.(OpenMp, 2008)

figure 4.4: The intel Xeon 7400. This processor features a single-die hexa-core design.

While shared memory can be used for communication among arbitrary collections of processes, most parallel programs are quite structured in their use of the virtual address space. They typically have a common code image, private segments for the stack and other private data, and shared segments that are in the same region of the virtual address space of each process or thread of the program. This simple structure implies that the private variables in the program are present in each process and that shared variables have the same address and meaning in each process or thread. Often straightforward parallelization strategies are employed; for example, each process may perform a subset of the iterations of a common parallel

9 A pointer is a programming language data type whose value "point to" another value stored elsewhere in the computer memory using its address.

loop or, more generally, processes may operate as a pool of workers obtaining work from a shared queue.

Therefore the main characteristics of shared memory can be summarized as follows:

- Easier to program: due to common memory address.

- Fast CPU communications: this is due to physical proximities of processing units and the communications using memory-CPU bus or fast intercore connections (figure 4.4).

- Limited parallel CPUs: this architecture can connect, at this moment, until one hundred CPUs.

In 2010, the consumer market offers configurations up to dual CPUs each with 6 physical computational cores. Professional and specific use can reach up to 4 exa-core CPUs. The computational core is equivalent to the old CPU definition but the communication interconnection between the same CPU's cores are faster than memory bus.

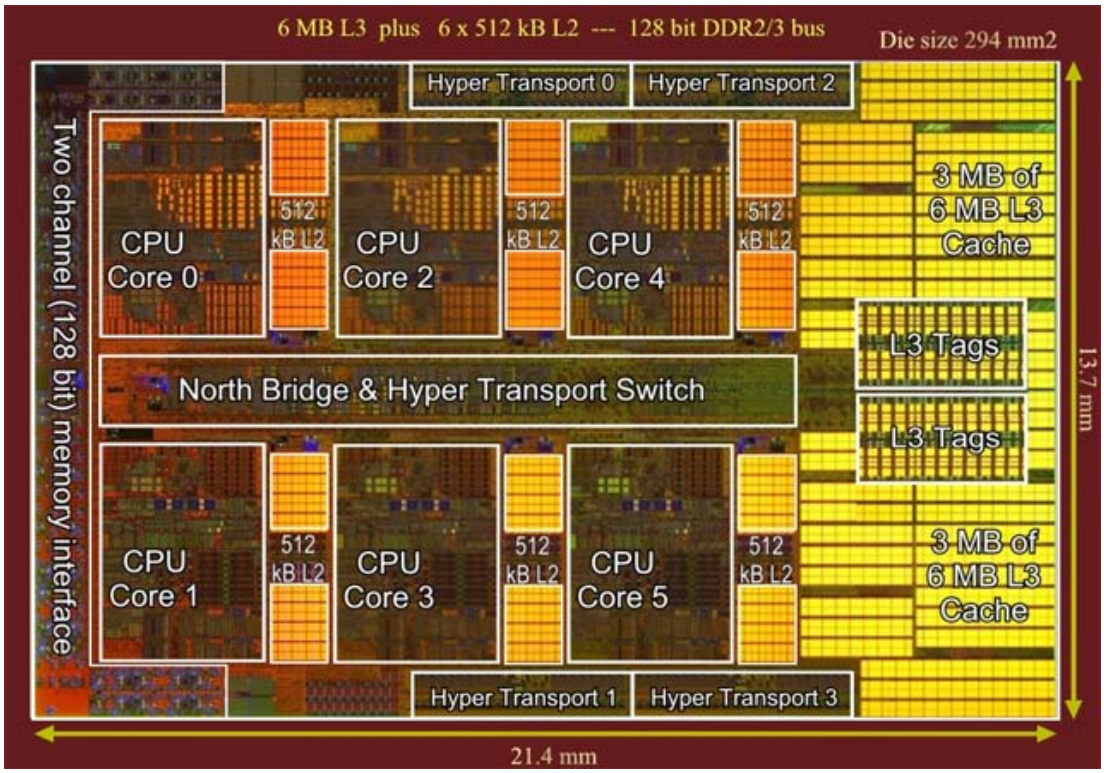

figure 4.5: The hexa-core CPU AMD Phenom II x 6. This is a real image of the chip. It is possible to observe the six single computational cores that are interconnected by a fast 4GHz dedicated bus (Hyper transport).

4.1.2. Distributed memory architecture

A second important class of parallel machines, distributed memory architectures, employ complete computers as building blocks, including the microprocessor, memory and I/O[10] system, and provide communication between processors as explicit I/O operations. This is also called message passing architecture because the communication is based on the message exchange between processing units. The primary difference with shared memory architecture is that communication is integrated at the I/O level, rather than in the memory system.

This style of design also has a lot in common with networks of workstations, or "clusters", except the packaging of the nodes is typically much tighter, there is no monitor or direct user access, and the network is of much higher capability than standard local area networks. The integration between the processor and the network tends to be much tighter than in traditional I/O structures, which support connection to devices that are much slower than the processor, since message passing is fundamentally processor-to-processor communication.

In message-passing there is generally a substantial distance between the programming model and the communication operations at the physical hardware level, because user communication is performed through operating system or library calls which perform many lower level actions, including the actual communication operation.

This is the common architecture used in a modern supercomputer and the main characteristics can be summarized as follows:

- Scalability of processor numbers and memory quantity: if you increase the number of processors than the size of memory increases proportionately; The number of processor can vary from hundreds to hundreds of thousands of CPUs or computational cores.

10 Input/output

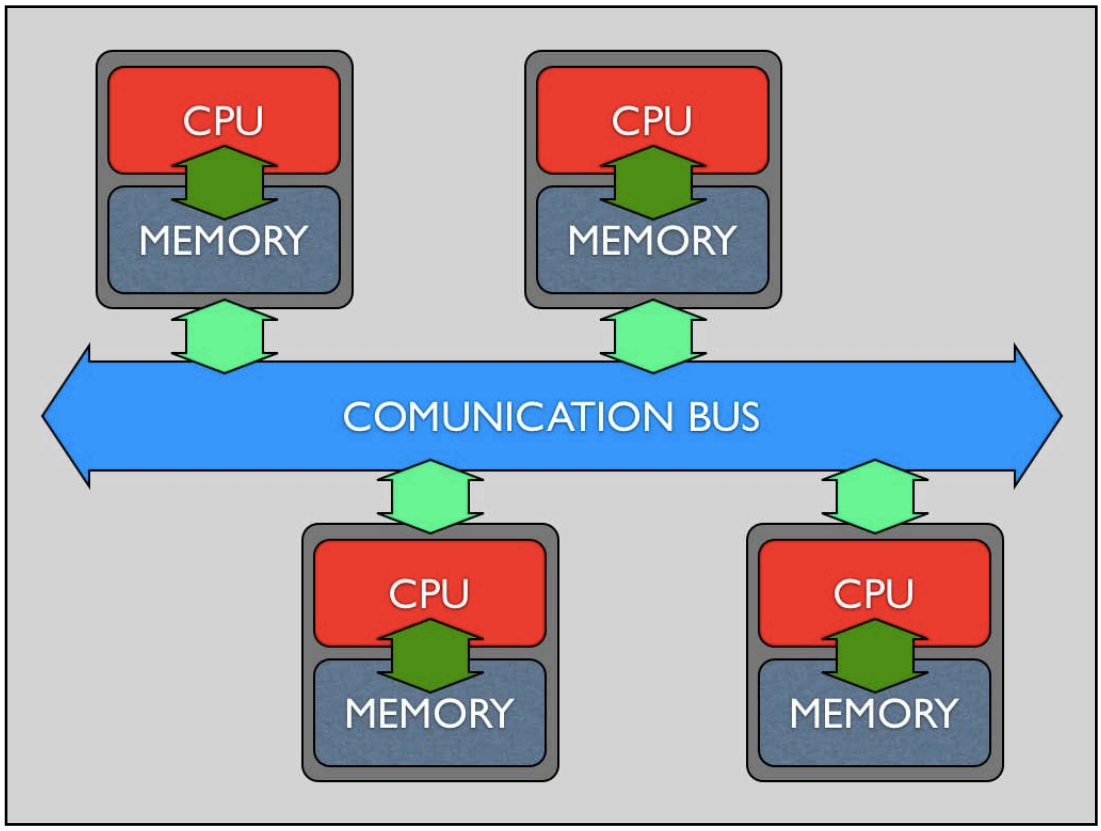

figure 4.6: distributed memory architecture diagram. The CPU have a private memory and the comunication are performed by a comunication bus.

- Exclusive memory access by every CPU: each processing unit can rapidly access its own memory without interference and without the overhead incurred with trying to maintain cache coherency.

- Difficult programming: the programmer is responsible for many of the details associated with data communication between processors.

- Communications speed: all CPU communication passes through the interconnection network that is slower than memory bus or dedicated core interconnections. The intercommunications latency is bigger than a shared memory system.

4.2. High Performance Computing

The maximum level of parallel programming and computing identify the High performance computing (HPC) which is the field that uses supercomputers and computer clusters to solve complex computational problems or huge domain problems or a combination of these two which are called advanced computation problems.

Today, computer systems approaching the teraflops-region are considered HPC-computers. Flops is the acronym for FLoating point OPerations per Second and it is a measure of a computer's performance, similar to the older and simpler instructions per second (IPS) but more indicative especially in scientific calculations that make heavy use of floating point numbers.

Using supercomputers implies a different approach to programming and the use of advanced programming languages, paradigms and techniques that are focused to use the supercomputer's architectural computational power.

There are different standard library interface specifications that allow programmers to write code for supercomputers. One of these is MPI, Message Passing Interface. MPI addresses primarily the message-passing parallel programming model, in which data is moved from the address space of one process to that of another process through cooperative operations on each process. Extensions to the "classical" message-passing model are provided in collective operations, remote-memory access operations, dynamic process creations, and parallel I/O.

MPI is a specification, not a language, and there are multiple implementations of MPI: all operations are expressed as functions, subroutines, or methods, according to the appropriate language bindings, which for C, C++, Fortran-77, and Fortran-95, are part of the MPI standard. The standard has been defined through an open process by a community of parallel computing vendors, computer scientists, and application developers.

The MPI standard allows portability and ease of use. In a distributed memory communication environment in which the higher level routines and/or abstractions are built upon lower level message-passing routines the benefits of standardization are particularly apparent. Furthermore, the definition of a message-passing standard

like MPI provides vendors with a clearly defined base set of routines that they can implement efficiently, or in some cases provide hardware support for, thereby enhancing scalability.

Key features of MPI standard are (mpi 2.2 report, 2009):

- Design an application programming interface.

- Allow efficient communication: Avoid memory-to-memory copying, allow overlap of computation and communication, and offload to communication co-processor, where available.

- Allow for implementations that can be used in a heterogeneous environment.

- Allow convenient C, C++, Fortran-77, and Fortran-95 bindings for the interface.

- Assume a reliable communication interface: the user need not handle difficult situations with communication failures. Such failures are dealt with by the underlying communication subsystem.

- Define an interface that can be implemented on many vendor's platforms, with no significant changes in the underlying communication and system software.

- Semantics of the interface should be language independent. The interface should be designed to allow for thread safety.

4.3. HIRESSS code

HIRESSS, HIgh REsolution Slope Stability Simulator, is developed with these main technical characteristics:

- Speed: code running time is crucial in a forecasting system for civil protection purposes.

- Portability: the code has to be usable by different machines and on different operating systems.

The code is written in C++ in conjunction with Open-MPI paradigm for the parallelization management. This coupling guarantees the portability of the code, because only different compilers are needed to make an executable file for different operating systems or machines. This is a characteristic that differentiates HIRESSS from tools dependent on an existent platform (ARCgis, Matlab,...etc). Moreover, the speed of the HIRESSS is free from the heavy programming mechanism of a platform that must be multi purpose. The languages C++ and the paradigm Open-Mpi are also supported by the majority of supercomputing centers, making the software porting easier. Usually in scientific computation fields the most widely used language is Fortran, the friendliest for managing many mathematical operators and usually considered faster than other programming languages, but it was preferred to develop HIRESSS in C++ for a better integration with a possible civil protection warning system. Usually C++ is the main language for multi purpose software, not only computational oriented, and it is the main reason for this choice. Moreover, at this moment the speed gap from Fortran is not so sensible. The supercomputing diffusion and better compilers have equaled the theoretical speed of two languages, even if there is still some unfriendly management of usual mathematical operations.

HIRESSS code is an approximately 5000 row code, 2500 of those are the computational core.

4.3.1. General structure

The general operation structure is illustrated in figure 4.7. HIRESS is organized in two principal blocks: the initialization and the computation.

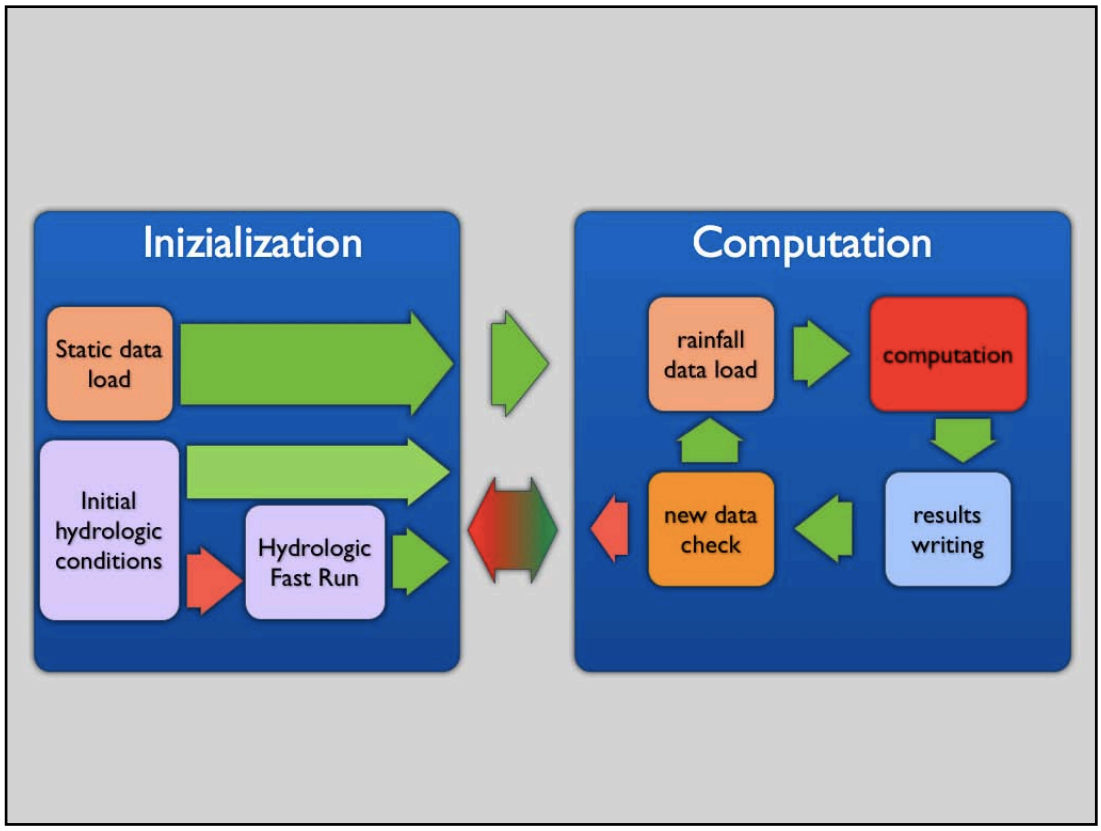

Figure 4.7: the functional diagram of HIRESSS (HIgh REsolution Slope Stability Simulator).

The initialization prepares the computation phase. The geotechnical and morphological data are static data because they do not change during the running of the simulation, therefore, they need to be loaded only once. At the same time, the hydrological initial condition is loaded, in terms of pressure head value, if available. If the value of pressure head is not available directly, it is possible to evaluate the initial condition from measured rainfall data. This is called "Hydrologic Fast run" because only the hydrological engine of HIRESSS is started, in a light form. Any intermediate results are not written on disk and only the final computation is written and passed to the computational phase. The hydrologic fast run is the 6% of a complete computation block running time for the same forecasting periods and temporal resolution. In this way it is possible to reconstruct the initial condition from a rainfall data at the same resolution of the rainfall data used in the evaluation of the factor of safety (FS).

The parallelization is very deep in the initialization phase. The number of static files read are eleven and they are loaded contemporarily by the first eleven CPUs if the processing units available are more then 11. The loading data is divided and balanced between processors if the CPU number is less then data files. This

technique is possible if the I/O architecture is strongly parallel because contemporary access is needed at the stored data. Using a supercomputer the data loading is up to 90% faster than a serial file reading. Unfortunately, a multicore personal computer or workstation does not have any benefits with a standard I/O system, in most cases it can increase the loading time up to 10% more than a sequential loading.

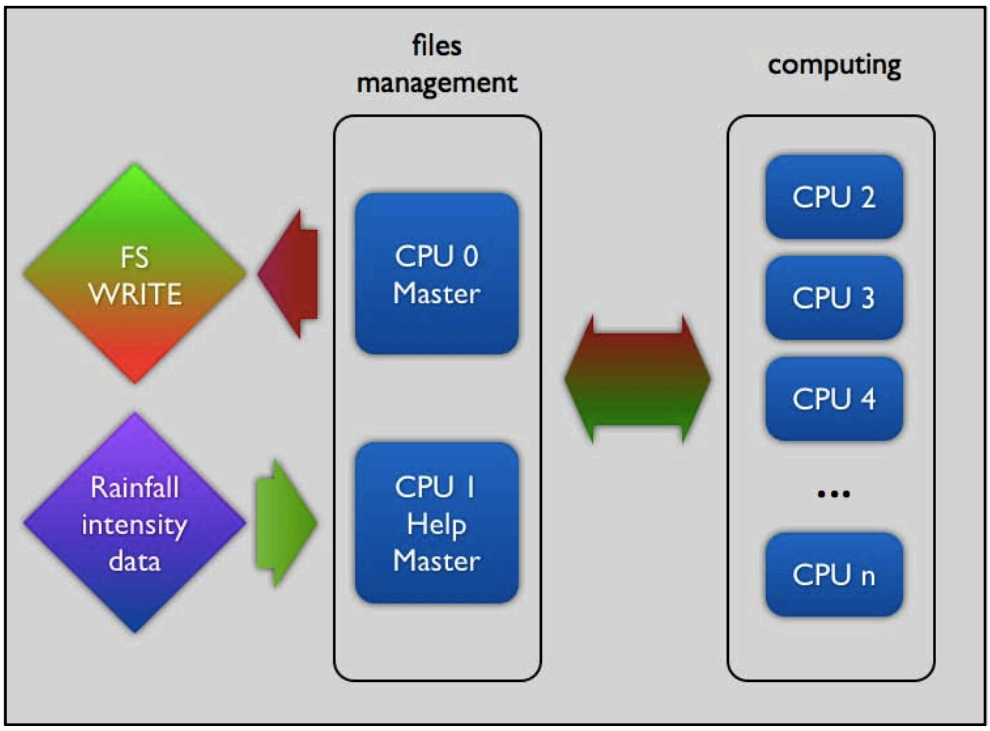

Figure 4.8: the functional diagram of the parallel data management ("multisave" function).

The computing phase infers the dynamical data, the rainfall input. This files represents the data that changes with the time: they can be forecasted rainfall intensity or real time measurements, in each case are data updated continuously or at fixed time interval. A first rainfall file is read and used to evaluate the FS by the computational core, then the results are written in an ASCII GRID map. Afterwards, a routine checks if there is new rainfall intensity data files and if there is a new sure initial condition. If the system receives new information about the initial condition, for example when the rainfall analyzed in the computation is forecasted data and a measured intensity is available that corrects the forecasted estimation, a hydrological fast run is started that updates the actual hydrological condition. If there is no initial condition update but only new intensity rainfall files the system queues the new data to processing and then the cycle starts again. A typical simulation of one day

forecasting or analysis with a temporal resolution of one hour consists of a twenty-four repetition of the computing phase.

In the computational phase the parallelization is the key for speed and occurs at various level. First, the domain of data, the analyzed area, is divided for the CPU numbers available, and it is passed to each computing processor memory; the evaluation of FS is independent between each processing unit. Two CPUs, “master” and “help master” are dedicated to managing the reading and writing of data (figure 4.8). The “master” CPU collects the calculation results that is written on disk, and at the same time the “help master” reads a new rainfall intensity and distributes the new data above the “computing” CPUs. In this way reading and writing are done contemporarily and clearly, if the physical data system can support it, the running time is reduced. The “computing” processor does not have to wait until the results are written and they can start to evaluate the next time step of simulation. This choice is also required because the reading and writing on physical support are relatively slow on a supercomputer, even slower than a common workstation, but are strongly parallel. The key of reading/writing speed is to take advantage of the parallel architecture of physical disk I/O. The execution time difference in a typical run[11] between a serial sequential read /write procedure and a parallel strategy (figure 4.7) can be up to 20%.

4.3.2. Computational core structure

The computational schema is illustrated in figure 4.9 and it is the cycle executed for each pixel of the area extension. First, the hydrological model is evaluated at different depths starting from the maximum soil depth. The pressure head computed results are inserted into the Montecarlo simulation that evaluates the pixel stability at the respective depths. The stability model gives the mean value of the factor of safety and the probability of instability (see chapter 3.3) at different depths which are compared and the minor value is taken. Then, the two results and the respective pressure head are passed to the “master CPU” and written on a physical disk.

The Montecarlo simulation needs a random number generator to pick casual values from the probability distribution of the input parameter.

---

11 Run is a computational technical term that indicate a complete execution of a code.

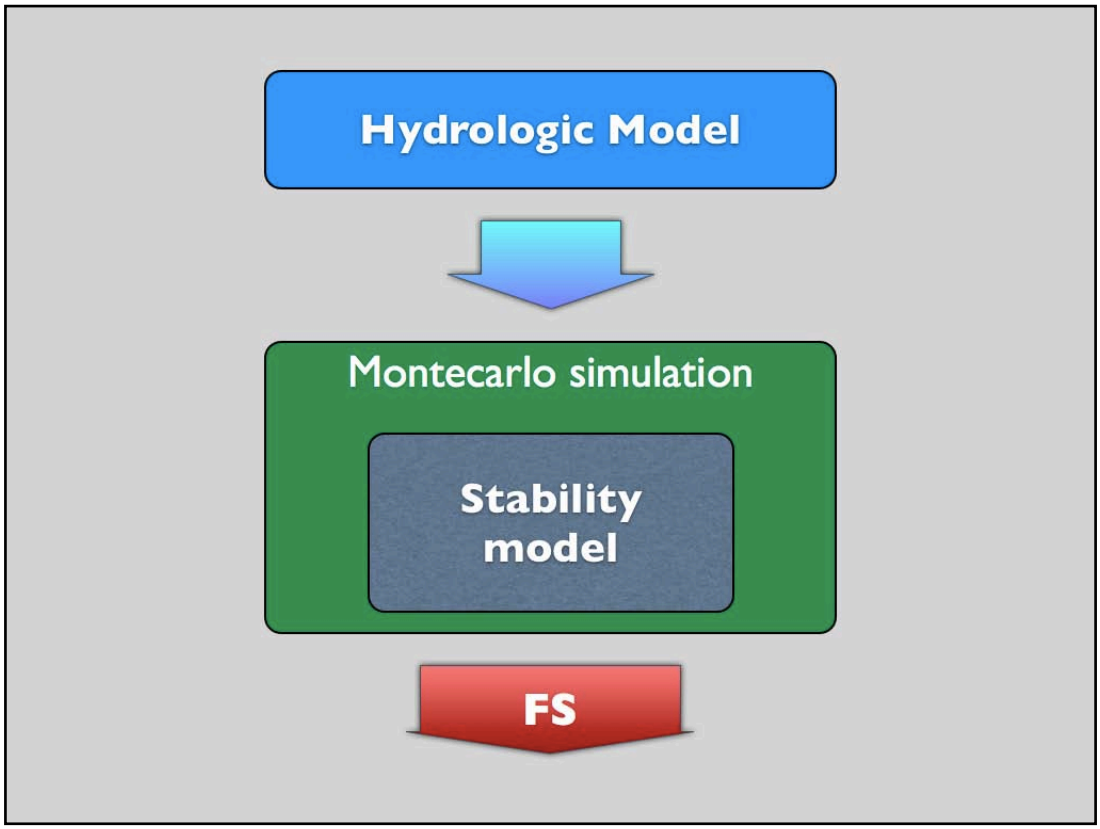

figure 4.9: functional diagram of the computational core.

A random generator library is used, for C++ that has these characteristics (Agner, 2008):

- Mersenne Twister: very good randomness and very long cycle length.
- High resolution.
- Support for multiple threads and multiple streams: helps parallelization.
- Fast and efficient: it is important that the parameters' pick up do not affect the computation time.
- Allow seeds of any length.
- Discrete uniform distribution over arbitrary interval is exact where other implementations have rounding errors.

- Continuous distributions supported: Uniform and normal.

- Discrete distributions supported: Uniform, Poisson, binomial, hypergeometric and various non-central hypergeometric distributions.

The Marsenne twister is a pseudorandom number generator developed by Makoto Matsumoto and Takuji Nishimura. It provides a fast generation of very high-quality pseudorandom numbers, having been designed specifically to rectify many of the flaws found in older algorithms (Matsumodo M. et al., 2008). Its name derives from the fact that period length is chosen to be a Mersenne prime: the randomness cycle is 2^{19937}-1 long. The sequence of random numbers is set up by the seed of the generator: a same seed generates an identical sequence of casual parameters. To avoid randomness problems, the seed is assigned differently by each processor and for every time step. When a CPU starts a Montecarlo simulation phase, it takes a seed equal to the system time at that instant. In this way every CPU has different seeds, because each execution's thread time is different and independent.

4.3.3. Operating procedures

HIRESSS is a terminal commands based software. There is no graphical interface because is not useful in a supercomputer environment. To start the software it is necessary to submit a string of commands and parameters:

mpirun -np <number of CPU> <HIRESSS executable> <static data folder> <initial condition folder> <Rainfall intensity folder> <results folder> <timestep> <shoots> <layer depth> <results saving methods> <Hydrologic model> <Diffusivity multiplier> <results probability methods> <Parallels files managements>

where the single parameters mean:

<number of CPU>: the number of CPUs that will be used in the simulation. It is an Open-MPI needed parameter to starting a parallel code execution.

<HIRESSS executable>: the name of the executable. Usually it is the name of the code with a suffix number version (ex. HIRESSS_1_0_0).

<static data folder>: the path of the folder that contains geotechnical and morphological static data.

<initial condition folder>: the path of the folder that contains initial condition data, initial pressure head or past rainfall data used to complete a fast run.

<Rainfall intensity folder>: the path of the folder that contains the rainfall intensity data, forecasted or real-time measured

<results folder>: the path of the folder where the results are stored

<timestep>: the time step of the simulation, expressed in seconds (integer). The time step is fixed by the period regarding rainfall intensity data. If the data intensity is referred to an hourly period then simulation time step is 1 hour.

<shoots> : the number, integer, that regulates the try cycles of Montecarlo simulation and consequently regulates the accuracy of results (chapter 3.3). Default is 100.

<layer depth> : an integer that sets the number of the intermediate depth where the model is evaluated. The depth of bedrock value is equally divided by the number of layers chosen.

<results saving methods>: a string parameter. It allows to save the pressure head value map beyond the FS and the probability of failure map. The parameter is “FS_yes” to save all three sets of data. Avoiding saving the pressure head results can save some running time.

<Hydrologic model>: a string that regulates the modeling of Hydraulic diffusivity. It is used only for testing purposes, and usually must be set to “idro_model_yes”.

<Diffusivity multiplier>: a multiplier of the hydraulic diffusivity (float). The default value is 1. It is possible to compensate the behavior of the stability model changing this value after a back analysis evaluation. A higher value accelerates the response at rainfall.

<results probability methods>: it is possible to choose two different methods to evaluate the failure probability. One is based on Gaussian distribution("prob"), the second is simply a counting of times that the FS, computed during the Montecarlo simulation , is under the stability thresholds (prob2).

<Parallels files managements>: this parameter allows parallel file management. Multiple read/write operations are possible only with specific hardware. Supercomputers boost the run time performance as said in chapter 4.3.1 and 4.3.2. The string value can be "multisave_yes" or "multisave_no".

An example string can be the following:

```
mpirun -np 8 HIRESSS_1_0_0 static initial rain results 3600 1000 3 FS_yes idro_model_no 10 prob2 multisave_yes
```

4.4. Parallel computing hardware used

There are two hardwares used to develop and test HIRESSS: a desktop workstation and a CINECA supercomputer.

CINECA is a non profit Consortium, made up of 46 Italian universities, The National Institute of Oceanography and Experimental Geophysics - OGS, the CNR (National Research Council), and the Ministry of Education, University and Research (MIUR). Today, it is the largest Italian computing centre, one of the most important worldwide. With more than three hundred and fifty employees, it operates in the technological transfer sector through high performance scientific computing, the management and development of networks and web based services, and the development of complex information systems for treating large amounts of data.

Access to the CINECA supercomputing facilities, like all the HPC resources, are computational time limited therefore, for the development it was preferable to use a workstation UNIX based. The development needs continuous testing and running of the code so having a testing machine available was very useful. Some code parallel

features are not usable on this workstation due to a non parallelized access to the physical disk: if used, the running time rises.

4.4.1. Apple Mac Pro

The workstation is an **Apple Mac Pro**, a shared memory architecture machine (see chapter 4.1.1), with the following characteristics:

- Operating system:Mac OSX 10.6
- CPU: two quad-core Intel Xeon 2.8 GHz (8 computational cores)
- RAM: 14GB DDR2 800 MHz ECC
- Disk space : 250 GB SATA 7200 rpm

Figure 4.10: the Apple Mac Pro

4.4.2. CINECA SP6

The supercomputing CINECA hardware used is an **IBM pSeries 575**, codename SP6, that was ranked at the 46th of the TOP500 (TOP500 List - June 2009). The TOP500 project was started in 1993 to provide a reliable basis for tracking and detecting trends in high-performance computing. Twice a year, a list of the sites operating the 500 most powerful computer systems is assembled and released. The best performance on a common benchmark, Linpack, is used as performance measure for ranking the computer systems. The list contains a variety of information including the system specifications and its major application areas.

The supercomputer SP6 has these main characteristics:

Figure 4.11: the SP6 supercomputer tower shelfs.

- Architecture: IBM P6-575 Infiniband Cluster
- Processor Type: IBM Power6, 4.7 GHz
- Computing Cores: 5376
- Computing Nodes: 168
- RAM: 21 TB (128 GB/node)

- Internal Network: Infiniband x4 DDR
- Disk Space: 1.2 PB
- Operating System: AIX 6
- Peak Performance: 101 TFlop/s
- Available compilers: Fortran90, C, C++
- Parallel libraries: MPI, OpenMP, LAPI

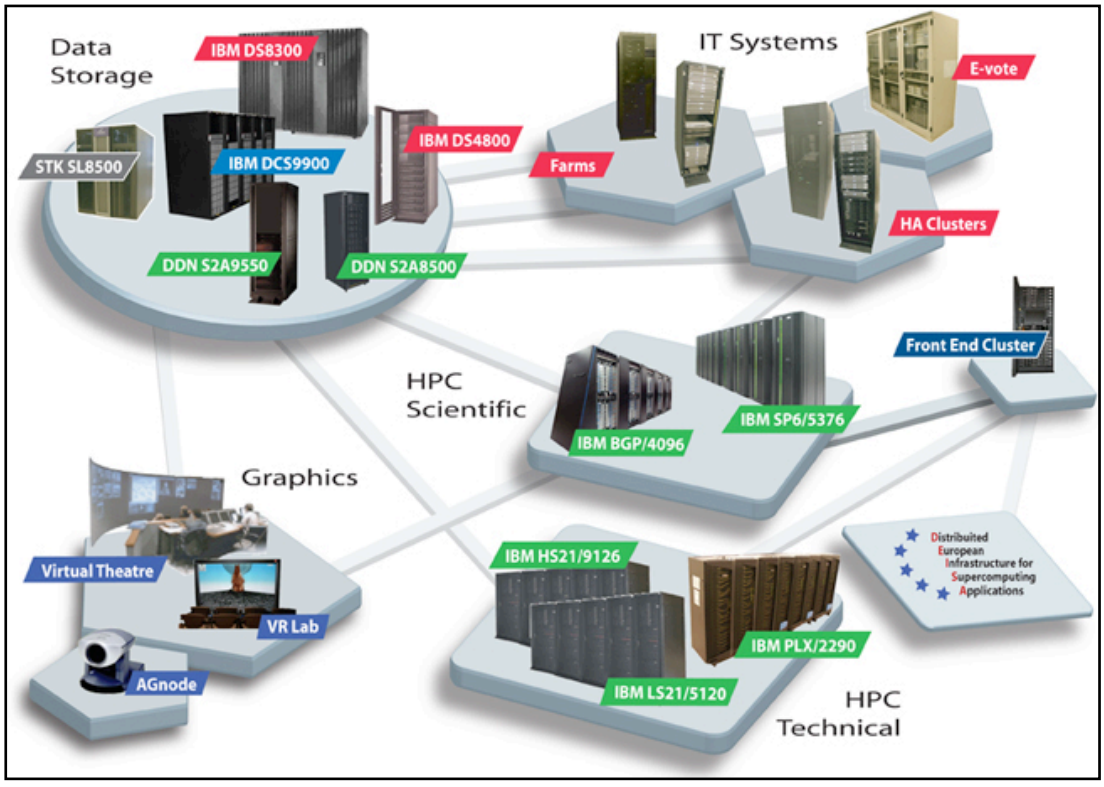

Figure 4.12: Diagram of CINECA hardware resources.

5. Test areas and input data collection

5.1. Armea basin

The Armea basin is located in the western part of the Liguria region, in the province of Imperia, not far from the border between Italy and France.

This basin has an extension of 38 km^2 and is entirely encompassed in the municipality of Ceriana and Arma di Taggia. The Armea stream begins in the Maritime Alps and flows into the Ligurian Sea with a total length of 16 km. In the northern part of the basin the watershed represented by the M. Colletazzo (1233m). M. Alpicella (1238), M. Merlo (10013) while in the western part there is the Punta Lodiro (1083), M. Bignone (1299) and M. Colma, and in the eastern part Punta Pistorin (483) and M. Santa Maria (463).

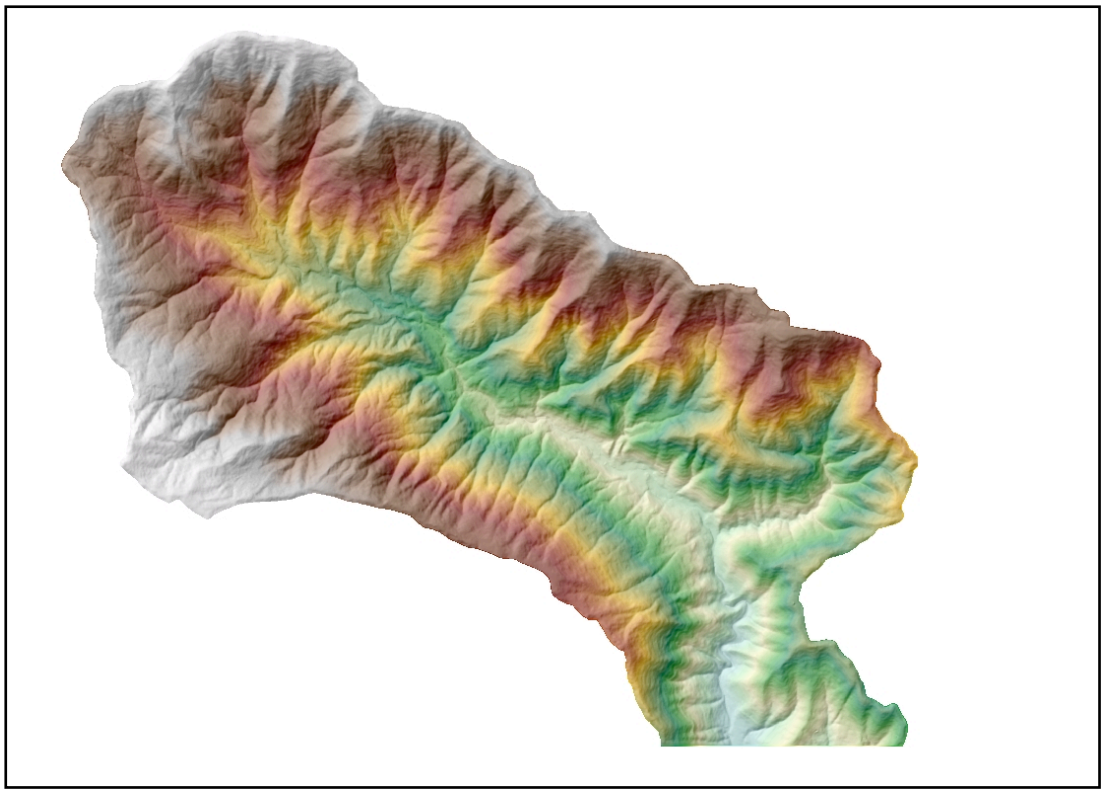

Figure 5.1: The Armea basin area.

Figure 5.2: the Amea basin geographical location.

The studied area is not the entire basin, but solely the middle and upper part for a total extension of 33 km^2. This part has been chosen because it is characterized by a mountainous morphology, consolidated bedrock and frequent occurrence of shallow landslides.

The test site is located in Liguria, a Region in Northwestern Italy, south of the Alps (figures 5.1 and 5.2). Meteorological conditions change at a local and regional scale due to localized storm cells or to regional cyclonic conditions. The latter is the case when moving from the Alpine–pre-Alpine sectors to the Tyrrhenian coast. Average annual precipitation ranges from 750–1250 mm in the west to 1350–1850 mm in the central and eastern parts of the Region.

Due to the geographical location and to the morphological and geological setting, landslides are frequent in Liguria. According to Italian archives of historical information on landslides and floods, in 1806 landslide events damaged 1,233 localities during the period 1800–2001 in the four Provinces of the Liguria Region. This historical information revealed that damaging events occurred most frequently in the rainy season, during the period from September through December, in all four Provinces. A strong control on soil slips is the presence of a shallow bedrock. A peculiarity of some failures is represented by the presence of old dry stone walls, completely covered by colluviated material, associated with the slide scar.

Landslides are quite a recurrent phenomenon: they are prevalently represented by soil slips, soil slumps and soil slip-debris flows. These landslides are the cause of economical losses and sometimes even casualties. They damage crops, settlements and pose hazards to people's safety. Soil slip-debris flows are gravity-induced mass movements and are one of the most hazardous natural phenomena. Their considerable hazard potential is related to the abundance of susceptible areas, the high areal density and the high velocity of the movements. These shallow landslides can be triggered by rainstorms of high intensity and short duration or by prolonged rainfall of moderate intensity. The area considered in this project has been affected by several rainfall-induced landslide events in the last decade. In November 2000, a high-intensity winter storm hit the coast of the Ligurian Sea. Damage was particularly severe in the Province of Imperia where landslides caused three fatalities and severely damaged infrastructure, private homes, agriculture, and the flower industry. Landslides were most abundant in Ventimiglia, near San Remo, and in the

Armea and Argentina valleys. Soil slips were also reported near Mentone, in France. After the event, 1024 rainfall induced landslides were inventoried in an area of about 500 km^2.

Landslides triggered by the high-intensity rainfall were both shallow and deep seated. Shallow landslides were mostly soil slips and debris flows. Most of the soil slips mobilized into debris flows. Debris flows travelled long distances (up to 1.5 km in the Armea valley), involving considerable volumes of material.

5.1.1. Geological setting

This sector of the Ligurian Alps chain has been widely studied in the past and many papers have been written about the evolution of each single geologic formation. As a support during the field work and during the following parametrization of the soil properties, a geologic map (scale 1:10,000) was used. This map was produced by researchers of the University of Pavia during their fieldwork for the basin plan called "Piano di Bacino del Torrente Armea e del Rio Fonti". This geologic map was carefully checked during the fieldwork conducted for this PhD thesis and some minor changes to the exact position of a few boundaries between formations have been added. The results are shown in figure 5.3.

In the Unit of Sanremo-Monte Saccarello from the bottom to the top the following geologic formations are included:

- Formazione di San Bartolomeo: this formation, also known as "Argilliti del Colle S. Bartolomeo", is composed of marine basin sediments characterized by a low sedimentation rate, mainly turbidites and hemipelagic sediments. The outcrops of this formation are located within the core of the anticline that characterize the structural setting of the middle Armea basin. This formation is in stratigraphic contact with the chaotic facies of the Ventimiglia flysch (Complesso di Progressione della Falda del Fly- sch ad Helmintoidi) on the bottom and with the Arenarie di Bordighera formation on the top. The lithologies are mainly quartzose-micaceous sandstones and brown-green pelites with manganese and iron oxides. In the upper part red and green clays, quartzose sandstone and thin layers of calcareous turbidites

appear. The age is Late Campanian - Barremian. The exact thickness of this formation cannot be estimated due to the intense tectonic deformation.

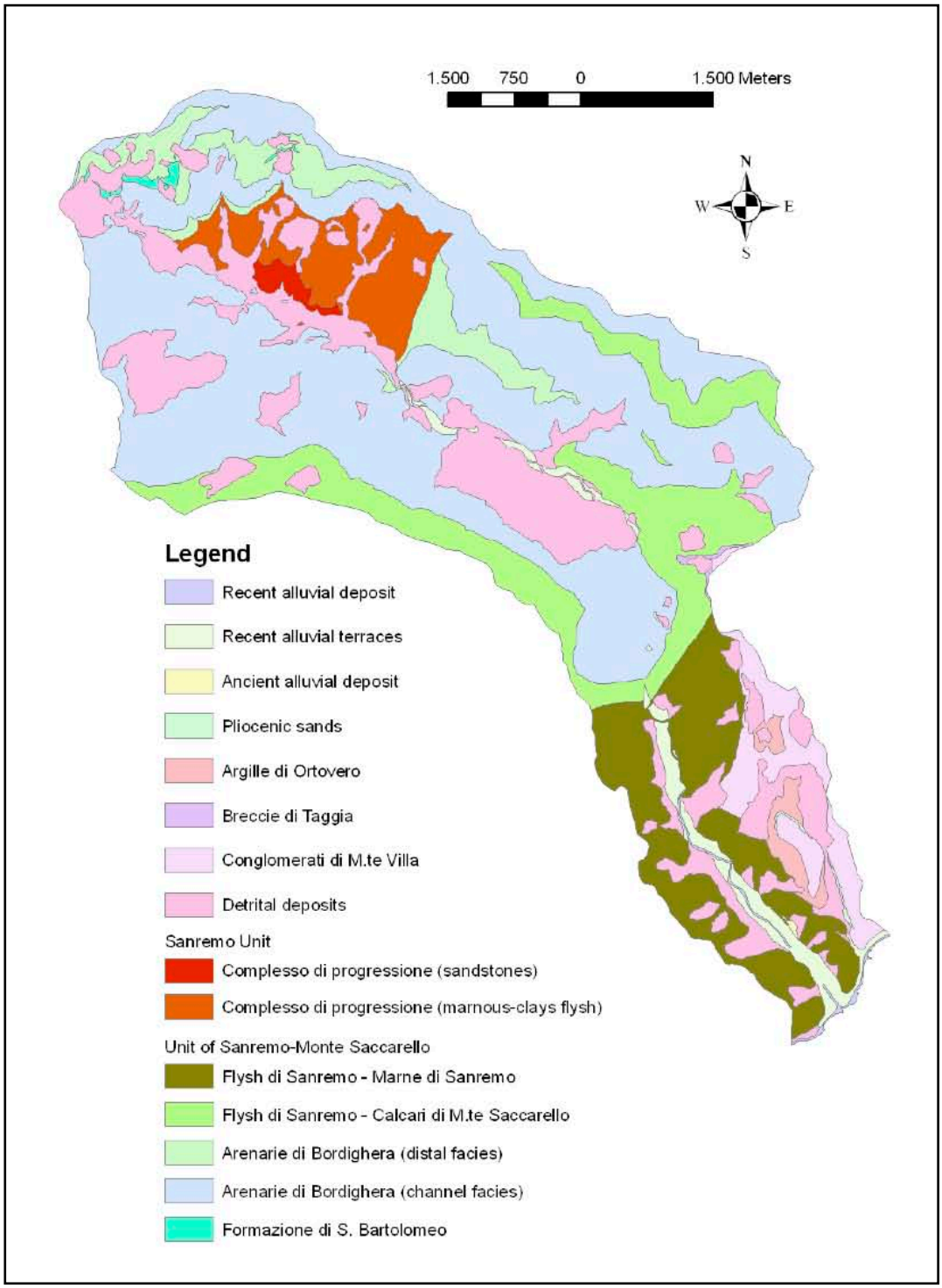

Figure 5.3: Geologic map of the Armea basin.

• Arenarie di Bordighera: this formation has been divided into two different sedimentary facies, a distal facies and a channel facies. The first one represents the distal part of a turbiditic submarine conoid (Sagri, 1980). This

facies crops out pervasively in the Armea basin with alternating thin turbidites and hemipelagites. The thickness of these layers varies between 5 cm and 30 cm. Lithologically it is composed of marnous limestone and calcareous marls with Helmintoides and Chondrites traces alternating with calcarenites, quartzose sandstone and micrites. The era has been attributed to Late Campanian and the maximum thickness in this area is about 50m. The second facies of the Arenarie di Bordighera formation are sedimentary deposits that can be related to the proximal part of the submarine conoid. This facies is composed of coarse channelized deposits with sandstones, conglomeratic sandstones, conglomerates and massive sandstones. Turbidites of varying thicknesses can be found intercalated between the proximal fan deposit, especially in the upper part of the formation. The passage to the upper formation is gradual and signed by the progressive increase in the marnous-calcareous layers. The era of this second facies is Late Campanian - Maastrichtian and the total thickness is between 400m and 500m.

- Calcari di Monte Saccarello: this formation is included in the group of "Helmintoides Flysch". The depositional environment was a narrow basin with high sedimentation rates below the carbonate compensation depth (ccd). Lithologically it is composed of marls and calcareous sandstones (lithofacies "b" of Sagri, 1984) with minor calcilutites and arenaceous turbidites. The main outcrops are located along the ridge on the southwestern part of the basin. The passage to the upper formation is gradual and signed by the progressive increase of the marnous-calcareous layers. The age of the Calcari di Monte Saccarello formation is Late Campanian - Maastrichtian and the maximum thickness is about 300m.

- Marne di Sanremo: this formation is composed of arenaceous and clay layers (lithofacies "d" of Sagri, 1984) with minor intercalations of calcilutites and arenaceous-marnous layers. Interlayers are constituted of silt and clay with thickness up to few decimeters. The age is Maastrichtian.

In the Delfinese-Elvetico-Provenzale Domain (Sanremo Unit) only one formation is included:

- Complesso di progressione della Falda del Flysch ad Helmintoidi: this formation represents the chaotic facies and stratigraphically higher, of the Ventimiglia Flysch formation. It is composed of marnous-clays olistostromes with sandstones and some detrital extra-basinal clasts included. The chaotic appearance is due not only to synsedimentary reasons but also to the intense tectonic deformation that occurred and especially to the final overthrusting of the Unit of Sanremo-Monte Saccarello. Outcrops of this formation are visible only in the tectonic window known as “Finestra tettonica di Ceriana”. The total thickness in unknown and the era is Priabonian.

The Quaternary Deposits present the area are:

- Alluvial terraces: these deposits are terraced embankments of loose material adjacent to the sides of the river valley. The granulometry of these sediments is heterogeneous with gravels, sands and silts. The gravels lithotypes are mainly sandstones and limestones. These terraces are often occupied by anthropic activities and different types of infrastructures. In the southern part of the Armea basin, not far from the coastline, these deposits can reach thicknesses of more than 20m, however, in the studied area, in the middle and northern part of the basin, the thicknesses are usually limited to a maximum of a few meters.

- Detrital deposits: these deposits are widely present in the Armea basin especially in areas occupied by the Arenarie di Bordighera formation (channel facies) where they can reach the thickness of more than 3m. They are composed of incoherent deposits with varying granulometry and composition that can be classified as eluvial deposits, colluvial deposits, paleolandslides and talus-debris slopes.

Lithotechnical area	Dry soil unit weight (N/m^3)	Friction angle (grade)	Hydraulic conductivity (m/s)
Recent alluvial deposit	22000	35	$1 \cdot 10^{-3}$
Recent alluvial terraces	20000	26	$2 \cdot 10^{-3}$
Ancient alluvial deposit	20000	27	$1 \cdot 10^{-3}$
Detrital deposits	20000	28	$1 \cdot 10^{-3}$
Pliocenic sands	21000	26	$1 \cdot 10^{-3}$
Argille di Ortovero	20000	20	$1 \cdot 10^{-6}$
Breccie di Taggia	21000	34	$4 \cdot 10^{-3}$
Conglomerati di Monte Villa	20000	30	$2 \cdot 10^{-3}$
Complesso di progressione (sandstones)	24000	27	$2 \cdot 10^{-4}$
Complesso di progressione (marnous-clays flysh)	23000	18	$3 \cdot 10^{-6}$
Flysh di Sanremo - Marne di Sanremo	24000	21	$3 \cdot 10^{-5}$
Flysh di Sanremo - Calcari di Monte Saccarello	24000	22	$2 \cdot 10^{-5}$
Arenarie di Bordighera (distal facies)	24000	27	$5 \cdot 10^{-4}$
Arenarie di Bordighera (channel facies)	24000	29	$8 \cdot 10^{-4}$
Formazione di San Bartolomeo	23000	27	$4 \cdot 10^{-5}$

Table 5.2: input parameters of the lithotechnical areas individuated in Armea basin.

5.1.2. Typical Landslides

The Armea basin is characterized by a widespread slope instability. The presence of many types of landslides, quiescent and active, is due to many reasons: the high slope gradients, the poor conditions of the bedrock, the widespread presence of detrital deposits and, especially in the northern part of the basin, to the bedding planes oriented in the direction of the slope.

The landslides occurred in the Armea basin are both deep and shallow with the latter being the most frequent. The deep landslides are usually characterized by a rotational-translational movement and can be classified as complex. Shallow landslides of the Armea basin are soil slip, soil slump, earth flow and debris flows. The majority of these landslides are located in the northern and central part of the basin, usually triggered by heavy rainfall events like those that occurred in November 2000 and in December 2006. Shallow landslide occurrence is a widespread phenomena throughout the basin and are usually located where the slopes are higher and the soil depth is between a few decimeters to one meter or more, independently of the lithology of the bedrock. Instead, deep landslides are located especially in correspondence to thick detrital deposit or where the bedrock alteration is quite deep and pervasive.

5.2. Ischia

The island of Ischia is located in the southern part of the Tyrrhenian sea, between 40°44’ North latitude and 13°56’ East longitude, 33 km from Naples. This island is 7 km wide from North to South and 10 km from East to West. The coastline is 39 km long and the total surface is 46 km^2.

The island of Ischia is a volcanic island even though the highest mountain, the Monte Epomeo (787 a.s.l.) is not a volcano but a horst of volcanic rocks uplifted by tectonic movements. The volcanic activity of Ischia has been characterized by small eruptions quite long in time between each other. The last one occurred in 1301 D.C. (the Arso eruption, a flow which reached the coastline in the eastern part of the island) while the previous occurred during the Roman age.

The island is divided into six municipalities: Ischia, Casamicciola, Lacco Ameno, Forio, Serrara Fontana and Barano. The total population is about 50000 but in the summer season it can increase up to 300000.

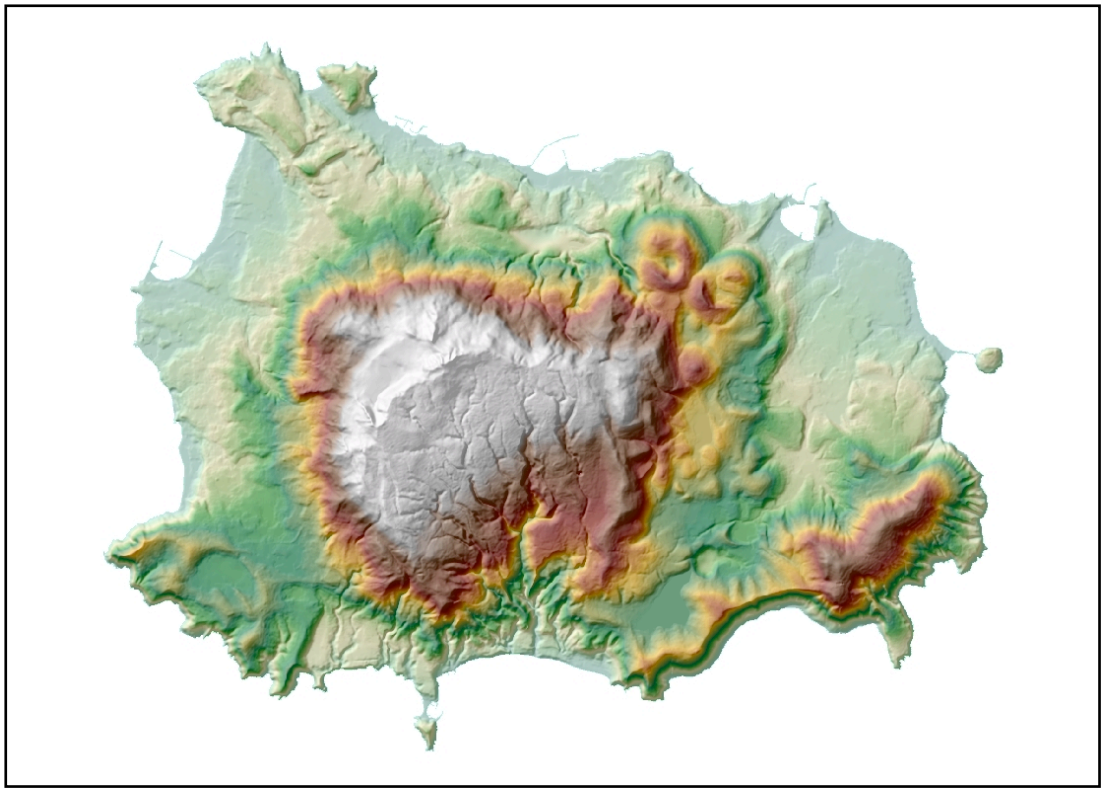

Figure 5.4: The Ischia island test area.

5.2.1. Geological setting

The geomorphological evolution of the island of Ischia is strictly related to its tectonic and volcanic activity and in particular to the development of the Monte Epomeo structural horst. The uplifting of this horst started about 30,000 years ago with an asymmetric movement that led to the development of different morphologies in different areas of island.

The southern slope of the Monte Epomeo horst, corresponding with the Fontana basin, is characterized by shallow detrital deposits derived from the superimposition of many debris flows, paleosoils and pyroclastic deposits (Bortoluzzi et al., 1983).

In the southern part of the Fontana basin more than one order of marine terraces can be recognized (Del Prete & Mele, 1999). A peculiarity of this basin is the dendritic drainage pattern with deep v-shaped valleys and widespread gully erosion.

The major vertical movements, due to the asymmetric uplifting of the horst, have taken place in the northern part of the island leading to the partition of the area in many isolated blocks bounded by slope faults. This area is characterized by a dendritic drainage pattern and a torrential regime.

The western sector of the island is similar to the northern one with sub-vertical slopes due to the fault movements and many fractured isolated blocks. Huge detritic deposits form an almost flat area characterized by slope angles lower than 10°. The drainage pattern is poorly developed in this sector with the only exception being the Corsare-Monterone torrent with many branches so as it can be classified as a second order stream.

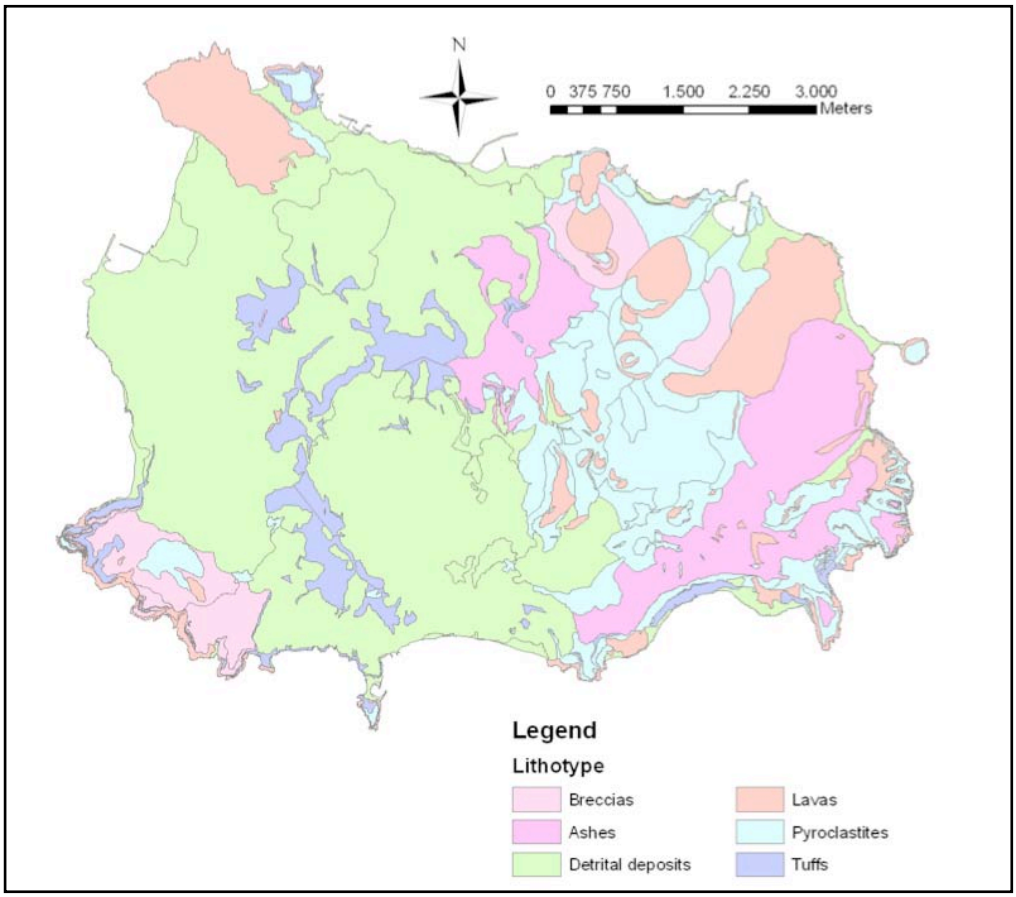

Figure 5.5: Schematic lithologic map of the Island of Ischia

The eastern part of the island is characterized by the presence of a near flat area, the Ischia graben, and it is limited towards South-East by the structural high represented by the Monte Vezzi, Monte Barano and Il Torone, towards West by the lava domes of Monte Trippodi and Costa Spariana, towards North- West by the

craters of Fondo Ferraro and Porto D'Ischia and the domes of Montagnone and Maschiata. All the geomorphological features presented in this sector are related to the volcanic activity and with the uprising of magmas through the main faults. The drainage pattern is poorly developed and often the streams don't reach the sea but flow into an endorheic basin.

Almost the entire island of Ischia is characterized by steep cliffs, up to 200 m high, for a total of 36 km. Locally, along the coastline it is possible to find small sandy and pebbly beaches, usually deposits of old landslides which occurred along the sheer cliffs behind.

Many areas of the island are obviously characterized by geomorphological features that can be related to the volcanic activity such as remains of old cones (e.g. Monte Vico and Monte Rotaro), craters (e.g. Campotese and Fondo Ferraro) and crater edges (e.g. Scarrupo cliff).

Lithotechnical area	Dry soil unit weight (N/m^3)	Friction angle (grade)	Hydraulic conductivity (m/s)
Pyroclastites	14000	19	$3 \cdot 10^{-4}$
Lavas	14000	37	$2 \cdot 10^{-6}$
Detrital deposits	14000	28	$2 \cdot 10^{-4}$
Tuffs	18000	26	$6 \cdot 10^{-4}$
Ashes	15000	36	$1 \cdot 10^{-6}$
Breccias	18000	25	$2 \cdot 10^{-4}$

Table 5.2: input parameters of the lithotechnical areas individuated in Ischia island.

5.2.2. Typical Landslides

For the Island of Ischia, the situation is more complex in respect to the Armea basin as fewer information is available. Prior to 2006, very little information regarding shallow landslides is available. These events certainly have occurred in the past as both the geologic and geomorphologic settings of the territory are very

similar to other areas in Campania, namely volcanic soils overlying steep massifs, where landslides have occurred frequently and with catastrophic effects. Moreover, many debris flows deposits have been found within the volcanic succession the same as geomorphologic evidences of deep landslide especially on the western side of the island and near Monte Vezzi (de Vita et al., 2006). However, as no precise documentation exists regarding earlier events it is not possible to create a comprehensive landslide inventory.

Accurate information exists only regarding the April 26, 2006 rainfall event that triggered four landslides and caused the deaths of four people. These landslides were inventoried and the resulting map has been used for validation. Radar rainfall data has been acquired from civil protection authorities.

5.3. Prato, Pistoia and Lucca province area

This test area is located in North-central Italy, in Tuscany, and includes part of the northern Apennines and has an extension of 3103 Km^2. This area has been chosen for a large scale test, it is 100 times bigger then Armea and Ischia test areas and it is more representative of a typical regional alert area. The resolution used to investigate this area is 10 meters square pixel, for a total of over 50 million of pixels.

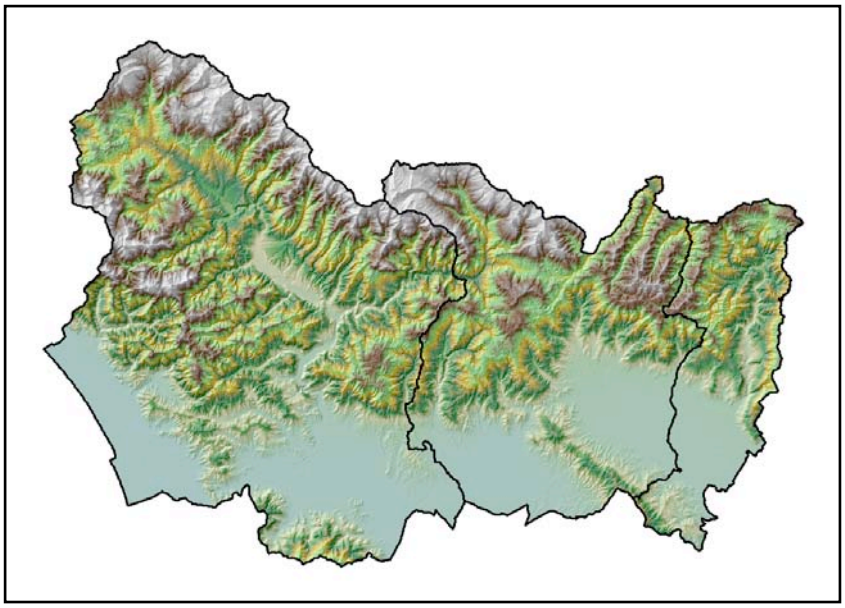

Figure 5.6: The Prato, Pistoia and Lucca province area.

This area is not only used as a potential verification and a computational stress test, but also for studying a methodology to collect data for a large regional area. In chapter 5.3.2 this important aspect will be analyzed.

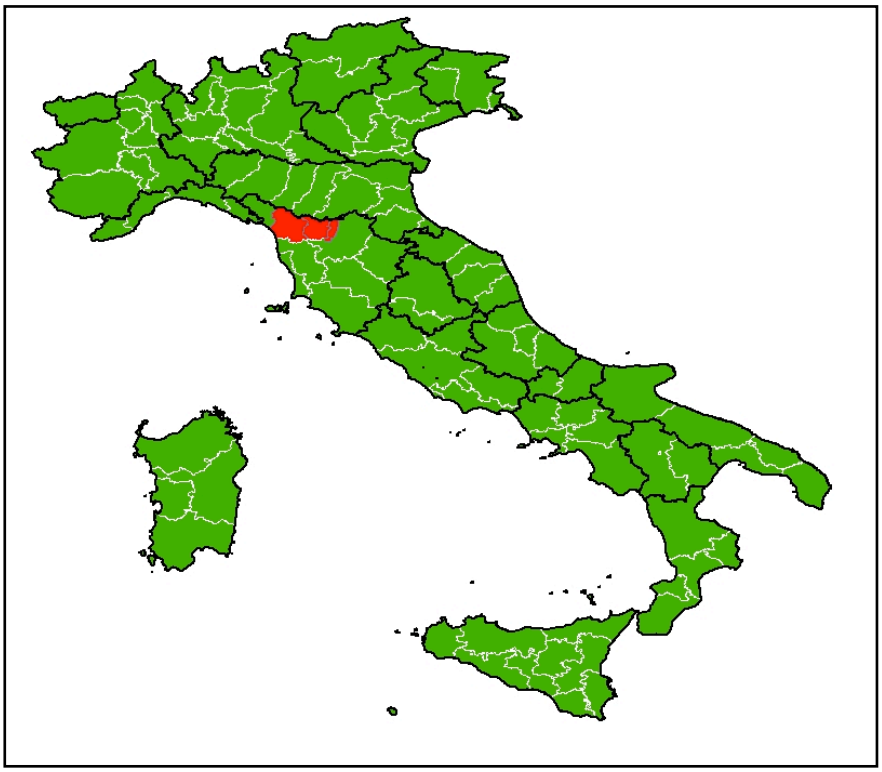

Figure 5.7: Geographic location of the Prato, Pistoia and Lucca province area.

5.3.1. Geological setting

The Northern Apennines is a complex thrust-belt system made up by the juxtaposition of several tectonic units, piled during the Tertiary under a compressive regime that was followed by extensional tectonics from the Upper Tortonian. The latter phase produced a sequence of horst-graben structures with an alignment NW-SE that resulted in the emplacement of Neogene sedimentary basins, mainly of marine (to the West) and fluvio-lacustrine (to the East) origin (Martini and Vai, 2001). Today, the morphology is dictated by the presence of NW-SE trending ridges where Mesozoic and Tertiary flysch and calcareous units outcrop, separated by Pliocene-Quaternary basins.

The inter-mountain basins formed from the Upper Tortonian (in the South-West) to the Upper Pliocene and Pleistocene (in the North-East). While the former experienced several episodes of marine regression and transgression during the

Miocene and Pliocene, the latter were characterized by a fluvio-lacustrine depositional environment and gave rise to the present typical Tuscan smooth landscape.

These geological settings clearly affect the typology and occurrence of surface processes, primarily through the differences in the mechanical properties linked to the various prevalent lithologies. On this basis six main lithotechnical categories can be distinguished, such as cohesive soils, granular soils, hard rocks, weak rocks, complex units with predominance of rock material and complex units with predominance of argillaceous material.

In particular the study area which is located in Northern Tuscany and it includes the provinces of Pistoia, Prato e Lucca show two different geological settings in the east and west sectors respectively.

In the west sector the ridges that divide the basins are usually made up of carbonaceous rocks with slope gradients of even greater than 60°, often subvertical or vertical. These slopes are usually rocky and with discontinuous vegetation, without forest. The carbonaceous rock faces are connected to the lower parts of the slopes, composed of metamorphic sandstone and phyllitic–schist, by talus and scree deposits. These slopes are usually moderately steep, especially in the intermediate areas (values ranging from 25° to 40°). There is, however, an increase in gradient in the lower slopes, as a consequence of the accentuation of erosive processes resulting from the Olocenic–Pleistocenic uplift of the Apuan metamorphic core.

The slopes are largely characterized by soils which typically cover the slopes underlain by predominantly phyllitic–schist and metamorphic–arenaceous rocks and are also mantled by dense forest (mainly chestnut). On the contrary, the calcareous and dolomitic slopes are usually rocky or with very thin soil cover. As shown below, the soils covering metamorphic sandstone and phyllite are usually the most involved in landsliding; these soils are rather thin (0.5–2 m thick).

The east sector shows a more uniform geological condition with the prevalence of flysch formation rock-type (Macigno) which is composed of quartz and feldspar sandstone alternated with layers of siltstone. The slope gradients varying from 0° in the plain and 55°. In the mid and upper sections of the valley, where most landslides usually occur, the stratigraphy consists of a 1.5 to 5 m thick layer of colluvial soil overlying the bedrock.

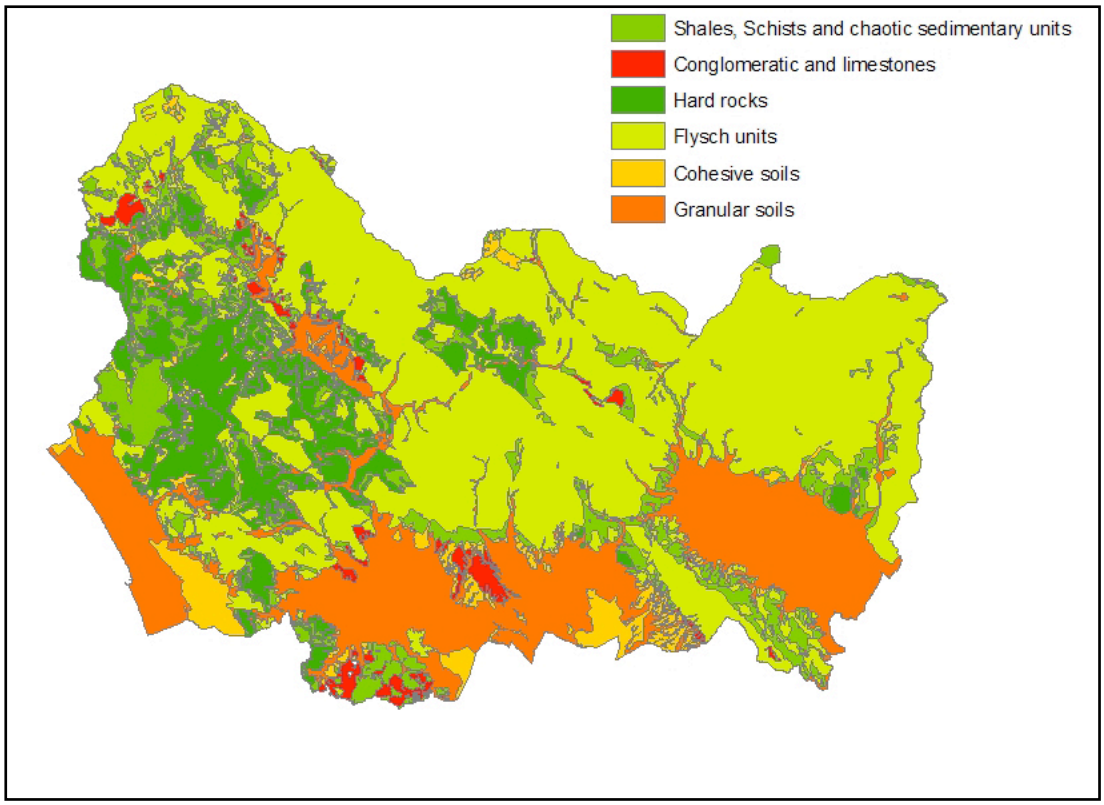

Figure 5.8: Schematic litohological map of the Prato, Pistoia and Lucca province area.

In Figure 5.8 is reported the litohological map of the area. In the south portion, mainly flat areas, cohesive and granular soils outcrop. In the East sector there is the predominance of flysh units, mainly complex units with predominance of rock material and complex units with predominance of argillaceous material. In the West sector there is the predominance of hard rocks, mainly phyllitic–schist and metamorphic–arenaceous rocks and secondarily shales, limestones and conglomerates.

5.3.2. Fieldwork

The provinces area of Pistoia, Lucca and Prato has been elected for a large fieldwork campaign of measurements.

There are two main problems to managing a large area with HIRESSS: the parameters incertitude value and the amount of measurements to be done.

HIRESS has the instruments to manage approximative and uncertain data but does not completely eliminate the need for field and laboratory measurements. The variation of the input data must be evaluated in order to provide Montecarlo

parameters that can allow less time for calculation. If the range of parameters incertitude is not too large, it is possible to obtain more accurate results employing less simulation shoots (see chapter 3.3). Moreover, the quantification of the field measures needed to run the simulation on a large scale is very important to plan a large scale fieldwork.

The measurements campaign proposed and executed is oriented to solve these two questions. After the identification of the soil lithotechnical classes from an analysis of lithological and geological 1:100000 chart, two series of measurements were planned: one to estimate the local range variation, a second to investigate the long range variation on the same lithotechnical area. The campaign was made up of 34 field measurements (figure 5.6).

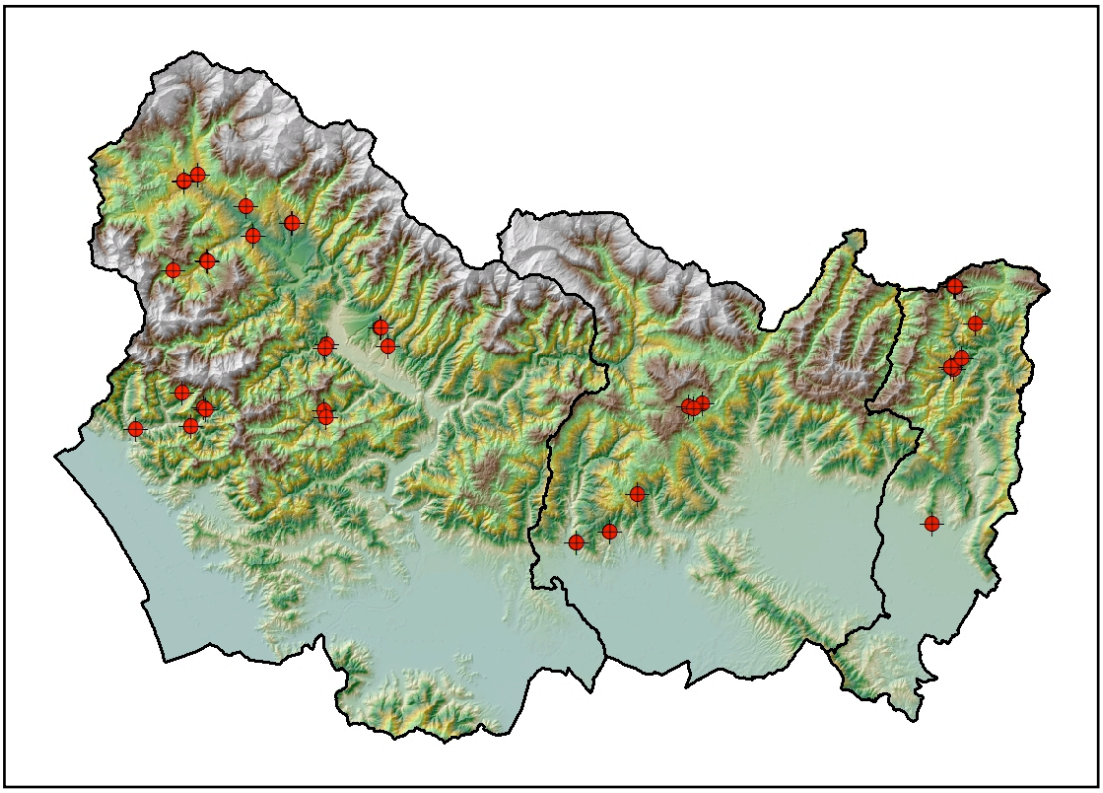

Figure 5.6: the distribution of the field measurements over Lucca, Pistoia and Prato province area.

The Shear strength parameters were evaluated in situ by using the Borehole Shear Test (BST, figure 5.7), obtaining values under natural conditions without disturbing the soil samples.

Figure 5.7: BST in situ measurements setup.

At the same depth as the BST, matric suction values were measured with tensiometers (figure 5.9). Saturated hydraulic conductivity within the unsaturated zone was measured in-situ using the Amoozemeter or Compact Constant Head Permeameter (CCHP) (figure 5.8).

Figure 5.8: Amoozemeter measurements setup.

The procedure used for measuring the hydraulic conductivity in the field is termed constant-head well permeameter technique (Philip 1985). Results were then entered into the Glover solution, which computes the saturated permeability of the soils. The measurements operated in situ are:

- Saturated hydraulic conductivity
- Friction angle
- Matric suction
- Soil water content

Figure 5.9: a tensiometer setup for matric suction measurements.

A sampling of soil was taken in each location to perform laboratory analysis and then to define the value of the other parameters used in the stability simulator, such as bulk density, porosity and grain size curve.

The local variation series of measurements was performed on the most extended lithotechnical area, the Flysch units, and the measurements points were in a range of 500 meters; at least two complete sets of measurements were executed for each

lithotechnical typology. The average and the maximum deviation was evaluated for all lithotechnical classes.

Analyzing the results it was possible to observe that the local variation of the measured parameters are comparable to the long distance ones. Moreover, the variation is almost consistent in value with the other lithotechnical classes.

These results permit a simplification of the input parameters assigning the same relative variation for each class of the entire area. Moreover, this characteristic is very important for large scale data collection. If the variation range can be considered as an intrinsic characteristic for any lithotechnical classes, it is possible to drastically reduce the number of field measurements and samplings needed to characterize each class.

The large area collecting campaign can be reduced to only a few measurements executed in different distant points in a same lithological class, making the work more time affordable. This is a possibility that will be extensively investigated in the future with more measurements.

Measured parameter	Average Value	Relative error
Friction Angle (grade)	38	20%
Hydraulic conductivity (m/s)	$3 \cdot 10^{-7}$	56%
Dry soil unit weight (N/m^3)	17000	21%

Table 5.3: local variation of the parameters measured in the Flysch units lithotechnical area.

Measured parameter	Average Value	Relative error
Friction Angle (grade)	34	15%
Hydraulic conductivity (m/s)	$6 \cdot 10^{-7}$	66%
Dry soil unit weight (N/m^3)	18000	15%

Table 5.4: long range variation of the parameters measured in the Flysch units lithotechnical area.

Lithotechnical area	Dry soil unit weight (N/m^3)	Friction angle (grade)	Hydraulic conductivity (m/s)
Shales, schists and chaotic sedimentary units	14000	35	$1 \cdot 10^{-6}$
Conglomerate and limestone	14000	30	$1 \cdot 10^{-6}$
Hard rocks	14000	32	$1 \cdot 10^{-7}$
Flysch units	18000	34	$1 \cdot 10^{-6}$
Cohesive soils	15000	29	$1 \cdot 10^{-6}$
Granular soils	18000	32	$6 \cdot 10^{-6}$

Table 5.5: input parameters of the lithotechnical areas individuated in the Pistoa, Prato and Lucca province area.

5.4. Input data

The input parameters can be divided in two classes: the static data and the dynamical data. Static data is a parameter that does not change during a simulation run such as geotechnical and morphological parameters. Dynamical data is an input that changes during the simulation, like rainfall intensity. Static data is read only once at the beginning of the simulation while dynamical inputs are continuously updated.

The static and dynamical data files are in ASCII GRID format to make the analysis and management easier because it is a well known standard for GIS softwares.

5.4.1. Static data

- Cohesion: the effective cohesion c' when the saturation condition is reached. Usually this is a low value chosen by literature values or laboratory test.

- Friction angle: this value is the result of in situ measurements (chapter 5.3.2).

- Slope: this parameter is computed from high resolution DEM (Digital Elevation Map) using GIS software. The DEM resolution usually sets the HIRESSS simulation results' resolution.

- Dry soil unit weight: this parameter, after an in situ sampling, is measured with laboratory test. Sometimes, depending on the test area, the value was chosen also from literature measurements.

- Soil depth: these parameters are the results of an empirical model developed at the Department of Earth Science in Florence and known as GIST (Catani et al., 2010). Several studies have shown that soil thickness is one of the most important parameters controlling shallow landslide initiation (Johnson & Sitar, 1990; Wu & Sidle, 1995; Van Asch et al., 1999; Segoni et al., 2010). The model is based on three morphometric attributes (slope gradient, slope curvature and position within the hillslope profile) and on geomorphological and lithological criteria. It is an empirical model that can produce distributed soil thickness maps at catchment scale with a high spatial resolution; it uses cheap and easily available data and gives a major importance to geomorphological and geological factors (Catani et al., 2010).

- Hydraulic conductivity: this parameter is measured in situ with Compact Constant Head Permeameter (chapter 5.3.2).

- Initial soil saturation: this parameter sets the initial condition of soil saturation. As discussed in chapter 4.3, the initial condition can be measured or computed from pluviometric data with a "hydrological fast run". This parameter can even be fixed by the operator for scientific analysis purposes.

- Pore size index distribution: in this work this parameter is evaluated and chosen by literature measurements and databases. (Rawls et al., 1982)

• Bubbling pressure: in this work this parameter is evaluated and chosen by literature measurements and databases. (Rawls et al., 1982)

• Porosity: this parameter is evaluated from laboratory measurements or from literature values, depending on analyzed area.

• Residual water content: in this work this parameter is evaluated and chosen by literature measurements and databases. (Rawls et al., 1982)

Parameters	Relative error
Cohesion	40%
Friction angle	20%
Slope	20%
Dry soil unit weight	21%
Soil depth	20%
Hydraulic conductivity	60%
Pore size index distribution	30%
Bubbling pressure	20%
Porosity	20%
Residual water content	30%

Table 5.6: the relative variations of each parameter considered in the Montecarlo simulation.

5.4.2. Dynamic data

Rainfall intensity is the only dynamical data used in HIRESSS. It is prevalently meteorological radar measurements, but during this PhD thesis work it was collected for future testing also by a pluviometer network.

- Armea basin Area: the rainfall intensity maps are measurements that come from the meteorological radar of Monte Settepani. The resolution of the maps is 1 Km.

- Ischia Island: the rainfall intensity maps are provided by the Italian air Force with the Grazzanise radar, near Naples. The resolution of the maps is 500 m

- Pistoia, Prato and Lucca province area: there are two available sets of rainfall intensity maps. The first set is an interpolation from automated pluviometers measurements of the Tuscan region network. The network updates the data every hour. The second set is a forecasted data of a 1 hour temporal resolution and 1 km spatial resolution. The data is provided by a meteorological model developed by CIRA (Centro Italiano Ricerche Aereospaziali).

6. Simulations Results and validations

HIRESSS performance was evaluated in the three test areas simulating historical events to estimate the reliability and the speed of the code. The objectives of the project are the spatial and temporal localization of an unstable area hit by rainfalls, and the computational time has to be compatible with a real time warning system for civil protection purposes. Clearly, good results are a compromise of the three factors of evaluation: an extremely precise spatial and temporal location is not useful to a warning system if it is ready after the triggering of a landslide. Moreover, the analyzed area is not a single slope deeply investigated and monitored with real time instrumentation. The simulator has to obtain useful results from data that is affected by large variability and incertitude.

The validation is not simple because of the lack of information regarding the shallow landslides positioning. It is very difficult to find an area where the landslides

are both spatially and temporally correctly located. Usually the problem is not related to the geographical positioning but to the temporal collocation. The spatial individualization is quite simple analyzing satellite images, but does not allow a precise temporal location because the data cannot be sufficiently updated: a satellite is not dedicated to observe a single area.

For this reason the HIRESSS validation is divided in three areas depending on available data. The spatial validation is performed in the Armea basin area, where the positioning of landslides comes from a satellite image, but with a large temporal incertitude. The temporal validation is performed in the test area of the island of Ischia, because a shallow landslide was correctly dated due to deadly consequences after the triggering. We do not have data regarding all of the island's landslides occurring the same day in order to also perform a complete spatial validation.

The third area, the larger, was used to test the code run time performance over a large area. This area will become the future testing area because it is the subject of a quite precise survey and reporting work on landslides. Moreover, it is possible to obtain real time and historical rainfall data measured from automated pluviometers and an hourly forecasting of precipitation intensity. In this work, the available data regarding an event at the end of december 2009 that triggered a huge amount of landslides but all correlated to a sudden snow melting. Unfortunately, this phenomena is not modeled in HIRESSS. The future data availability and quality, especially meteorological data, will be pushed to perform even a real time test, that is the best validation for a slope stability model.

6.1. Results and spatial validation

The spatial validation was performed in the Armea basin area simulating the event which occurred the day of December 6, 2006. This historical event wasn't extremely intense compared to typical events in this area, but the rainfall data available on that day was measured by the Monte Settepani radar: radar measurements are very high quality data compared to the satellite or pluviometric data. In table 6.1 all the data available for the simulation is summarized.

Rainfall data	Radar - 24 hours resolution 1 hour - spatial resolution 1 Km^2
DEM resolution	5 meters
Depth Layers	3
Montecarlo simulation shoots	1000
Initial soil saturation	< 20%

Table 6.1: Main characteristics of the Spatial Validation performed in the Armea basin area.

The simulation is a 24 hour forecasting simulation, with spatial resolution of 5 meters and temporal resolution of 1 hour. The results validation was performed in three different methods:

- Pixel by pixel landslide area: this method is the most arduous because it consists of comparing the pixel instability with the pixel that was actually involved in a landslide. It is hard to have a good performance because that means localizing a landslide with 5 meters of precision; the georeferentiation error can be comparable and it is only the most evident problem tied at this type of validation. However, it can be an indicator of the general behavior of the model.

- Aggregation by 1st basin order defined with Horton methods: it is a more reasonable method that consists of aggregating the results in a 1st basin order and then comparing basin to basin. The method is reasonable because it provides a stability evaluation of an area that will be quite homogeneous; moreover, the physical model does not take into account the parameters that can be determinant to trigger a landslide in a particular point and not in another only few meters away that has the same apparent characteristics. Therefore, the aggregation allows us to take into partial account the chaotic

components of real soil. Moreover, shallow landslides are very dangerous when they group and flow in the channels, so it can be useful to understand the stability situation of an entire micro-basin.

- Aggregation by 2nd order basin defined with Horton methods: the same methods with a higher aggregation area.

The probabilistic results are another HIRESSS characteristic that require a different validation approach. We do not have absolute results but a probability of instability. Therefore, a risk analysis will be needed to find the threshold levels of warning but in this work this type of study is not performed. However, reasonable thresholds were defined to evaluate and understand the results better.

Starting with the pixel by pixel landslide area validation, the single pixel was considered unstable if it reached the reasonable thresholds of 80% of instability probability. In the 24 hour simulation, if a pixel exceeds that threshold more then one time it is considered only once.

The landslides localized are 34% and the percentage of false positive, pixels that reach the instability in the simulation but will be stable, are 12%. If the false positive result is more deeply investigated and we count the times that the same pixel exceeds the instability thresholds, only 7% of them are unstable more than three times during the entire day. The results are summarized in table 6.2 .

Pixel by pixel validation (unstable pixel probability > 80%)	
Landslides correctly localized	34%
False positive (percentage of pixel unstable over stable area)	low probability: 5%
	high probability: 7%

Table 6.2: Pixel by pixel validation results.

The results are good considering the ratio true positive over false positive and the arduous validation method. Moreover, the landslide validation data refers to a larger period, because it was derived from a satellite photo that was taken some days after

the event. Therefore, it is not certain that all the landslides occurred in the simulated day, even if testimonies report most of them that day.

The aggregate validation, as said, is conceptually more reasonable. The pixel instability was evaluated with the same procedure of pixel by pixel validation, then, the results are aggregated in a small area defined from Horton methods: an area is considered unstable if more the 1% of them are over the 80% of instability probability. The average area of this 1st order basin is around 90000 m^2. The results are summarized in table 6.3.

In the contingency table four classes are presented:

- true-positive: the unstable area correctly localized by the simulation (hit).
- false-negative: the unstable area not localized by the simulation (miss).
- true-negative: the area correctly defined stable by the simulation (correct rejection).
- false-positive: the area that is stable but defined unstable by the simulation (false alarm).

It is possible to observe that the true negative and false positive are characterized by an instability probability. The probabilistic results of HIRESSS help the reliability of the results. We do not have a deterministic exact value, but a result that helps to quantify the level of instability. False negatives areas, the misses, do not reach the reasonable thresholds fixed in this validation to define them as unstable, but are characterized by an average and maximum instability reasonably higher than the stable areas. Reading the true negative and false positive stats, it is possible to state that the stable areas are correctly classified. In the figure 6.1 and figure 6.2 it is possible to see the graphical representations of the contingency table 6.3.

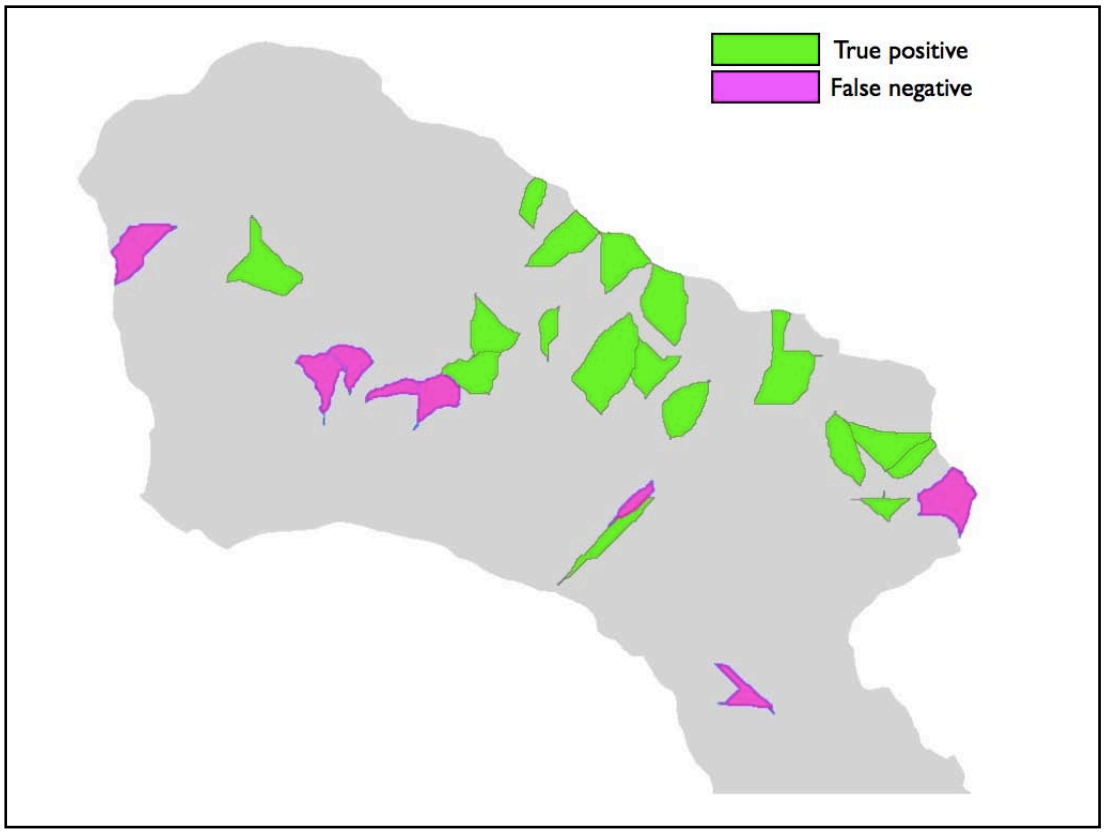

Figure 6.1: graphical results of the true positives (hits) and false negatives (misses) by 1st basin order aggregation.

1st basin order validation		
true positive	68%	
false negative	32%	average instability probability: 30 %
		maximum instability probability: 58 %
true negative	average instability probability: 4 % maximum instability probability: 22%	
false positive		

Table 6.3: validation results of 1st basin order aggregation.

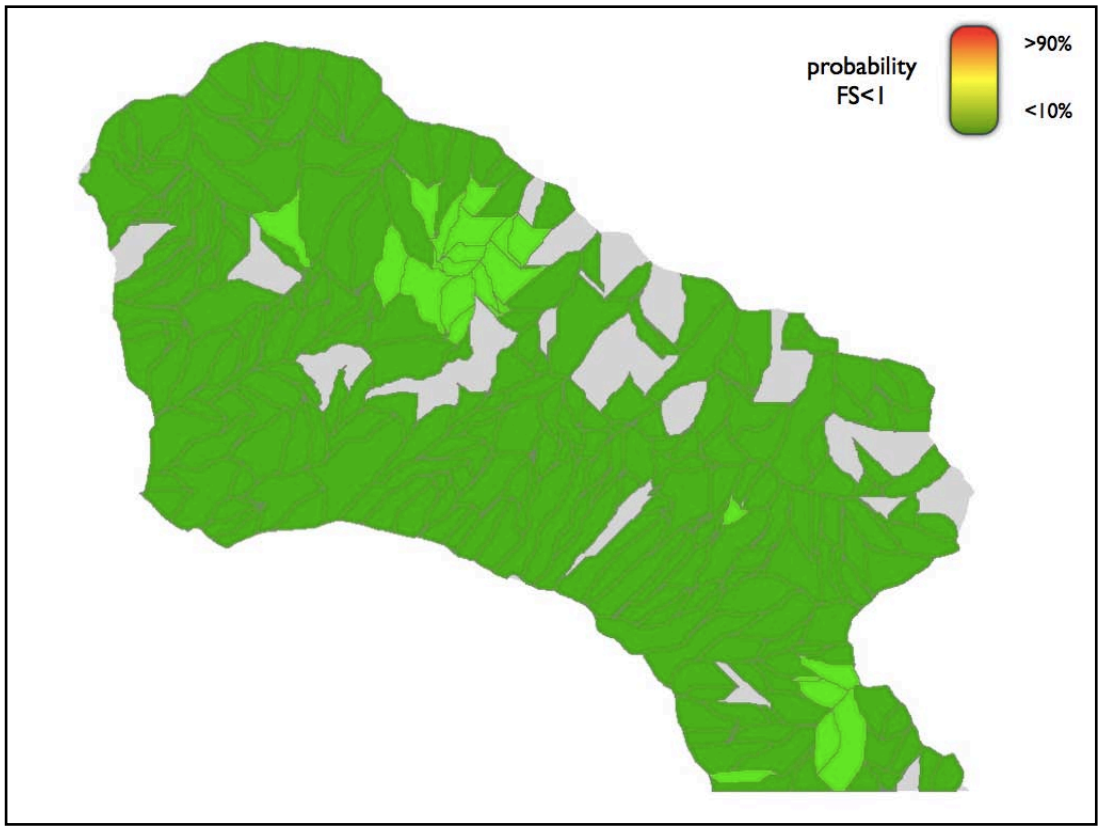

Figure 6.2: graphical representation of the instability probability simulation results of the stable area.

In table 6.4 the validation results of 2nd basin order aggregation are summarized. The results are graphically represented in figures 6.3 and 6.4. The true positives percentage increases to 94% without affecting the correct stable areas detection and losing an acceptable grade of resolution.

2nd basin order validation		
true positive	94%	
false negative	6%	average instability probability: 34 %
true negative	average instability probability: 4 % maximum instability probability: 19%	
false positive		

Table 6.4: validation results of 1st basin order aggregation.

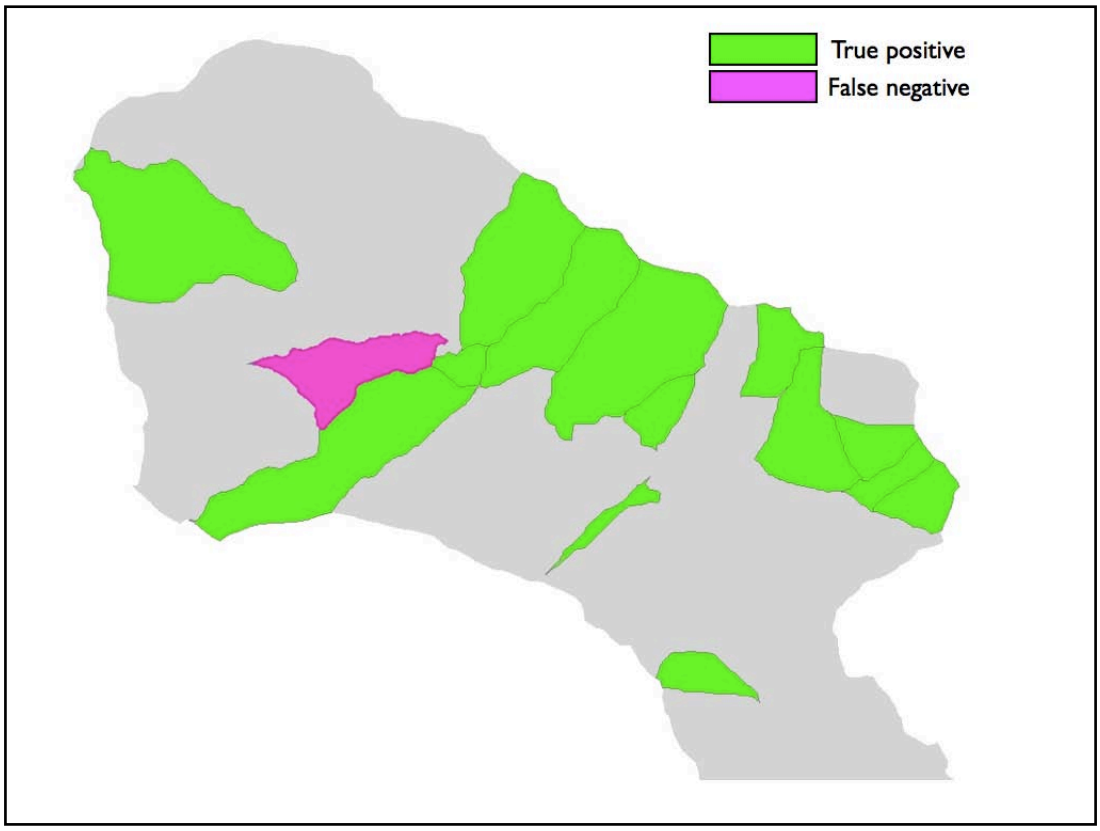

Figure 6.3: graphical results of the true positives (hits) and false negatives (misses) by 2nd basin order aggregation.

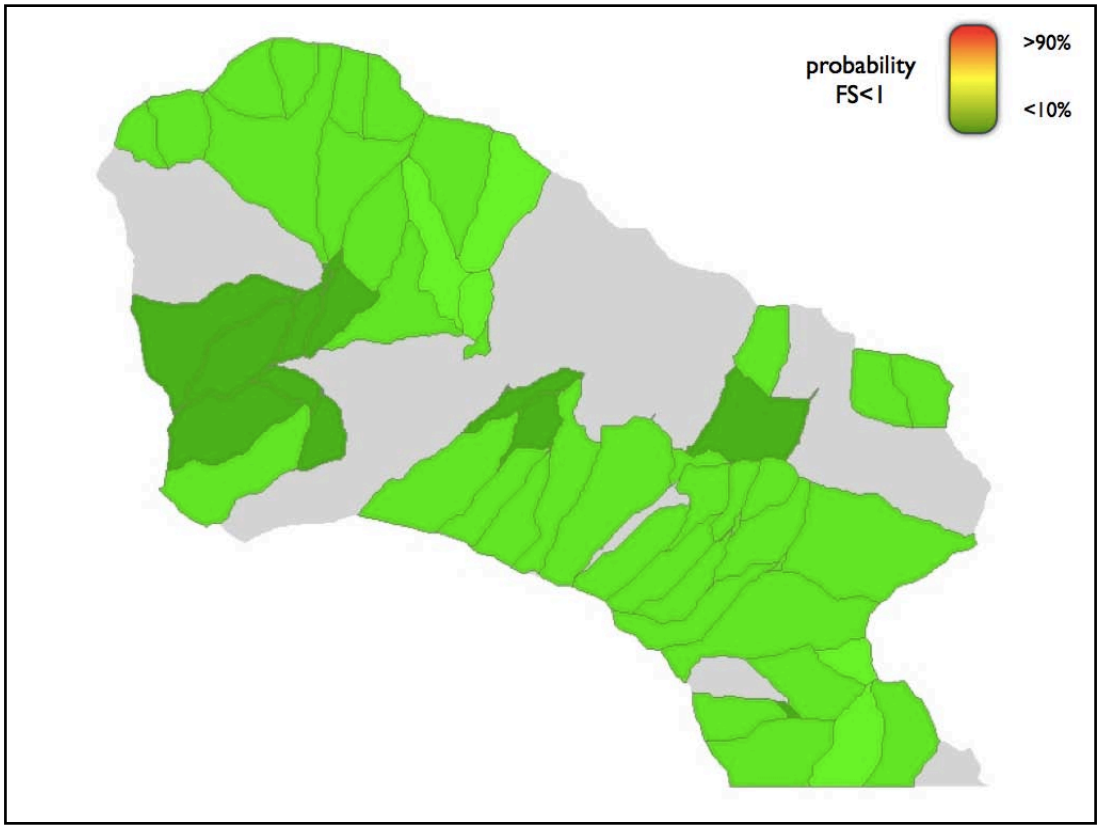

Figure 6.4: graphical representation of the instability probability simulation results of the stable area.

6.2. Results and temporal validation

The temporal validation is performed by simulating a deadly event on the April 30, 2006 on the island of Ischia. Four debris flows (figure 6.5) occurred along the northern flank of Monte Vezzi between the 6:00 and the 8:30 am, in the locality of Piano Liguori, triggered by heavy rainfall. These landslides involved two buildings, a quarry and a garbage compactor and four persons were killed in their home. It is important to point out that this meteorological event didn't exceed the alert thresholds for the areas that were subjected to hydrogeological monitoring.

The simulation was performed over two days, the 29th and the 30th of April, at the spatial resolution of 5 meters and at the temporal resolution of 30 minutes. The validation is focalized in the area of the occurred landslides. The average of the factor of safety and the failure probability is calculated over the Monte Vezzi failed slope from the single 30 minute map.

Figure 6.5: Landslide triggered by a heavy rainstorm in the morning of April 30, 2006.

Rainfall data	Radar - 48 hours resolution 30 minutes - spatial resolution 500 m^2
DEM resolution	5 meters
Depth Layers	3
Montecarlo simulation shoots	1000
Initial soil saturation	< 20%

Table 6.5: Main characteristics of the Spatial Validation performed in Armea basin area.

The FS average resulting from HIRESSS simulation is shown in figure 6.6. The simulation shows that the instability is reached when the landslides actually occurred. Observing the rainfall intensity measured by the Grazzanise radar (figure 6.7) we can observe that there is a preparatory phase that starts to undermine the slope stability before the final intense precipitation.

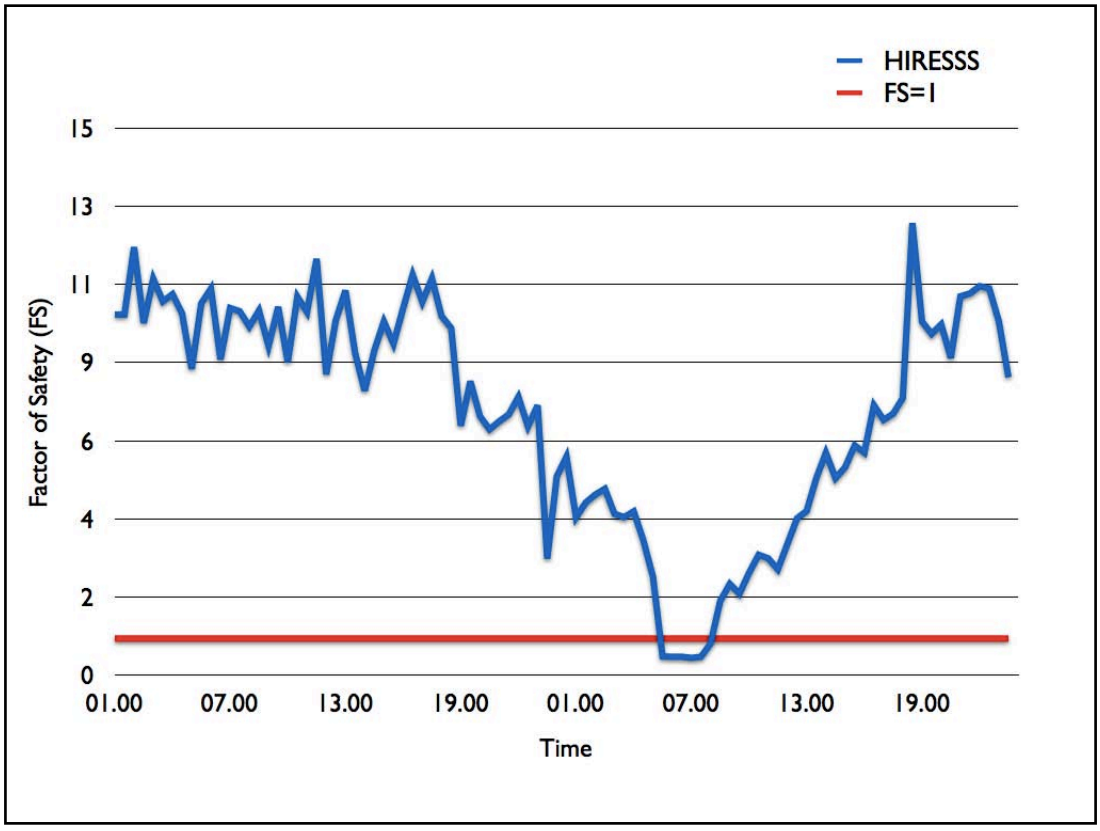

Figure 6.6: The average FS of the Monte Vezzi failed slope simulating event which occurred the 29th and 30th of April, 2006.

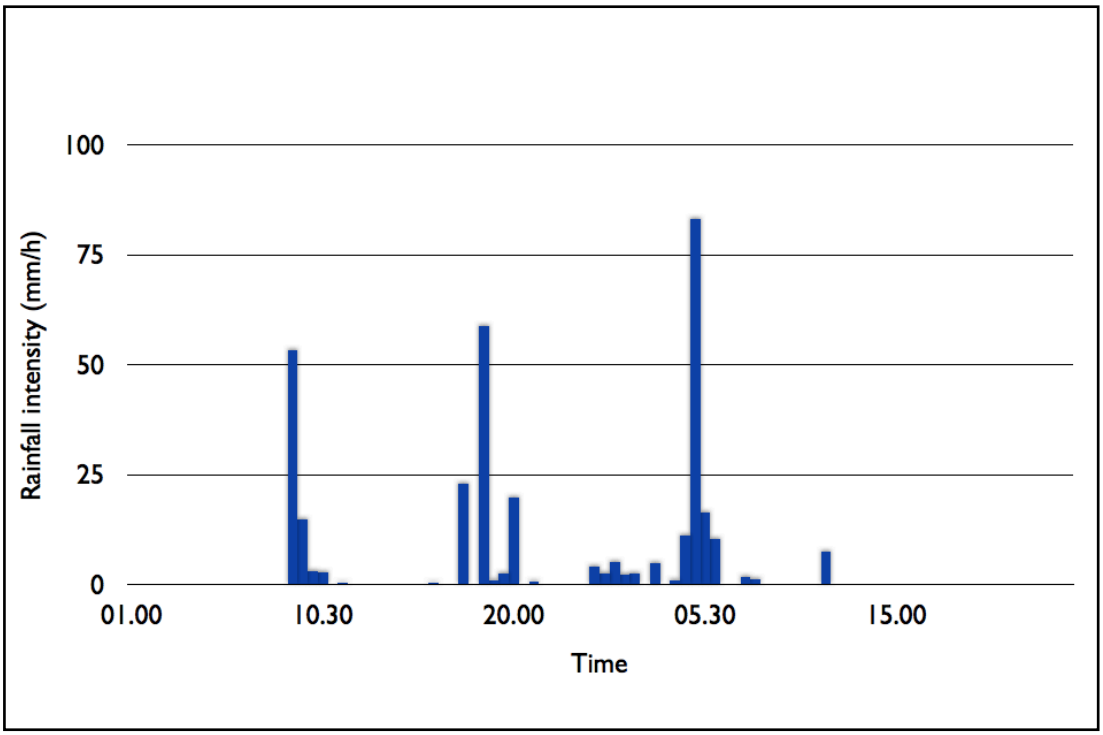

Figure 6.7: The rainfall intensity recorded by Grazzanise radar the 29th and 30th of April, 2006

The simulated behavior is quite progressive to the instability, showing that the pluviometric path is justly taken into account. This result, like the Armea basin one, is obtained from data extracted from geological chart, literature parameters and not intensive or real time measurement. This kind of data collecting is affordable in almost any area of any extension.

6.3. HIRESSS runtime performance

The spatial and temporal validation shows a promising reliability and behavior but the code running time is very important. In the Monte Vezzi validation we saw a correct temporal localization, an index of a good model behavior that is good for scientific purposes, and surely not the only one or the best that can be funded in the scientific community. For civil protection purposes we have to obtain the results in a reasonable amount of time before an event occurs. Moreover, HIRESSS is not conceived to be focalized in one or a few critical slopes, but, to control a large area, thousands of square kilometers at the resolution comparable with single slope case study investigation models.

As said in chapter 4.4.1 the development and testing of HIRESSS involved a desktop workstation and a supercomputer.

In figure 6.8, a general comparison between serial and parallel execution of HIRESSS code is presented. Disabling the Montecarlo simulation, HIRESSS shows a slight increase in performance from a parallelized execution. This is an index of a good optimization and a rationalized structure of the code if analyzed together with the graph on the right in figure 6.8: the right graph shows that the Montecarlo simulation receives great benefits from parallelization. Moreover, in the same simulation conditions, HIRESSS reduces the runtime by another 68%, in the 8 CPUs code execution, using the "multisave" file management (see chapter 4.3.1).

The running times of the Armea area simulation, performed with the SP6 supercomputer, are plotted in the graph in figure 6.9 in relation to CPUs used. The simulation involves 24 hours at spatial and temporal resolutions respectively of 5 meters and 1 hour. They are the same setting used in the spatial validation. The time needed to complete the simulation varies from 12 hours using 1 CPU to 13 minutes using 512 CPUs.

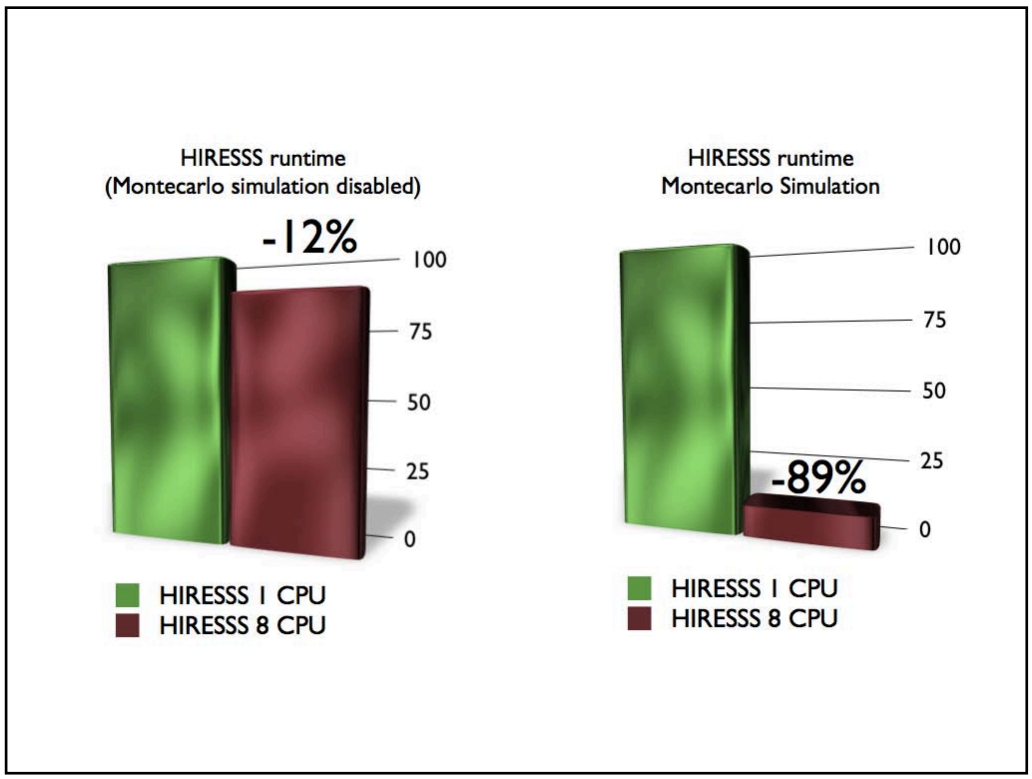

Figure 6.8 : Comparative runtime graph: on the left the effect of parallelization in the code without the Montecarlo simulation (only timing results, the FS results are not usable). Right graph shows the benefits from parallelization. The graphs refer to the same simulation conditions.

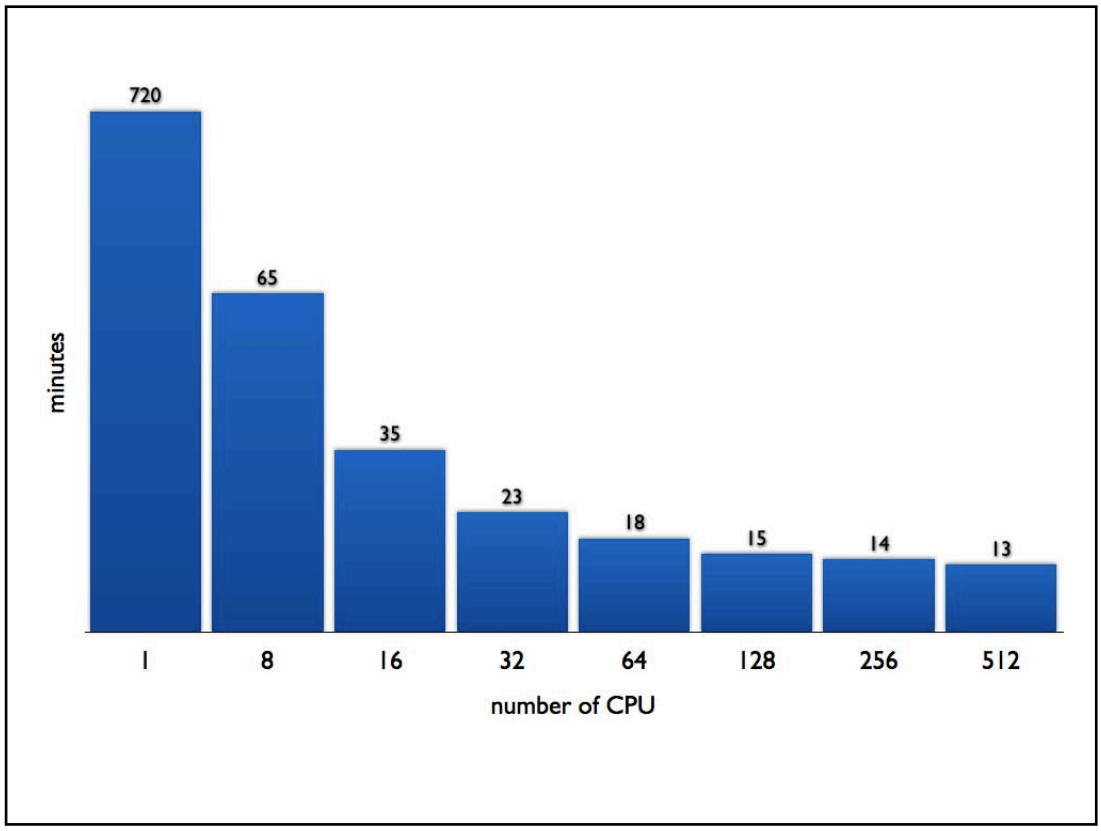

Figure 6.9: The runtime of HIRESSS code in the SP6 supercomputer for a 24 hour simulation of the Armea basin area. The spatial resolution is 5 meters and the time step resolution is 1 hour.

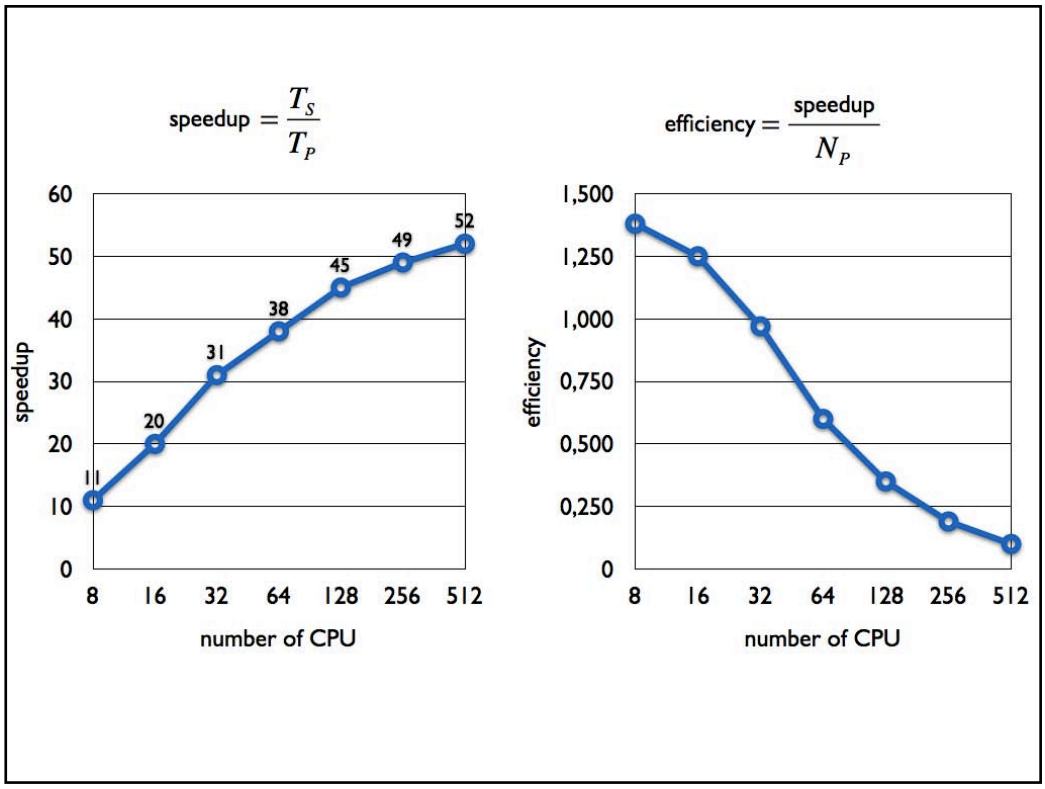

Figure 6.10: Speedup and efficiency are the two usual parameters to evaluate a code parallelization.In parallel computing, speedup refers to how much a parallel algorithm is faster than a corresponding sequential algorithm.

It is possible to observe that even using only 8 CPUs the time is compatible with civil protection purposes because in only one hour we have the “forecasting” of the slope stability situation for the next 23 hours. Raising the number of CPUs used, the runtime decreases with a high efficiency (figures 6.9 and 6.10) up until 32 processors: the runtime is halved every time the number of CPUs is doubled. Between 32 and 64 processors the efficiency decreases but stays at good level, after that number we have improvements that are not worth the resources employed.

The runtime results show that resources over 32/64 CPUs can be used to improve the quality of simulation. For example, it is possible to compute the results at more layers of the soil depth or increase the number of shoots of the Montecarlo simulation if we have very uncertain input data. Clearly the analyzed area can be simply extended which is the objective of this work.

We tested HIRESSS with a bigger area, the entire province of Lucca, Pistoia and Prato (chapter 5.3). The area is approximately 3000 square kilometers, investigated with the spatial resolution of 10 meters and a hourly temporal step.

The first attempt, using the same strategy adopted for the smaller area, wasn't encouraging. Using 1024 CPUs, the runtime for a 24 hour simulated forecasting was 5.3 hours. This is not an absolutely bad result because we computed the model over 50 millions of pixels but it is limiting to plan a major extension of the applied area.

The problem is the writing and reading of the data. For this reason, the computing strategy must be changed for large areas. The new strategy is shown in figure 6.11.

If we have extremely short computational time over a certain area we can “manage” a bigger area executing contemporarily the code over same extension areas. Therefore, the area dimension and the simulation settings are compared with parameters of maximum efficiency that define the dimension of a sub-areas. The smaller sub-areas are assigned to a sub-computational group that manages the simulation independently. Each computational group has to write smaller result files, decreasing the runtime. The runtime of HIRESSS decreases to approximately 30 minutes, more importantly using less CPUs: 640.

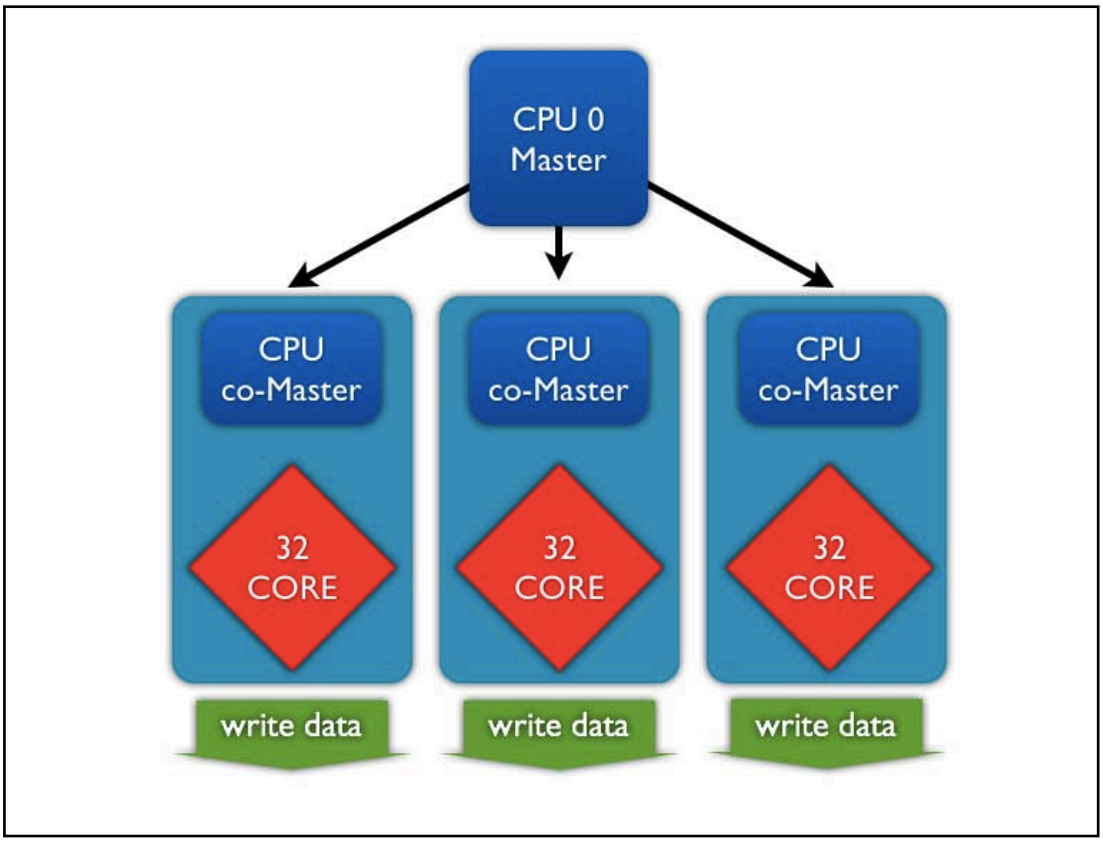

Figure 6.11: The dividing strategy used to improve runtime over extremely large areas.

This strategy can be used until the maximum parallel access to the data is reached and depends on the supercomputer's architecture: when the limit is reached the runtime will increase again.

The runtime speed test shows that HIRESSS on a supercomputer is fast enough to be useful for civil protection purposes, managing a very extended area with very high spatial and temporal resolution. Moreover, HIRESSS can be employed in relatively smaller areas using more affordable workstation computers. In table 6.6 the computational time results for the main simulation performed are shown.

Area	Spatial resolution	Temporal resolution	Time steps	Runtime	CPU
Spatial validation area (~38 Km^2)	5m	1h	24	13 min	512
Temporal validation area (~46 Km^2)	5m	0.5h	96	60 min	512
Large area test (~3100 Km^2)	10m	1h	24	32 min	640

Table 6.6: Summary of best runtime results over each test areas.

7. Discussion and Conclusions

7.1. Conclusions

The objectives of is PhD thesis concerned the development of a physically based distributed slope stability simulator for the purpose of analyzing shallow landslide triggering in real time and on a large scale.

The development culminated in HIRESSS, High REsolution Slope Stability Simulator, that has these main characteristics:

- High temporal and spatial resolutions physically based analysis.
- Operating on a large scale area.
- Probabilistic failure results.
- Fast computational time.

The physical model proposed is composed of two parts: hydrological and geotechnical. The hydrological model receives the rainfall data as dynamical input and provides the pressure head as perturbation to the geotechnical stability model, that provides results in factor of safety (FS) terms. The physical model is inserted into a Montecarlo simulation, to overcome the exact computation problems. This technique is introduced to manage the typical geotechnical parameters' incertitude, which is the common weak point of the deterministic models and large area management. The main characteristics of the physical model implemented in HIRESSS are:

- The Richards equation based hydrological model.
- The Modeling of Hydrological Diffusivity.
- The Modeling of soil suction effects in the stability model.
- Soil mass depending on saturation conditions.
- The Montecarlo simulation to overcome the input parameters' incertitude problems.

The high resolution analysis over a large area and the Montecarlo simulation implementation required the use of advanced techniques of parallel programming and the computational power of high performance computing machines. The software was written in C++ language and the parallelization used the Open-MPI paradigm. HIRESSS runtime were reduced using a high parallelization of the computation and a use of parallel data management architecture, typical of supercomputer. The HIRESSS software code main characteristics are:

- Portability over different operating systems and hardware architecture.
- Parallelized code
- Developed to run in HPC (High Performance Computing) hardware and supercomputers.

- Can be compiled and used in modern workstations

During the development of HIRESSS, a large scale geotechnical measurements campaign was conceived and performed in order to study a data collecting methodology that can be adopted extending the analysis area without penalizing the reliability. The campaign consisted of 34 geothecnical measurements of saturated hydraulic conductivity, friction angle, matric suction and soil water content over an area of approximately 3100 Km^2. This measurement was focalized to quantify the local and the long distance variability of the geotechnical parameters in the same lithotechnical area. The measures suggest that in the same lithotechnical class the two variabilities are comparable and the relative incertitude seems to be the same over different lithotechnical classes. In this case, the methodology to collect data can be simplified and limited to a few measurements for each lithotechnical class individualized, making the procedure on a large scale affordable. The parameters' variabilities individualized in this test area are a key input for the Montecarlo simulation implemented in HIRESSS, and they were associated even over the other studied area.

HIRESSS was tested on the SP6 supercomputer hosted in the Cineca HPC facilities and validations in three areas were performed to evaluate the spatial and temporal results' reliability and the computational speed. The validation results confirmed a good model behavior and a high reliability while managing very uncertain input data. The model parameters were deliberately extracted from literature measurements, geological and lithological charts combined with a small amount of geotechnical measurements to prove the ability of HIRESSS to work with data affordably collectible on a large scale.

The reliability of the model does not have huge computational time, indeed HIRESSS proved fast enough to be a core of a real time landslide forecasting system for civil protection purposes.

7.2. Considerations on extremely large scale area extensions

HIRESSS has extremely short computational time, but is it possible to extend the analyzed area to a national scale like a weather forecasting system?

It is possible to make some projections from the runtime results collected with the regional test area in the northern Apennines, clearly assuming the resolution of the huge data collection problem.

The Italian territory extension without sea and plains is approximatively 220000 km^2. A forecasting run of 24 hours at the same spatial resolution of 10 meters with a time step of 1 hour could be performed in 30 minutes employing approximatively 44000 CPUs. Clearly this amount of processing units can be found only in a few supercomputers in the world. The runtime and the resolution are the same as the large test areas analyzed in this PhD thesis. Decreasing the spatial resolution, 20 meters, the entire national territory could be analyzed in 1 hour using approximately 5000 CPUs: this is a more reasonable amount of resources, comparable to the Cineca SP6 supercomputer.

Operatively, the smart choice is not the slope stability evaluation of all national territories without filters that can help to save resources: it is useless to compute the slope stability of an area that is not subjected to precipitations and rarely can a storm hit the entire territory simultaneously. The resources saved by using filters can even be used to improve the physical model, improving the reliability of the results.

This is currently only a projection exercise, but, it is useful to understand how fast HIRESSS can be on a supercomputer and its future potential.

Acknowledgements

Il primo ringraziamento è per Jen, che con mia grande felicità ha accettato di sposarmi in questi anni di dottorato. La sua serenità e il suo supporto sono stati indispensabili per affrontare questi anni con tranquillità. Non riuscirò mai a ringraziarla abbastanza per aver letto e riletto questa tesi revisionando pazientemente il mio inglese "italianizzato".

Ringrazio come sempre i miei "supporters" affezionati, i miei genitori, Ennio e Patrizia, per il loro affetto, sostegno continuo e la loro curiosità per le cose che faccio. Ormai a tutti gli effetti contributori della ricerca (si spera apprezzata) in Italia.

Un ringraziamento speciale lo rivolgo al Professor Casagli e ai professori Moretti e Catani per avermi messo a disposizione il supporto e mezzi per completare la mia formazione e per permettermi di continuare a fare ricerca.

Un ulteriore particolare ringraziamento lo rivolgo al mio tutore Filippo, preziosa guida e piacevole interlocutore anche al di fuori dell'ambito lavorativo.

Un sentito grazie a Veronica e Samuele per la loro professionalità e per il "supporto geologico" assolutamente indispensabile a un fisico, proveniente dallo spazio e che ha voluto impugnare, almeno qualche volta, il temibile martelletto da geologo!

Un ringraziamento al CINECA e in particolare al dott. Giovanni Erbacci e a tutto il suo staff, partner tecnologico d'eccellenza del lavoro di tesi.

Un ulteriore ringraziamento a tutti i "ragazzi del laboratorio" (o quasi) Goffredo, Alessandro, Ascanio, Melania, Silvia, Chiara, Ping, Lorenzo, Giacomo, Angelo e il mitico onnipresente sistemista Gabriele, compagno di keynote di questi ultimi anni...

Un ringraziamento a tutti gli altri appartenenti al fantastico il gruppo di ricerca di geologia applicata: Francesco, Giovanni ... troppo numeroso da elencare.

E chiaramente non posso non citare loro, il solito gruppone instancabile, ormai multidisciplinare e multinazionale (purtroppo), compagni unici oramai di n 1000 avventure: Tommi, Lumao, Andre, Luca, Ghigone, Celo e Marcos!

References

And inspiring readings.

Aleotti P, 2004 “A warning system for rainfall-induced shallow failures” Engineering Geology 73 247–265

Aleotti P, Chowdhury R, 1999 “Landslide hazard assessment: summary review and new perspectives” Bulletin of Engineering Geology and the Environment 58 21–44

Alonso E, Gens A, Josa A, 1990 “A constitutive model for partially saturated soils” Géotechnique 40–3

Anbalagan R, Singh B, 1996 “Landslide hazard and risk assessment mapping of mountainous terrains—a case study from kumaun himalaya, india” Engineer- ing Geology 43 237–246

Annunziati A, Focardi A, Focardi P, Martello S, Vannocci P (2000) - Analysis of the rainfall thresholds that induced debris flows in the area of Apuan Alps – Tuscany, Italy (19 June 1996 storm). In: Proc. EGS Plinius Conf. on Mediterranean Storms, Maratea, Italy, pp 485–493.

Apuani T, Corazzato C, Cancelli A, Tibaldi A, 2005 “Physical and mechanical properties of rock masses at Stromboli: a dataset for volcano instability evaluation” Bulletin of Engineering Geology and the Environment 64 419–431

Arboleda RA, Martinez ML (1996) - 1992 lahars in the Pasig- Potrero River system. In: Fire and mud: eruptions and lahars of Mount Pinatubo (Newhall CG, Punongbayan RS, eds). Philippine Institute of Volcanology and Seismology. Seattle: Quezon City and University ofWashington Press, 1126 pp.

Baeza C, Corominas J, 2001 “Assessment of shallow landslide susceptibility by means of multivariate statistical techniques” Earth Surface Processes and Landforms 26 1251–1263

Bagnold R, 1954 “Experiments on a gravity-free dispersion of large solid spheres in a newtonian fluid under shear” Proceedings of the Royal Society of London. Series A, Mathematical and Physical Sciences (1934-1990) 225 49–63

Baum R, Coe J, Godt J, Harp E, Reid M, Savage W, Schulz W, Brien D, Chleborad A, McKenna J, et al., 2005 “Regional landslide-hazard assessment for seattle, washington, usa” Landslides 2 266–279

Baum R, Savage W, Godt J, 2002 “Trigrs: A fortran program for transient rainfall infiltration and grid-based regional slope-stability analysis” Open-file Report. U. S. Geological Survey

Bear J, 1972 “Dynamics of fluids in porous media”

Beven K, Lamb R, Quinn P, Romanowicz R, Freer J, 1995 “Topmodel” Computer Models of Watershed Hydrology 18 627–668

Birkeland P, 1984 “Soils and geomorphology” New York

Bishop A, 1955 “The use of the slip circle in the stability analysis of slopes” Geotechnique 5 7–17

Bishop A, 1959 The Principles of Effective Stress (Norges Geotekniske Institutt)

Bolley S, Oliaro P (1999) - Analisi dei debris flows in alcuni bacini campione dell’Alta Val Susa. Geoingegneria Ambientale e Mineraria, Marzo, pp 69–74.

Bolt G, 1956 “Physico-chemical analysis of the compressibility of pure clays” Geotechnique 6 86–93

Bortoluzzi G, Grimaldi R, Italiano A, 1983 “Osservazioni geomorfologiche sul versante meridionale dell’isola d’Ischia” Centro studi sull’isola d’Ischia: Ricerche, contributi e memorie II 257–265

Braun J, Heimsath A, Chappell J, 2001 “Sediment transport mechanisms on soil-mantled hillslopes” Geology 29 683–686

Brooks, R. H., Corey A. T., 1966. “Hydraulic proprieties of porous media affecting fluid flows”. J. Irrg. Drain. Div., Am. Soc. Civil Eng. 92(IR2):61-88

Brooks, R. H., Corey A. T., 1964 “Hydraulic properties of porous media”, Hydrology Paper no. 3, Civicl Engineering Dep., Colorado State University., Fort Collins, Colo.

Buchanan P, Savigny K, 1990 “Factors controlling debris avalanche initiation” Canadian Geotechnical Journal 27 659–675

Burton A, Bathurst J, 1998 “Physically based modelling of shallow landslide sediment yield at a catchment scale” Environmental geology(Berlin) 35 89–99

Caine N, 1980 “The rainfall intensity-duration control of shallow landslides and debris flows” Geografiska Annaler 62 23–27

Calcaterra D, Coppin D, Palma B, Parise M, Orsi G, de Vita S, di Vito M, 2003 “Slope processes in weathered volcaniclastic rocks of the camaldoli hill (naples, italy): Geomorphologic and engineering-geological aspects” in “EGS- AGU-EUG Joint Assembly, Abstracts from the meeting held in Nice, France, 6-11 April 2003, abstract# 10281”

Calcaterra D, Parise M, Palma B, Pelella L (2000) - The influence of meteoric events in triggering shallow landslides in pyroclastic deposits of Campania, Italy. In: Proc. 8th Int. Symp. on Landslides (Bromhead E, Dixon N, Ibsen ML, eds), vol. 1. Cardiff: A.A. Balkema, pp 209–214.

Campbell R, 1975 “Soil slips, debris flows and rainstorms in the santa monica mountains and vicinity, southern california” U.S. Geological Survey Profes- sional Paper 851 51pp.

Cannon S, Ellen S, 1985 “Rainfall conditions for abundant debris avalanches, san francisco bay region, california” California Geology 38 267–272

Cannon SH, Gartner JE (2005) - Wildfire-related debris flow from a hazards perspective. In: Jakob M, Hungr O (eds) Debris flow hazards and related phenomena. Springer, Berlin, pp 363–385.

Cardinali M, Galli M, Guzzetti F, Ardizzone F, Reichenbach P, Bartoccini P (2006) - Rainfall induced landslides in December 2004 in Southwestern Umbria, Central Italy. Nat Hazard Earth Sys Sci 6: 237–260.

Carslaw, H. S., and J. C. Jaeger, Conduction of Heat in Solids, Oxford Univ. Press, New York, 1959.

Carson M, Kirkby M, 1972 Hillslope form and process (Cambridge University Press)

Casadei M, Dietrich W, Miller N, 2003 “Testing a model for predicting the timing and location of shallow landslide initiation in soil-mantled landscapes” Earth Surface Processes and Landforms 28 925–950

Casagli N, Nocentini M, Farina P, Falorni G, Lombardi L, Righini G, Tofani V, Vannocci P, 2007 “Analisi dei fenomeni franosi avvenuti nel versante settentrionale del monte vezzi (isola di ischia) il 30 aprile 2006” Rapporto n◦2.1 - Dipartimento di Protezione Civile

Casagrande A, 1979 Liquefaction and Cyclic Deformation of Sands: A Critical Review (Harvard University)

Catani, F., S. Segoni, and G. Falorni (2010), An empirical geomorphology-based approach to the spatial prediction of soil thickness at catchment scale, Water Resour. Res., 46, W05508, doi:10.1029/2008WR007450.

Chien-Yuan C, Tien-Chien C, Fan-Chieh Y, Sheng-Chi L, 2005 “Analysis of time-varying rainfall infiltration induced landslide” Environmental Geology 48 466–479

Cho S, Lee S, 2001 “Instability of unsaturated soil slopes due to infiltration” Computers and Geotechnics 28 185–208

Chleborad AF (2003) - Preliminary evaluation of a precipitation threshold for anticipating the occurrence of landslides in the Seattle Washington Area, US Geological Survey Open-File Report 03-463.

Conacher A, Dalrymple J, 1977 The Nine Unit Landsurface Model: An Approach to Pedogeomorphic Research (Elsevier Scientific Pub. Co.)

Costa J, 1984 “Physical geomorphology of debris flows” Developments and applications of geomorphology 268–317

Crosta G, Dal Negro P, 2003 “Observations and modelling of soil slip-debris flow initiation processes in pyroclastic deposits: the sarno 1998 event” Natural Hazards and Earth System Sciences 3 53–69

Crosta G, Frattini P, 2002 “Rainfall thresholds for triggering soil slips and debris flow” Proc. 2nd Plinius Int. Conf. on Mediterranean Storms, Siena, Italy, in press

Crosta G, Frattini P, 2003 “Distributed modelling of shallow landslides triggered by intense rainfall” Natural Hazards and Earth System Sciences 3 81–93

Crozier M, Glade T, 1999 “Frequency and magnitude of landsliding: fundamental research issues” Zeitschrift fur Geomorphologie 115 141–155

Cruden D, 1991 “A simple definition of a landslide” IAEG Bull. 27–29

Cruden D, Varnes D, 1996 “Landslides type and processes” Landslides: Investigation and Mitigation 39–75

De Vita S, Sansivero F, Orsi G, Marotta E, 2006 “Cyclical slope instability and volcanism related to volcano-tectonism in resurgent calderas: The ischia island (italy) case study” Engineering Geology 86 148–165

Del Prete O, Mele R, 1999 “L’influenza dei fenomeni d’instabilità di versante nel quadro morfoevolutivo della costa dell’isola di’ischia” Bollettino della Società geologica italiana 118 339–360

Denlinger R, Iverson R, 1990 “Limiting equilibrium and liquefaction potential in infinite submarine slopes” Mar. Geotechnol 9 299–312

Dhakal A, Sidle R, 2004 “Distributed simulations of landslides for different rainfall conditions” Hydrological Processes 18 757–776

Dietrich W, Bellugi D, de Asua R, 2001 “Validation of the shallow landslide model, shalstab, for forest management” Water Science and Application 2 195–227

Dietrich W, Montgomery D, 1998 “Shalstab: a digital terrain model for mapping shallow landslide potential” NCASI (National Council of the Paper Industry for Air and Stream Improvement) Technical Report, February

Dietrich W, Reiss R, Hsu M, Montgomery D, 1995 “A process-based model for colluvial soil depth and shallow landsliding using digital elevation data” HYDROLOGICAL PROCESSES 9 383–383

Ellen S, 1988 “Description and mechanics of soil slip/debris flow in the storm of january 3-5, 1982, in the the san francisco bay region, california” U.S. Geological Survey Professional Paper 1434 64–111

Ferraris L, Gabellani S, Rebora N, Provenzale A, 2003 “A comparison of stochastic models for spatial rainfall downscaling.” Water Resources Research 39 1368

Ferraris L, Rudari R, Siccardi F, 2002 “The uncertainty in the prediction of flash floods in the northern mediterranean environment” Journal of Hydrometeorology 3 714–727

Floris M, Mari M, Romeo RW, Gori U (2004) - Modelling of landslide-triggering factors – a case study in the Northern Apennines, Italy. In: Lecture Notes in Earth Sciences 104: Engineering Geology for Infrastructure Planning in Europe (Hack R, Azzam R, Charlier R, eds). Berlin Heidelberg: Springer, pp 745–753.

Fonseca F, 1870 Geologia dell’Isola d’Ischia

Frattini P, Crosta G, 2005 “Deliverable 3 - report on spatially distributed deterministic models and rainfall thresholds” LESSLOSS Risk Mitigation for Earthquakes and Landslides Integrated Project

Frattini P, Crosta G, Fusi N, Dal Negro P, 2004 “Shallow landslides in pyroclastic soils: a distributed modelling approach for hazard assessment” Engineering Geology 73 277–295

Fredlund D, 1987 “Slope stability analysis incorporating the effect of soil suction” Slope Stability: Geotechnical Engineering and Geomorphology. John Wiley and Sons New York. 1987. p 113-144, 31 fig, 10 tab, 25 ref.

Fredlund G, Rahardjo H, 1993 Soil mechanics for unsaturated soils (John Wiley and Sons)

Fuchs C, 1873 “Monografia geologica dell’isola d’ischia con carta geologica 1:25.000” Mem. per serv. alla descrizione della carta geologica d’Italia

Gabet E, Burbank D, Putkonen J, Pratt-Sitaula B, Ojha T, 2004 “Rainfall thresholds for landsliding in the himalayas of nepal” Geomorphology 63 131– 143

Gallipoli D, Gens A, Sharma R, Vaunat J, 2003 “An elasto-plastic model for unsaturated soil incorporating the effects of suction and degree of saturation on mechanical behaviour” Geotechnique 53 123–136

Gee M, 1992 “Classification of landslide hazard zonation methods and a test of predictive capability, vol. 2” Proc. 6th International Symposium on Landslides, Christchurch, New Zealand 947–952

Giannecchini R. (2005), Rainfall triggering soil slips in the southern Apuan Alps (Tuscany, Italy), Advances in Geosciences, 2: 21-24.

Giannoni F, Roth G, Rudari R, 2000 “A semi-distributed rainfall-runoff model based on a geomorphologic approach” Physics and Chemistry of the Earth, Part B 25 665–671

Giannoni F, Roth G, Rudari R, 2005 “A procedure for drainage network identification from geomorphology and its application to the prediction of the hydrologic response” Advances in Water Resources 28 567–581

Gillot P, Chiesa S, Vezzoli L, 1982 “33000 yr k-ar dating of the volcano-tectonic horst of the isle of ischia, gulf of neaples” Nature 229 242–244

Glade T, 2000 “Applying probability determination to refine landslide-triggering rainfall thresholds using an empirical “antecedent daily rainfall model”” Pure and Applied Geophysics 157 1059–1079

Green W, Ampt G, 1911 “Studies on soil physics, 1. the flow of air and water through soils” J. Agric. Sci 4 1–24

Guillot G, Lebel T, 1999 “Approximation of sahelian rainfall fields with meta-gaussian random functions” Stochastic Environmental Research and Risk Assessment 13 113–130

Guimarães R, Montgomery D, Greenberg H, Fernandes N, Trancoso Gomes R, de Carvalho O, 2003 “Parameterization of soil properties for a model of topographic controls on shallow landsliding: application to rio de janeiro” Engineering Geology 69 99–108

Guzzetti F, 2000 “Landslide fatalities and the evaluation of landslide risk in italy” Engineering Geology 58 89–107

Guzzetti F, Cardinali M, Reichenbach P, Cipolla F, Sebastiani C, Galli M, Salvati P, 2004 “Landslides triggered by the 23 november 2000 rainfall event in the imperia province, western liguria, italy” Engineering Geology 73 229– 245

Guzzetti F, Carrara A, Cardinali M, Reichenbach P, 1999 “Landslide hazard evaluation: a review of current techniques and their application in a multi-scale study, central italy” Geomorphology 31 181–216

Guzzetti F., S Peruccacci, M Rossi, CP Stark 2008. The Rainfall intensity-duration control of shallow landslides and debris flows: an update. Landslides.

Hammond C, Hall D, Miller S, Swetik P, 1992 “Level i stability analysis (lisa) documentation for version 2” General Technical Report INT-285, USDA For- est Service Intermountain Research Station 121

Heimsath A, E. Dietrich W, Nishiizumi K, Finkel R, 1999 “Cosmogenic nuclides, topography, and the spatial variation of soil depth” Geomorphology 27 151– 172

Hillel D, 1982 “Introduction to soil physics” New York Hsu M, 1994 A grid-based model for predicting soil depth and shallow landslides
Ph.D. thesis University of California, Berkeley

Hungr O, 1996 “A model for the runout analysis of rapid flow slides, debris flows, and avalanches” International Journal of Rock Mechanics and Mining Sciences and Geomechanics Abstracts 33 88A–88A

Hungr O, Evans S, Bovis M, Hutchinson J, 2001 “A review of the classification of landslides of the flow type” Environmental and Engineering Geoscience 7 221

Hurley D, Pantelis G, 1985 “Unsaturated and saturated flow through a thin porous layer on a hillslope” Water Resources Research 21

Innes J, 1983 “Debris flows” Progress in Physical Geography 7

Iverson R, 1997 “The physics of debris flows” Reviews of Geophysics 35 245–296

Iverson R, 2000 “Landslide triggering by rain infiltration” Water Resources Research 36 1897–1910 Iverson R, LaHusen R, 1989 “Dynamic pore-pressure fluctuations in rapidly shearing granular materials” Science 246 796–799

Iverson R, Reid M, Iverson N, LaHusen R, Logan M, Mann J, Brien D, 2000
“Acute sensitivity of landslide rates to initial soil porosity”

Iverson R, Reid M, LaHusen R, 1997 “Debris-flow mobilization from landslides 1” Annual Reviews in Earth and Planetary Sciences 25 85–138 Janbu N, 1973 “Slope stability computations” Embankment Dam Engineering:

Casagrande Vol., John Wiley & Sons, New York 47–86

Jan CD, Chen CL (2005) - Debris flows caused by typhoon Herb in Taiwan. In: Debris flow hazards and related phenomena (Jakob M, Hungr O, eds). Berlin Heidelberg: Springer, pp 363–385

Jibson RW (1989) - Debris flow in southern Porto Rico. Geological Society of America, special paper 236, pp 29–55.

Johnson A, Rodine J, 1984 “Debris flow” Slope Instability 257–361

Johnson K, Sitar N, 1990 “Hydrologic conditions leading to debris-flow initiation” Canadian Geotechnical Journal 27 789–801

Keefer D, Wilson R, Mark R, Brabb E, Brown W, Ellen S, Harp E, Wieczorek G, Alger C, Zatkin R, 1987 “Real-time landslide warning during heavy rainfall” Science 238 921–925

Kienholz H, 1978 “Maps of geomorphology and natural hazards of grindelwald, switzerland, scale 1: 10.000” Arctic and Alpine Research 10 169–184

Kim J, Park S, Jeong S, 1998 “Effect of wetting front suction loss on stability of unsaturated soil slopes” in A S of Civil Engineers, ed., “Advances in Unsaturated Soil, Seepage, and Environmental Geotechnics (GEOTECHNICAL SPECIAL PUBLICATION)”,

Krahn J, 2004 “Seepage modeling with seep/w” Alberta: Geoslope

Larsen M, Simon A, 1993 “A rainfall intensity-duration threshold for landslides in a humid-tropical environment, puerto rico” Geografiska annaler. Series A. Physical geography 75 13–23

Lee S, Chwae U, Min K, 2002 “Landslide susceptibility mapping by correlation between topography and geological structure: the janghung area, korea” Geomorphology 46 149–162

Lee S, Ryu J, Min K, Won J, 2003 “Landslide susceptibility analysis using gis and artificial neural network” Earth Surface Processes and Landforms 28 1361–1376

Lee S, Ryu J, Won J, Park H, 2004 “Determination and application of the weights for landslide susceptibility mapping using an artificial neural network” Engineering Geology 71 289–302

Lu N, ASCE M, Likos W, 2006 “Suction stress characteristic curve for unsaturated soil” Journal of Geotechnical and Geoenvironmental Engineering 132 131

Martini, I.P., Vai, G.B (eds) (2001) Anatomy of an Orogen: the Apennines and Adjacent Mediterranean Basins. Kluwer Acad. Publ., Dordrecht, 632 pp.

Matsumoto, M.; Nishimura, T. (1998). "Mersenne twister: a 623-dimensionally equidistributed uniform pseudo-random number generator". ACM Transactions on Modeling and Computer Simulation 8 (1): 3–30. doi:10.1145/272991.272995

Merizzi G, Seno S, 1991 “Deformation and gravity-driven translation of the s. remo-m. saccarello nappe (helminthoid flysch, ligurian alps)” Bollettino della Società Geologica Italiana 110 757–770

Metternicht G, Hurni L, Gogu R, 2005 “Remote sensing of landslides: An analysis of the potential contribution to geo-spatial systems for hazard assessment in mountainous environments” Remote Sensing of Environment 98 284–303

Mitchell J, Soga K, 2005 Fundamentals of soil behavior. (John Wiley & Sons Ltd Chichester, UK)

Montgomery D, Dietrich W, 1994 “A physically based model for the topographic control on shallow landsliding” Water Resources Research 30 1153–1172

Montgomery D, Sullivan K, Greenberg H, 1998 “Regional test of a model for shallow landsliding” HYDROLOGICAL PROCESSES 12 943–955

Montrasio L, Valentino R, 2003 “Experimental analysis on factors triggering soil slip” Proceedings of int. conf. on fast slope movements prediction and prevention for risk mitigation, Patron Ed., Bologna 371–378

Moore I, Gessler P, Nielsen G, Peterson G, 1993 “Soil attribute prediction using terrain analysis” Soil Science Society of America Journal 57 443

Morgenstern N, Price V, 1965 “The analysis of the stability of general slip surfaces” Geotechnique 15 79–93

Moser M, Hohensinn F, 1983 “Geotechnical aspects of soil slips in alpine regions” Engineering Geology 185–211

MPI: A Message-Passing Interface Standard version 2.2, 2009 , Message passing interface forum 4 sept. 2009.

Neitsch S, Arnold J, Kiniry J, Williams J, King K, 2001 “Soil and water assessment tool theoretical documentation version 2000” Grassland, Soil and Water Research Laboratory, Temple, Texas

Okimura T, Ichikawa K, 1985 “A prediction method for surface failures by movements of infiltrated water in surface soil layer” Nat. Disaster Sci. 7 41–51

O’Loughlin E, 1986 “Prediction of surface saturation zones in natural catchments by topographic analysis” Water Resources Research 22 794–804

Pack R, Tarboton D, Goodwin C, 1998 “The sinmap approach to terrain stability mapping” in “8th Congress of the International Association of Engineering Geology, Vancouver, British Columbia, Canada”,

Pack R, Tarboton D, Goodwin C, 2001 “Assessing terrain stability in a gis using sinmap” in “15th Annual GIS Conference, GIS”,

Pareschi M, Santacroce R, Sulpizio R, Zanchetta G, 2002 “Volcaniclastic debris flows in the clanio valley (campania, italy): insights for the assessment of hazard potential” Geomorphology 43 219–231

Perica S, Foufoula-Georgiou E, 1996 “Model for multiscale disaggregation of spatial rainfall based on coupling meteorological and scaling descriptions” Journal of Geophysical Research. D. Atmospheres 101 26347–26361

Paronuzzi P, Coccolo A, Garlatti G (1998) - Eventi meteorici critici e debris flows nei bacini montani del Friuli. L’Acqua, Sezione I Memorie, pp 39–50.

Paronuzzi P., Gnech D. (2007) - Frane di crollo indotte da piogge intense: la casistica del Friuli – Venezia Giulia (Italia NE). Giornale di Geologia Applicata 6 (2007) 55-64, doi: 10.1474/GGA.2007-06.0-06.0179.

Pierson T, 1980 “Piezometric response to rainstorms in forested hillslope drainage espressions” Journal of Hydrology of New Zeland 19 1–10

Pierson T, 1983 “Soil pipes and slope stability” gsqjegh 16 1–11 Pradel D

Raad G, 1993 “Effect of permeability on surficial stability of homoge-
neous slopes” Journal of Geotechnical Engineering 119 315

Rebora N, Ferraris L, Von Hardenberg J, Provenzale A, 2006 “Rainfall downscaling and flood forecasting: a case study in the mediterranean area” Natural Hazards and Earth System Sciences 6 611–619

Reid M, 1994 “A pore-pressure diffusion model for estimating landslide-inducing rainfall” The Journal of Geology 102 709–717

Renau S, Dietrich W, 1997 “Size and location of colluvial landslides in a steep forested landscape” in R Beschta, T Blinn, G Grant, F Swanson, G Ice, eds., “Erosion and Sedimentation in the Pacific Rim”, Number 165 (Int. Assoc. Hyd. Sci. Pub.) pp. 39–49

Richards L, 1931 “Capillary conduction of liquids through porous media” Physics 1 318–333

Rigon R, Bertoldi G, Over T, 2006 “Geotop: A distributed hydrological model with coupled water and energy budgets” Journal of Hydrometeorology 7 371– 388

Ritter J, 2004 “Landslide and slope stability analysis: using an infinite slope model to delineate areas susceptible to translational sliding in the cincinnati, oh area, computational science module, dept. of geol” Wittenberg U., Spring- field, OH

Rittmann A, Gottini V, 1980 “L’isola d’ischia-geologia” Bollettino del Servizio 101

Rosso R, Rulli M, Vannucchi G, 2006 “A physically based model for the hydrologic control on shallow landsliding” Water Resour. Res 42

Rawls W.J., Brakensiek D.L., Saxton K. E. 1982 “ Estimation of soil water properties” Trans. Amer. Soc. of Agric. Engin. 25(5)1316-1320, 1328.

Rulon J, Freeze R, 1985 “Multiple seepage faces on layered slopes and their implications for slope-stability analysis” Canadian Geotechnical Journal

Sagri M, 1980 “Le arenarie di bordighera: una conoide sottomarina nel bacino di sedimentazione del flysch ad elmintoidi di san remo (cretaceo superiore, liguria occidentale)” Bollettino della Società Geologica Italiana 98 205–226

Sagri M, 1984 “Litologia, stratimetria e sedimentologia delle torbiditi di piana di bacino del flysch di san remo (cretaceo superiore, liguria occidentale)” Mem. Soc. Geol. It 28 577–586

Salciarini D, Godt J, Savage W, Conversini P, Baum R, Michael J, 2006 “Modeling regional initiation of rainfall-induced shallow landslides in the eastern umbria region of central italy” Landslides 3 181–194

Sassa K, 1984 “The mechanism starting liquefied landslides and debris flows”Proceedings of 4 thInternational Symposium on Landslides, Toronto, June 2 349–354

Saulnier G, Beven K, Obled C, 1997 “Including spatially variable effective soil depths in topmodel” Journal of Hydrology 202 158–172

Schmidt J, Turek G, Clark M, Uddstrom M, Dymond J, 2008 “Probabilistic forecasting of shallow, rainfall-triggered landslides using real-time numerical weather predictions” Natural Hazards and Earth System Science 8 349–357

Schmugge T, Jackson T, McKim H, 1980 “Survey of methods for soil moisture determination” Water Resources Research 16

Scott K, Pringle P, Vallance J, 1992 “Sedimentology, behavior, and hazards of debris flows at mount ranier, washington” Available from Books and Open Files Reports Section, USGS Box 25425, Denver, CO 80225. USGS Open File Report 90-385, 1992. 106 p, 21 fig, 8 tab, 123 ref, 1 plate.

Seggiani M, 2008 “Zonazione dell’innesco di frane superficiali nellisola di ischia” Università delgli Studi di Firenze, Tesi di Laurea

Segoni S, 2008 Elaborazione ed applicazioni di un modello per la previsione dello spessore delle coperture superficiali Ph.D. thesis Università degli Studi di Firenze

Segoni S., Rossi G., Catani F. Improving basin-scale shallow landslides modelling using reliable soil thickness maps. In revision on Natural Hazards

Selby M, 1993 “Hillslope materials andprocesses” Siccardi F, 1996 “Rainstorm hazards and related disasters in the western
mediterranean region” Remote Sens. Rev 14 5–21 Siccardi F, Boni G,

Ferraris L, Rudari R, 2004 “A hydrometeorological approach
for probabilistic flood forecast” J. Geophys. Res 110

Sidle R, Swanston D, 1982 “Analysis of a small debris slide in coastal alaska”
Canadian Geotechnical Journal 19 167–174

Simoni S, Zanotti F, Bertoldi G, Rigon R, 2008 “Modelling the probability of occurrence of shallow landslides and channelized debris flows using geotop-fs” HYDROLOGICAL PROCESSES 22 532

Skempton A, 1960 “Significance of terzaghi’s concept of effective stress” From theory to practice in soil mechanics 42–53

Skempton A, DeLory F, 1957 “Stability of natural slopes in london clay” Proceedings of the 4th International Conference on Soil Mechanics and Foundation Engineering 2 378–381

Soeters R, van Westen C, 1996 “Slope instability recognition, analysis and zonation” Landslides Investigation and Mitigation 129–177
Spencer E, 1967 “A method of analysis of the stability of embankments assuming parallel inter-slice forces” Geotechnique 17 11–26

Takahashi T, 1978 “Mechanical characteristics of debris flow” Journal of the Hydraulics Division 104 1153–1169

Takahashi T, 1981 “Debris flow” Annual Reviews in Fluid Mechanics 13 57–77

Taylor G, Eggleton R, 2001 Regolith Geology and Geomorphology (Wiley)

Terzaghi K, 1936 “The shearing resistance of saturated soils and the angle be- tween the planes of shear” Proc. 1st Int. Conf. Soil Mech. Found. Engng, Cambridge, MA 1 54–56

Tofani V, Dapporto S, Vannocci P, Casagli N, 2006 “Infiltration, seepage and slope instability mechanisms during the 20–21 november 2000 rainstorm in tuscany, central italy” Natural Hazards and Earth System Sciences 6 1025– 1033

Tsai T, 2008 “The influence of rainstorm pattern on shallow landslide” Environmental Geology 53 1563–1569

Tsai T, Chen H, Yang J, 2007 “Numerical modeling of rainstorm-induced shallow landslides in saturated and unsaturated soils” Environmental Geology 1–9

Tsai T, Yang J, 2006 “Modeling of rainfall-triggered shallow landslide” Environmental Geology 50 525–534 USDA, 2006 “National soil survey characterization data” Soil Survey Laboratory National Soil Survey Center, USDA-NRCS, Lincoln, NE

Van Asch T, Buma J, Van Beek L, 1999 “A view on some hydrological triggering systems in landslides” Geomorphology 30 25–32

Van Genuchten M. Th., 1980 “A closed form equation for predcting the hydraulic conductivity of unsaturated soils. Soil Sci. Soc. Am

Vanapalli S, Fredlund D, Pufahl D, Clifton A, 1996 “Model for the prediction of shear strength with respect to soil suction” CANADIAN GEOTECHNICAL JOURNAL 33 379–392

Vanossi M, 1991 “Guide geologiche regionali-alpi liguri” Soc. Geol. It., Milano

Varnes D, 1978 “Slope movements: types and processes.” Landslide analysis and control Special Report 11–33

Varnes D, 1984 “Iaeg commission on landslides (1984)." landslide hazard zonation: a review of principles and practice”

Wieczorek G, 1987 “Effect of rainfall intensity and duration on debris flows in central santa cruz mountains, california” Debris Flows/Avalanches: Process, Recognition, and Mitigation 93–104

Wieczorek G, 1996 “Landslide triggering mechanisms” AK Turner and RL Schuster, op. cit 76–90

Wu W, Sidle R, 1995 “A distributed slope stability model for steep forested basin” Water Resources Research 31 2097–2110

Yin K, Yan T, 1988 “Statistical prediction models for slope instability of metamorphosed rocks” Proceed 5 1269–1272

Zêzere J, Ferreira A, Rodrigues M, 1999 “Landslides in the north of lisbon region (portugal): Conditioning and triggering factors” Physics and Chemistry of the Earth, Part A 24 925–934

Zezere JL, Trigo RM, Trigo IF (2005) - Shallow and deep landslides induced by rainfall in the Lisbon region (Portugal): assessment of relationships with the North Atlantic Oscillation. Nat Hazard Earth Sys Sci 5: 331–344.